ISTANBUL TECHNICAL UNIVERSITY ★ GRADUATE SCHOOL

THE EFFECT OF USING DIFFERENT FEATURE SETS AND FLIGHT DATA ENVELOPES ON THE FIDELITY OF DEEP LEARNING BASED SYSTEM IDENTIFICATION OF A FIGHTER AIRCRAFT

M.Sc. THESIS

Mehmet Can ŞEN

Department of Aeronautical and Astronautical Engineering

Aeronautical and Astronautical Engineering Programme

JULY 2024

ISTANBUL TECHNICAL UNIVERSITY ★ GRADUATE SCHOOL

THE EFFECT OF USING DIFFERENT FEATURE SETS AND FLIGHT DATA ENVELOPES ON THE FIDELITY OF DEEP LEARNING BASED SYSTEM IDENTIFICATION OF A FIGHTER AIRCRAFT

M.Sc. THESIS

Mehmet Can ŞEN
(511201170)

Department of Aeronautical and Astronautical Engineering

Aeronautical and Astronautical Engineering Programme

Thesis Advisor: Ass. Dr. Barış BAŞPINAR

JULY 2024

ISTANBUL TEKNİK ÜNİVERSİTESİ ★ LİSANSÜSTÜ EĞİTİM ENSTİTÜSÜ

FARKLI FEATURE SETLERİ VE UÇUŞ VERİ ZARFLARININ KULLANIMININ BİR SAVAŞ UÇAĞININ DERİN ÖĞRENME TABANLI SİSTEM TANIMLAMASININ DOĞRULUĞU ÜZERİNDEKİ ETKİSİ

YÜKSEK LİSANS TEZİ

Mehmet Can ŞEN
(511201170)

Uçak ve Uzay Mühendisliği Anabilim Dalı

Uçak ve Uzay Mühendisliği Programı

Tez Danışmanı: Dr. Öğr. Üyesi Barış BAŞPINAR

TEMMUZ 2024

Mehmet Can Şen, a M.Sc. student of İTU Graduate School student ID 511201170 successfully defended the thesis/dissertation entitled "THE EFFECT OF USING DIFFERENT FEATURE SETS AND FLIGHT DATA ENVELOPES ON THE FIDELITY OF DEEP LEARNING BASED SYSTEM IDENTIFICATION OF A FIGHTER AIRCRAFT", which he prepared after fulfilling the requirements specified in the associated legislations, before the jury whose signatures are below.

Thesis Advisor :	**Ass. Dr. Barış BAŞPINAR** İstanbul Technical University	....
Jury Members :	**Prof. Dr. Gökhan İNALHAN** Istanbul Technical University	....
	Ass. Dr. Mevlüt UZUN Cranfield University	....

Date of Submission : 01 July 2024
Date of Defense : 03 July 2024

To my spouse and family,

FOREWORD

Firstly, I would like to express my sincere gratitude to Turkish Aerospace for providing me with the opportunity and resources to pursue this research. The support and collaborative environment at the company have been very helpful. This thesis represents not only the learnings of my academic efforts but also the practical experiences and knowledge I have gained throughout my career.

I would like to express my deepest gratitude to my thesis consultant, Barış Başpınar, for his invaluable guidance and support throughout this journey. His insights and encouragement have been critically important in preparing this thesis.

I would like to express my deepest gratitude to my spouse Ecem Cibar, whose patience and support have been my anchor throughout this challenging journey. Her encouragement and understanding have been invaluable to me. I am also profoundly grateful to my family, who have always stood behind me, providing their unconditional love and support every step of the way. Additionally, I must acknowledge my former friend and classmate Esin Dağkolu, with whom I shared countless hours of study and mutual assistance. Our teamwork and friendship were key to getting through our tough classes. Thank you all for your steadfast support and belief in me.

I am also immensely grateful to my colleagues and managers at Turkish Aerospace. Their continuous support and the collaborative environment helped me immensely at this journey.

Thank you all for your contributions to this significant milestone in my academic and professional career.

July 2024 — Mehmet Can ŞEN
(Modeling and Simulation Engineer)

TABLE OF CONTENTS

Page

ABBREVIATIONS

SP	: Short Period maneuver
BTB	: Bank to Bank maneuver
DR	: Dutch Roll maneuver
ANN	: Artificial Neural Network
OEM	: Output Error Method
EOM	: Equation Error Method
FEM	: Filter Error Method
CG	: Center of Gravity
BP	: Backpropagation
MSE	: Mean Squared Error
MAE	: Mean Absolute Error
LG	: Landing Gear

SYMBOLS

C_D	: Drag Coefficient
C_L	: Lift Coefficient
C_Y	: Side Force Coefficient
C_R	: Roll Moment Coefficient
C_M	: Pitch Moment Coefficient
C_N	: Yaw Moment Coefficient
P	: Roll Rate
Q	: Pitch Rate
R	: Yaw Rate
α	: Angle of Attack
β	: Sideslip Angle
ρ	: Density
q_{bar}	: Dynamic Pressure
β	: Sideslip Angle

Ix, Iy, Iz, Ixy, Iyz, Ixz: Inertia values of the aircraft

B_{ref}	: Span length
L_{ref}	: Chord length
S_{ref}	: Wing Area
a_x, a_y, a_z	: Linear Accelerations
$\dot{p}$, $\dot{q}$, $\dot{r}$	: Angular Accelerations

LIST OF TABLES

Page

LIST OF FIGURES

Page

THE EFFECT OF USING DIFFERENT FEATURE SETS AND FLIGHT DATA ENVELOPES ON THE FIDELITY OF DEEP LEARNING BASED SYSTEM IDENTIFICATION OF A FIGHTER AIRCRAFT

SUMMARY

Aircraft models that accurately reflect flight dynamics are critically important for aircraft design, development, and certification. To achieve high-fidelity results, flight dynamics models are developed through System Identification using flight data. Recently, Deep Learning-based approaches have gained prominence. However, collecting flight data is highly expensive, and accurately estimating the nonlinear region have significant challenges. This study aims to improve flight dynamics models in the nonlinear region by using different feature sets and optimize the flight test campaign by making flight envelope analyses with using deep learning-based system identification methodology.

First, a generic F-16 flight model was modified to obtain flight data. Short Period, Bank to Bank, and Dutch Roll maneuvers were executed in this model at various speeds and altitudes to be used for aerodynamic database predictions. Parameters required for System Identification were measured and obtained during these flights tests.

Next, data preprocessing was conducted. This involved preparing an infrastructure to calculate the total force and moment coefficients of the aircraft using mass-inertia, thrust values, and the flight data. Subsequently, an algorithm was developed to prepare deep learning-based models for the prediction algorithm. The models were trained using different feature sets and flight envelopes.

The purpose of using different feature sets was to enhance the accuracy of the flight model in the nonlinear region. Instead of using input sets directly for training, different exponents of the inputs and their coupled parameters were added to the feature set using knowledge of flight dynamics and aerodynamics. This provided the model with various input combinations during training the models. Initially, models were trained using simplified feature sets. Then, another feature sets with added exponential and coupled parameters were used for training with the same flight data. The models were compared using validation test maneuvers.

The study also focused on the subject of costs of the flight tests, a critical aspect of System Identification studies. Optimizing flight test maneuvers and inputs is essential for cost efficiency. Typically, performance and stability analyses are conducted in isolated regions thus the flight data does not lead to have sufficient distribution to reflect all flight envelope. In other cases, flight envelope is scanned at very high frequency which leads to very high costs. Second part of this study examined focused on model accuracy changes with the amount of data by examining system identification with different flight test maneuvers and envelopes. Models were trained using data from only the nonlinear region, only the linear region, and the full flight

envelope, each with different data densities. In total, six different cases were tested and compared.

In conclusion, comparing both feature sets for all force and moment coefficients revealed that they produce similar results in the linear regime. However, as nonlinearity increases near the extreme points of the flight envelope, the accuracy of the complex feature sets is significantly higher than that of the simpler feature sets. Flight test comparisons indicate that adding complex parameters to feature sets is necessary to improve accuracy in regions with increasing nonlinearity. Examining the effect of flight test envelopes used during training shows that using data only from nonlinear or linear regions is insufficient to represent the entire flight envelope. Even with increased data density in isolated regions, it is necessary to collect data from both linear and nonlinear regions for an accurate model across the entire flight envelope. Properly executed maneuvers demonstrate that increasing data density does not enhance accuracy cost-effectively.

For future applications, optimizing feature sets and flight test campaigns in System Identification studies can yield a model that performs accurately across the entire flight envelope. Additionally, significant budget savings can be achieved by conducting a cost-effective flight test campaign.

FARKLI FEATURE SETLERİ VE UÇUŞ VERİ ZARFLARININ KULLANIMININ BİR SAVAŞ UÇAĞININ DERİN ÖĞRENME TABANLI SİSTEM TANIMLAMASININ DOĞRULUĞU ÜZERİNDEKİ ETKİSİ

ÖZET

Uçuş dinamiklerini doğru bir şekilde yansıtan uçak modelleri, uçak tasarımı, geliştirme ve sertifikasyon gibi birçok çalışmanın gerçekleştirilemesi açısından kritik öneme sahiptir. Yüksek sadakat seviyesine sahip modeller geliştirebilmek için ise, uçuş dinamiklerini yansıtan modeller, uçuş verilerini kullanıldığı Sistem Tanımlama çalışmaları ile geliştirilmektedir. Son zamanlarda, derin öğrenme tabanlı çalışmalar ön plana çıkmaktadır. Ancak, uçuş verilerinin toplanması yüksek bütçe gerektirmekte ve lineer olmayan bölgelerin doğru bir şekilde tahmin edilmesinde zorluklar yaşanmaktadır. Bu çalışmanın amacı, farklı özellik setlerini kullanarak lineer olmayan uçuş zarfının olduğu bölgelerde uçuş dinamiği modellerini iyileştirmek ve farklı uçuş zarflarınının kullanıldığı sistem tanımlama analizlerini kullanarak uçuş testi kampanyasını optimize etmektir.

İlk olarak, uçuş verilerini elde etmek için jenerik kullanım için üretilmiş bir F16 uçuş dinamiği benzetim modeli modifiye edilmiştir. Daha sonra bu modelde Short Period, Bank-to-Bank ve Dutch Roll manevraları gerçekleştirilmiştir. Bu manevralar, farklı hız ve irtifa koşullarında gerçekleştirilmiştir. Bu uçuşlar sırasında, sistem tanımlama kullanılacak parametreler ölçülmüştür.

İkinci olarak, veri ön işleme çalışmaları gerçekleştirilmiştir. Bu çalışmalar kapsamında, uçağın ağırlığı, eylemsizlik momenti ve itki değerleri ile beraber uçuş verileri kullanarak uçağın toplam kuvvet ve moment katsayılarının hesaplanabildiği bir altyapı hazırlanmıştır. Bu altyapı içerisinde, elde edilen uçuş test verileri işlenerek aerodinamik kuvvet ve moment katsayıları oluşturulmuştur. Bunun için ise birçok parametrenin ayrıştırılması gerekmektedir. Lineer ivmeler ve açısal ivmeler total kuvvet ve momementlerin çıkarılmasında temel katkıyı sağlayan parametrelerdir. Ancak, uçuş testlerinde genellikle ölçülen parametreler lineer ivmeler ve açısal hızlardır. Sistem tanımlama çalışmalarında, açısal ivmeler açısal hızlardan türetilmektedir. Toplam kuvvet ve moment katsayılarının hesaplanmasında, açısal ve lineer ivmelerin merkez kütle noktasında hesaplanması gerekmektedir. Bu nedenle, ölçümler kütle merkezi noktasına taşınmıştır.

Toplam kuvvet ve moment katsayıları hesaplandıktan sonra, uçağın durum parametreleri ve kontrol yüzeyi verileri toplam katsayılarla birleştirilerek mat dosyalarında saklanmıştır. Temel Python kodunda tahmin algoritması ile sistem tanımlaması yapılırken veriler bu mat dosyaları ile kullanılmıştır. İlk olarak veriler, yapay sinir ağı eğitim modellerinde kullabilmesi için giriş ve çıkış gruplarına ayrılmıştır. Uçağın durum parametreleri ile kontrol yüzeyleri derin öğrenme modellerinin girdileri olarak tanımlanmıştır. Toplam kuvvet ve moment katsayıları ise tahmin algoritmasının çıktıları olarak tanımlanmıştır. Daha sonra giriş bölümünde kullanılacak tüm parametrelerin normalizasyonu yapılmıştır. Modelin yüksek doğrulukla tahmin edilmesi için normalizasyon gerekmektedir. Aksi takdirde, bazı

parametrelerin etkisi diğerlerine göre çok daha belirgin hale geldiği görülmüştür. Bu da tahmin algoritmasının uçak özelliklerini tam olarak yakalayamamasına ve düşük doğruluklu tahminlere yol açmasına sebep

olmuştur. Son olarak, veriler tahmin ve doğrulama olarak ayrılarak tahmin algoritmasına ayrıştırılmıştır.

Uçağın aerodinamiklerini tahmin etmek için veriler hazırlandıktan sonra, uçağın aerodinamiklerini tanımlayan model yapısı belirlenmiştir. Sinir ağı tabanlı modellemeyi tahmin işlemine uygulamak için Python ortamında TensorFlow framework yapısı kullanılmıştır. Bu çalışmada, kolaylık ve yüksek tutarlılık özelliği nedeniyle Keras API seçilmiştir. Bu yapı ile birçok farklı model, katman ve özellik setini test etme imkanı bulunmuştur. Model türü olarak sequantial model seçilmiştir. Uçuş verileri ile birçok deneme yanılma işlemi gerçekleştirilerek yapay sinir ağı katmanlarına system tanımlama çalışmalarının nasıl tepki verdiği incelenmiştir. Uçakların karmaşıklığı nedeniyle, Keras ardışık modeldeki katman sayısı ve her katmanda bulunan düğüm sayısı, her bir özellik seti ve uçağın durumu için yüksek parametre sayısı göz önünde bulundurularak yüksek yoğunlukta tasarlanmıştır. Parametrelerin birbiriyle doğrusal olmayan ilişkisi nedeniyle, tüm iç katmanlarda aktivasyon fonksiyonu olarak Relu seçilmiştir. Çıkış katmanında ise her bir parametrenin basit toplamını temsil etmek için aktivasyon fonksiyonu lineer olarak seçilmiştir. Son olarak, tahmin edilen model için optimize edici olarak Adam algoritması ve kayıp fonksiyonu olarak ortalama kare hatası seçilmiştir.

Veriler ve gerekli eğitim algoritmaları hazırlandıktan sonra, çalışmanın ilk aşaması olan, sinir ağı tabanlı sistem tanımlama çalışmalarının farklı feature setleri ile eğitilip karşılaştırılması gerçekleştirilmiştir. İlk olarak ilgili modeller, temel girdi setini tanımlayan parametreleri oluşturan set ile eğitilmiştir. Bu basit sette, ilgili moment ve kuvvet katsayısını efektik olarak etkileyen euler açıları, hızlar, hücum açısı, kayma açısı ve kontrol yüzeyi açılarını içermektedir. İkinci olarak ise üstel ve birleşik parametreler eklenerek başka bir kompleks feature seti üretilmiştir. Bu parametreler, uçuş dinamiği bilgisi kullanılarak elde edilmiştir. Örnek olarak elevator açısının etkinliği, uçağın hücum açısına ve Mach sayısına bağlı değişmektedir. Bu nedenle, elevator – hücum açısı ve elevator – Mach birleşik parametreleri yeni özellik setine eklenmiştir. Her özellik setinin oluşturulmasından sonra modeller aynı uçuş test verileriyle eğitilmiştir. Son olarak modeller doğrulama çalışmaları için ayrılmış uçuş test manevralarıyla karşılaştırılmıştır. Bu çalışmada farklı feature setlerinin kullanılmasının temel amacı, doğrusal olmayan bölgelerde uçuş modelinin doğruluğunu arttırmaktır. Bu amaçla eğitimde giriş setlerini doğrudan kullanmak yerine, uçuş dinamikleri ve aerodinamik bilgisi kullanılarak, girişlerin farklı üsleri ve birleşik durumları özellik setine eklenmiştir. Böylece, çözüm için eğitim sırasında modele farklı giriş kombinasyonları sağlanmıştır.

Çalışmanın ikinci kısmında ise uçuş testlerinin maliyetleri konusuna da odaklanılmıştır, bu sistem tanımlama çalışmalarının efektif bir şekilde gerçekleştirilebilmesi için kritik öneme sahip bir konu olmaktadır. Uçuş test manevralarının ve girdilerinin optimize edilmesi maliyet etkinlik için gerekli olmaktadır. Genellikle performans ve stabilite analizleri izole bölgelerde yapılmaktadır, bu nedenle, bu çalışmalar kapsamında toplanan uçuş verileri tüm uçuş zarfını yansıtacak yeterli dağılıma sahip olamamaktadır. Diğer durumlarda ise, uçuş zarfı çok yüksek sıklıkta taranmaktadır ve bu da çok yüksek maliyetlere yol açmaktadır. Bu çalışmanın ikinci kısmı, farklı uçuş test manevraları ve zarfları kullanılarak sistem tanımlaması yapılırken veri miktarının model doğruluğundaki değişikliklerine odaklanmaktadır. Modeller yalnızca doğrusal olmayan bölgeden, yalnızca doğrusal bölgeden ve tüm uçuş zarfından elde edilen verilerle, her bir senaryoda farklı veri yoğunluklarıyla eğitilmiştir. Toplamda altı farklı durum test edilip karşılaştırılmıştır.

Sonuç olarak bu tez kapsamında, çeşitli uçuş koşulları altında uçak dinamiklerinin kapsamlı analizleri yapılmış ve aerodinamik davranışların yakalanmasında basit ve karmaşık özellik setlerinin etkinliği incelenmiştir. Sonuçlar, farklı uçuş zarflarında tahmin modellerinin performansı hakkında önemli içgörüler sunmaktadır.

İlk olarak, Short Period uçuşlarıyla yapılan longitudinal aerodinamik parametrelerin analizi için, hem basit hem de karmaşık özellik setlerinin lineer uçuş zarfında birbirleriyle benzer ve kabul edilebilir sonuçlar verdiği gözlenmiştir. Ancak uçuş koşulları zarfın uç noktalarına yaklaştıkça non-lineer özelliklerin belirginleştiği ve kompleks feature setinin uçuş verisine çok daha uyumlu olduğu görülmüştür. Bu durum daha yüksek doğruluk için özellik setine karmaşık parametrelerin dahil edilmesinin gerekliliğini göstermektedir. Bu şekilde farklı koşullar altında aerodinamik davranışları doğru bir şekilde temsil eden tahmin modelleri geliştirilirken, tüm uçuş zarfını kapsayacak parametrelerin dikkate alınmasının önemi ortaya çıkmaktadır.

İkinci olarak, Dutch Roll ve Bank-to-Bank manevralarının incelenmesinde benzer eğilimler ortaya çıkmış, basit özellik setlerinin lineer uçuş zarfında yeterli performans gösterdiği ancak stall açılarına yaklaştıkça ve transonik bölgelerde lineer olmayan etkileri yakalamakta sıkıntı yaşadığı görülmüştür. Böylece, kompleks özellik setlerinin, bu zorlu uçuş senaryolarında daha yüksek doğruluk elde etmek için gerekli olduğu ortaya çıkmaktadır.

Tezin ikinci aşamasında ise, farklı uçuş zarflarında eğitilmiş olan modellerin uçuş testi sonuçları karşılaştırmaları yapılmıştır. Eğitilen modellerin performansını göstermek için uçuş zarfının lineer ve lineer olmayan bölgelerinden uçuş test noktaları seçilmiştir. Sonrasında ise eğitilen modellerin her iki koşul altındaki performansı incelenmiştir. Tüm senaryolar incelendiğinde, kayıp fonksiyon değerleriyle ilgili yapılan karşılaştırma analizleri, modellerin eğitildiği uçuş test bölgelerinin uçak modelinin doğruluğu üzerindeki önemini göstermiştir. Sonuçlar, tüm uçuş zarfı verileriyle eğitilen modellerin üstün başarısını göstermektedir. Tüm uçuş zarfı verileriyle eğitilen modellerin, lineer veya lineer olmayan bölgelerin izole verileriyle eğitilenlere göre sürekli olarak daha iyi performans sergilediği görülmüş olup doğru tahmin modelleri için kapsamlı veri kapsamının önemini göstermektedir.

Sonuç olarak bu tez, uçak dinamikleri için tahmin modellerinin geliştirilmesine değerli içgörüler sağlamaktadır ve çeşitli uçuş koşulları altında aerodinamik davranışları doğru bir şekilde temsil etmede karmaşık özellik setlerinin ve kapsamlı eğitim verilerinin kritik rolünü göstermektedir. Bu bulgular, uçak tasarımı, uçuş simülasyonu ve kontrol sistemi geliştirme konusunda iyileştirilmiş performans ve güvenlik sağlayarak havacılık alanında önemli katkılar sunmaktadır.

1. INTRODUCTION

1.1 System Identification

System identification is the mathematical processes of defining a system in a adequate form based on its observed behaviors (Jategaonkar, 2006). Fundamentally, the main objective of the system identification can be framed as an optimization problem, aiming to discover a set of parameters of a model and that minimize the prediction error between the observed data and the model's output (Behera and Rana, 2014). In the process of aircraft developments, system identification plays a crucial role because the results of the system identification are creation of models that are sufficiently precise and validated mathematical models of the aircraft (Jategaonkar, 2006).

The general representation of the system identification is shown as Figure 1.1 by Behera and Rana (2014).

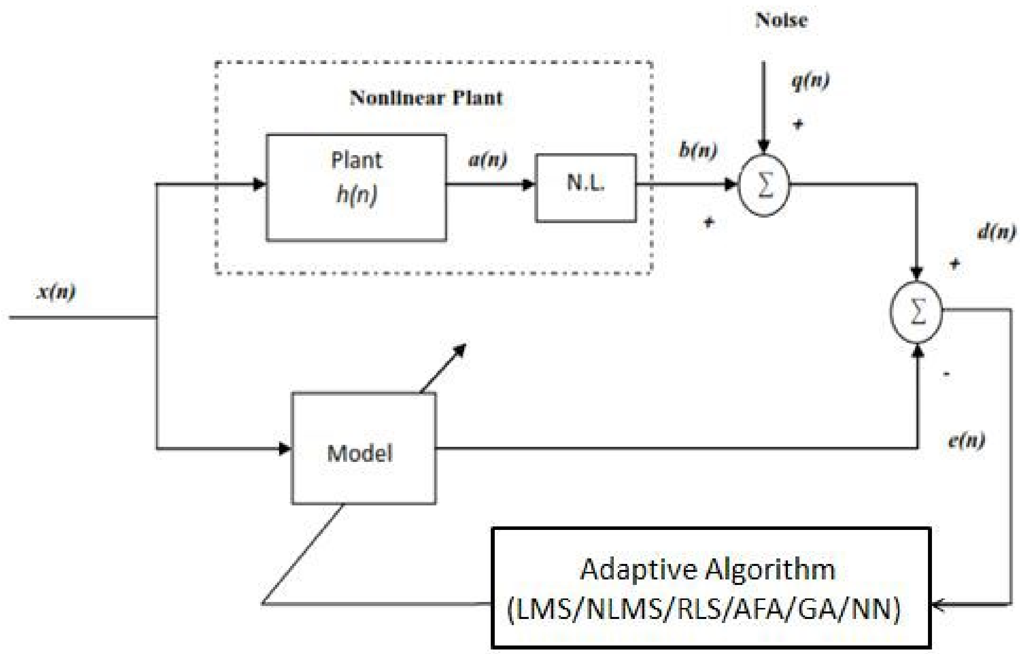

Figure 1.1 : General flow of the system identification (Behera and Rana, 2014).

The adaptive algorithm, non-linear plant, model sections can be altered in their self, however the general logic flow of the work of minimizing the difference between representative model and plant stays same.

1.2 Literature Review

1.2.1 Necessity of aircraft modeling and high-fidelity requirement

The process of designing an aircraft is highly complex and requires careful consideration of various flight characteristics, performance metrics, stability, control, analyses. In order to realize these studies, multiple tools are needed for flight science analyses. One of the most preferred tools used are flight dynamics models, which brings the ability of testable environments for the aircraft design studies (Dubois, 2018). When the significant cost associated with producing an aircraft and conducting these analyses are considere, flight dynamics models play a crucial role. These models are essential not only for the development of simulators but also for conducting accident analyses and improving aircraft design (Stevens et al., 2003).

The most important aspect of a model is its effectiveness in fulfilling its intended purpose (Morelli and Klein, 2006). The accuracy of the model is particularly critical in certain scenarios, such as the design of flight control systems, the final stages of aircraft design, and efforts to enhance aircraft design.

1.2.2 Importance of system identification

The primary goal of System Identification is to develop a defining structure for a system based on observations. System Identification is excellent at revealing the principal characteristics and underlying dynamics of a system from observation data. This approach is applied in various scientific fields, including medical research, civil engineering, economics, and flight vehicles (Jategaonkar, 2006). In this thesis, the focus will be on the identification of flight vehicles.

To use aircraft flight dynamics models effectively in various stages of design and improvement, the model must accurately represent the aircraft based on flight test data. Various inconsistencies and non-linearities are likely to be encountered in aircraft models. Particularly for flight control system designs and handling quality analyses, the aircraft model needs to be of high fidelity (Tischler and Remple, 2012).

1.2.3 Information on time and frequency domain identification techniques

The focal point of System Identification studies often revolves around two fundamental methodologies: time domain and frequency domain identification techniques. Time domain methodologies primarily center on measuring an aircraft's response over a defined time interval, whereas frequency domain approaches focus on the aircraft's response to periodic inputs. The principal aim of frequency domain methodologies is to characterize system dynamics, while time domain methodologies concentrate on producing both linear and non-linear models (Tischler and Remple, 2012).

Numerous studies delve into both time and frequency domains, sometimes viewing them as competing methodologies (Millidere, 2021). However, the overarching conclusion is that both time and frequency domain approaches are theoretically and informationally equivalent. Transitioning data between these domains does not alter the informational content, enabling tasks achievable in one domain to be accomplished in the other. Nonetheless, in practical terms, certain information may be more readily accessible in one domain over the other (Schoukens et al, 2004).

However, for this study, the focus lies on time domain system identification methodologies. This preference stems from the observation that aircraft modeling developed within a state-space representation in the time domain tends to offer greater accuracy for physical environments. Therefore, this study centers on time domain system identification methodologies.

1.2.4 Information on EEM, OEM, FEM and ANN methodologies

There are many different methodologies within time-domain system identification. Mainly, time-domain-based system identification studies focus on four main methodologies: Output Error Method (OEM), Filter Error Method (FEM), Equation Error Method (EEM), and Artificial Neural Network (ANN).

The Output Error Methodology involves conducting system identification studies by iteratively improving the parameters of the model to minimize the error between flight data and model outputs (Jategaonkar, 2006). Many methodologies employ a similar approach, where aircraft states such as angle of attack and angular rates are considered in the minimizing functions (Murat Millidere, 2021). This concept of system identification is commonly selected in the early stages of such studies, and its usage remains prevalent with periodic updates made to the solver algorithm (Jategaonkar, 2006). Therefore, this methodology continues to be one of the main methodologies used in system identification studies (Millidere et al, 2019; Morelli and Klein, 2004).

The Filter Error Methodology's algorithm is very similar to the output error method and is defined as logical extensions of the output error methodology to account for turbulence and airflow unsteadiness (Jategaonkar, 2006). This methodology is widely used to improve the poor performance of the output error method under turbulent and noisy conditions (Grauer and Morelli, 2015; Patel, 2007).

The Equation Error Methodology is another widely used system identification technique. This methodology also focuses on minimizing the cost function in a system of input-output coupling; however, the cost function is not focused on probability. The cost function is built on matrix algebraic operations for momentarily discrete measurements (Jategaonkar, 2006). Therefore, it is widely used for its mathematical simplicity (Liu et al, 2019; Millidere et al, 2021; Paris and Bonner, 2004).

Artificial Neural Network identification methodologies are becoming increasingly relevant in recent studies (Zheng and Xie, 2018). Especially with developing technology and the ability to obtain large amounts of data, neural network methodologies' high processing capabilities make them more useful in current studies (Andersson et al, 2019; Chauhan and Singh, 2017; Harris et al, 2016; Kirkpatrick et al, 2013; Roudbari and Saghafi, 2016; Zheng and Xie, 2018;).

1.2.5 Current ANN related studies and their conditions

Generating aircraft models presents numerous challenging obstacles, particularly when aiming for high-fidelity representation. One of the most critical challenges involves achieving fidelity in the non-linear flight region. Various methodologies have been explored to address this issue, including estimating aircraft aerodynamics near stall conditions that comes with high angle of attack (Bagherzadeh, 2018) and understanding aircraft behavior in transonic regions (Roudbari and Saghafi, 2016). In some instances, extensive wind tunnel and computational fluid dynamics analyses are conducted to cover these regions. However, these methodologies either consume significant time and budget resources or do not rely on actual flight data, leaving room for uncertainties that may impact the accuracy of results. Therefore, the high data processing capability of neural network methodology is increasingly recognized as crucial for overcoming these challenges (Zheng and Xie, 2018).

1.2.6 Non-linear region identification issue definition

One of the primary challenges associated with artificial neural network (ANN) techniques is their predominant use for identifying specific flight envelope regions. Consequently, models generated through simplistic ANN methodologies are not expected to comprehensively cover the entire flight envelope (Roudbari and Saghafi, 2016). Numerous studies and approaches are dedicated to addressing this issue. Some methodologies focus on blending different structures of ANN methodologies. For instance, Chauhan and Singh (2017) have achieved favorable results using the Feed Forward Neural Network (FFNN) methodology. Andersson et al. (2019) analyses employing the temporal convolutional network (TCN) have demonstrated promising outcomes with limited flight data. Additionally, studies by Bansal et al. (2016) and Putra Amiruddin et al. (2019) using recurrent neural networks have shown commendable performance under nonlinear conditions. Recurrent neural network methodology also tested by Moreira and Soares (2003), Kumar et al. (2006) with promising results. Hybrid structures combining convolutional and recurrent neural networks have also yielded promising results (Echevarría Corrales, 2021). In this study, the effects of utilizing different feature sets and flight envelopes in artificial neural networks are compared.

1.2.7 Thesis outline

Chapter 2: Flight Data Production

At this chapter an overview of flight data production processes is described. Aircraft models utilized in flight tests, the observation of flight test data, and essential information regarding the flight test envelope topics are investigated. Additionally, insights how essential of the scatter of flight data for system identification and validation studies.

Chapter 3: Data Pre-processing Studies

This section details the complication and necessity of data pre-processing. This section begins by examining the observation of Mass-Inertia and Thrust data throughout flight tests, including insights into engine and mass block details. Subsequently, the calculations of total force and moment coefficients derived from flight test data are detaily elaborated.

Chapter 4: Deep Learning System Identification

This chapter provides a comprehensive understanding of substructures of the deep learning section of the system identification studies. The data structure constructed for estimations and the utilization of the TensorFlow library is descrived in this part. Moreover, introduction about various feature sets that used in the estimation studies are provided.

Chapter 5: Comparison of Feature Sets

Here, the thesis compares different feature sets concerning the fidelity of system identification. It starts by explaining simplistic and complex feature sets. It then describes the flight test envelope utilized in identification studies. Lastly, it showcases force and moment comparisons between simplistic and complex feature sets based on flight data.

Chapter 6: Comparison of Flight Regions

This chapter compares the usage of different flight regions' test data in system identification studies. It elucidates flight test envelopes and case definitions before delving into a comparison of the fidelity of each case. Validation tests for special regions conclude the chapter.

2. DATA PRODUCTION

2.1 Simulator Model

This chapter focuses on the generation of necessary data. It begins by describing the 6-degree-of-freedom (6DOF) aircraft simulation model used for the flight test maneuvers. Using simulator based flight data is a cruically helpful practice for development of the system identificaiton studies (Çetin, 2018). Detailed insights into the flight test survey and the input schemes employed during these maneuvers are provided. Finally, the chapter offers brief information on the measured parameters and the integration of combined data.

2.1.1 Generic non-linear F-16 aircraft model

This chapter outlines the creation of the 6-degree-of-freedom (6DOF) aircraft model, utilizing the F-16 aircraft model developed by Russel (2003) as the foundation. The model encompasses both low and high-fidelity settings based on studies by Stevens et al. (2003) and Nguyen (1979). Typically employed for controller design studies and simulations, the model chosen for this study prioritizes high fidelity to analyze both linear and non-linear regions effectively.

The primary distinction between the two fidelity models lies in their aerodynamic databases. The low fidelity F-16 model's database covers an angle of attack range from -10 to 45 degrees and a sideslip angle range from -30 to 30 degrees. In contrast, the high fidelity F-16 model's aerodynamic database spans an angle of attack range from -20 to 90 degrees and a sideslip angle range from -30 to 30 degrees.

The general structure of the aircraft model is given at Figure 2.1

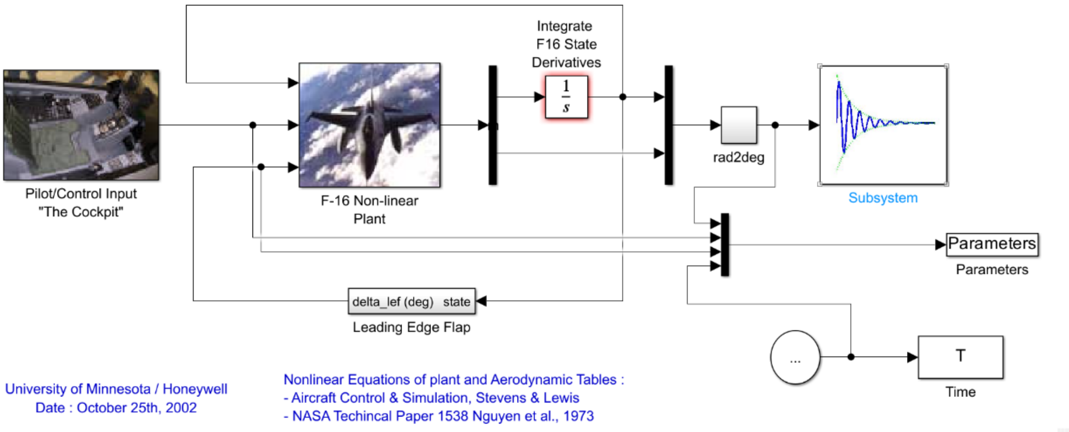

Figure 2.1 : 6DOF Model Structure (Russel, 2003).

2.1.2 Input block manipulation

In this chapter, the manipulation and excitation of inputs in the high-fidelity aircraft model are discussed. The high-fidelity F16 model offers four manually manipulable inputs, namely aileron, rudder, elevator, and thrust parameters. Additionally, it features a leading-edge flap (LEF) control surface, which functions based on angle of attack and dynamic pressure.

To facilitate the execution of necessary maneuvers in the flight model, the input block is modified to enable control via a Joystick controller. Initially, the trim calculation codes are protected to ensure stability during the trim process, during which joystick input features are disabled. Once the trim process is completed, the joystick controller block is activated, with joystick inputs integrated into the aircraft model by being added to the trim outputs. It is essential to maintain trim conditions for the first 5 to 10 seconds to enable the aircraft to sustain its trim condition even when there is zero input from the joystick.

Subsequently, joystick inputs are introduced to the system in real-time, allowing maneuvers to be flown according to the pilot's inputs. Finally, a recording block is incorporated to capture the control inputs for use in the system identification process.

The structure of the input block is outlined given at Figure 2.2.

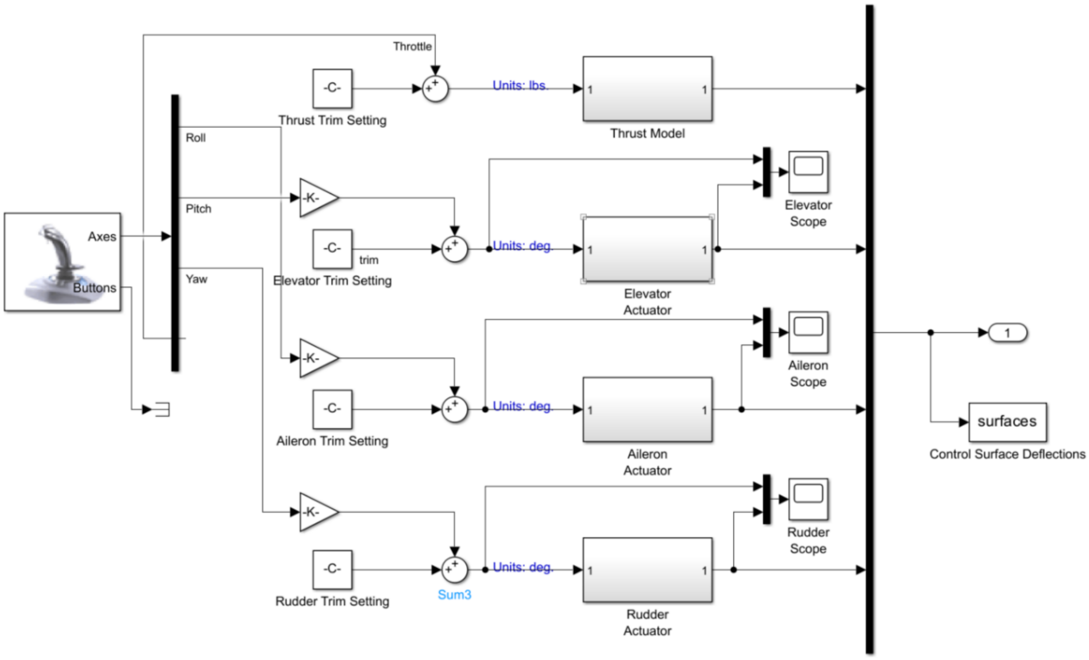

Figure 2.2 : Input block for integrating pilot inputs (Russel, 2003).

2.1.3 Data observation block

In order to use the flight test data on the system identification, the defining parameters of the aircraft must be recorded. Therefore, a block for recording necessary parameters of the system identification is added to the 6DOF aircraft model. In this block, states, control surfaces and atmospheric information in the flight tests are recorded in real time. With this block is correlation between inputs and outputs at each discrete time frame is observed.

2.2 Flight Test Survey

2.2.1 Decided flight test maneuvers

This chapter discusses the selection of maneuvers to estimate longitudinal, lateral, and directional force and moment coefficients. For estimating longitudinal coefficients, a short period maneuver is chosen, emphasizing the aircraft's longitudinal characteristics across various angles of attack. The trim section at the beginning of the flight test is instrumental in estimating static force and moment coefficients, as well as control surface coupling. Additionally, the aircraft's dynamic response to elevator inputs provides valuable insights into pitch rate-related coefficients and control surface effectiveness.

For lateral and directional coefficients, Bank to Bank and Dutch Roll maneuvers are selected. Bank to Bank maneuvers primarily provide information about the Roll Moment coefficient, while Dutch Roll maneuvers offer data about Yaw Moment and Side Force Coefficients. During Bank-to-Bank maneuvers, dynamic and static Roll Moment coefficient parameters are identified through the application of Aileron input to the dynamic system. Different magnitudes of roll accelerations and observations of roll angles are recorded when Aileron input is applied at various flight conditions. Said flight test maneuvers are shown at the Figure 2.3 and Figure 2.4

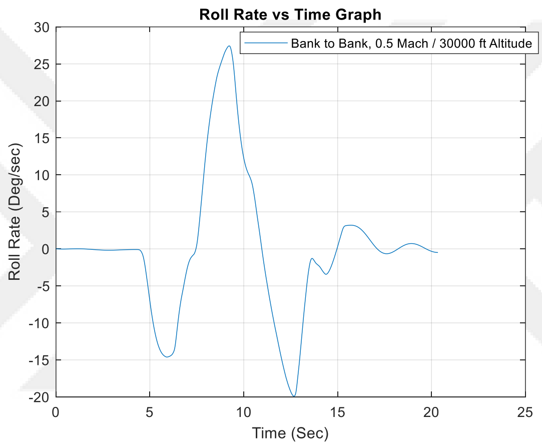

Figure 2.3 : Bank to Bank maneuver, low amplitude input.

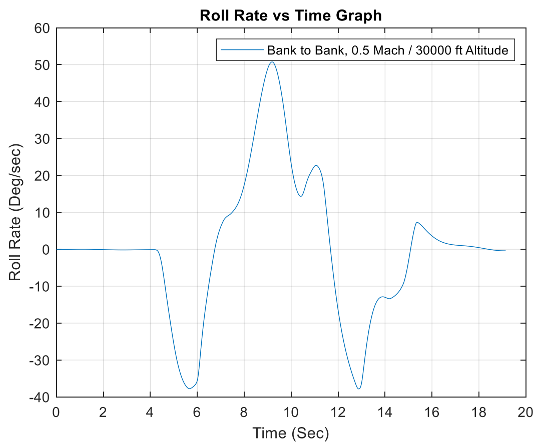

Figure 2.4 : Input Bank to Bank maneuver, high amplitude input.

With this observation, System Identification algorithm will have many different points of parameter to focus on solving stage. Therefore, the database points will be more widely dispersed. Thus, a larger area will be scanned and data accuracy will increase. Different magnitude of Roll Angles are shown in the Figure 2.5 and Figure 2.6

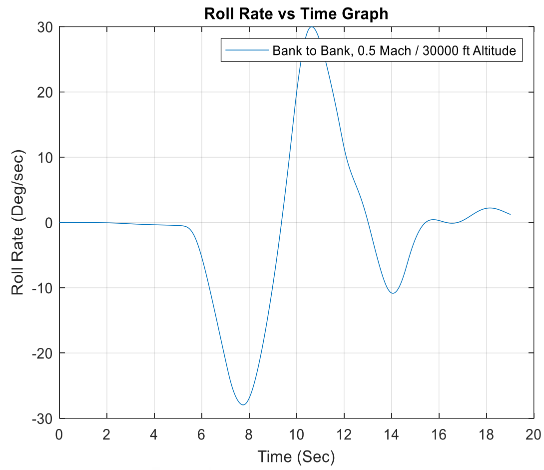

Figure 2.5 : Bank to Bank maneuver, low bank angle.

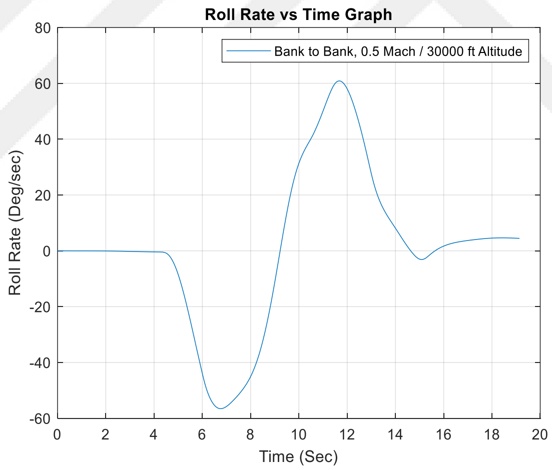

Figure 2.6 : Bank to Bank maneuver, low bank angle.

With the Dutch Roll maneuvers, targeted areas are Side Force and Yaw Moment Coefficients. To excite the Dutch Roll maneuver, 1 – 2 – 1 Rudder input is applied. After that Sideslip Angle change is observed. In order to calculate the necessary magnitude of Rudder angle, Sideslip Angles are observed to be change in between +-5 and +-10 degrees. With this maneuver, effects of different range of Sideslip angle, Rudder and yaw rate on aerodynamic parameters observed. Observation of the low and high side slip angle dutch roll maneuvers can be seen at the Figure 2.7 and 2.8

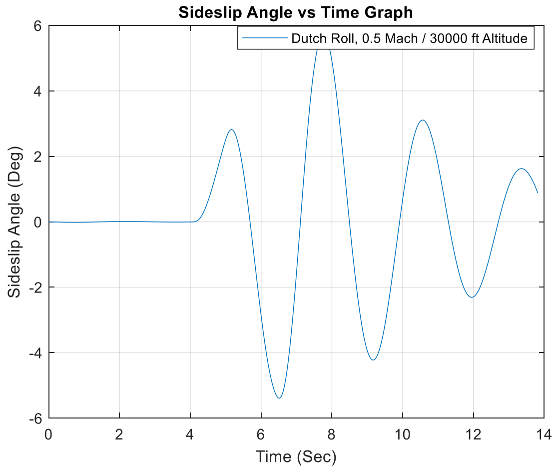

Figure 2.7 : Dutch Roll maneuver, low sideslip angle change.

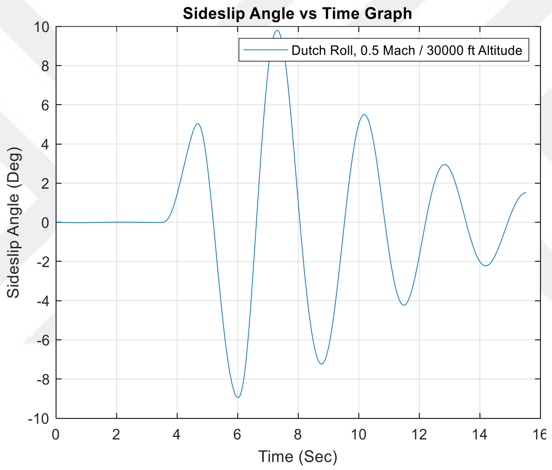

Figure 2.8 : Dutch Roll maneuver, high sideslip angle change.

With this data, main parameters of Side Force and Yaw Moment coefficients are observed. After that the estimation of these force and moment coefficients are made.

There are some important parameters are needed to be considered in estimation of the lateral and directional force and moment coefficients. Firstly, there are coupled effects between yaw moment and roll moment coefficients. Dynamic parameters of each coefficient are effective on one another. Secondly, Aileron and Rudder control surfaces are both affective on roll and yaw moment coefficients. Therefore, in order to calculate the coupled effects of the aerodynamic parameters, Dutch Roll maneuvers also has to be examined in roll moment coefficients and bank to bank maneuvers also should be examined in yaw moment coefficients. With this way, complexities of the lateral and directional coefficients are observed.

2.2.2 Flight test envelope

In order to estimate aerodynamic parameters of the f16 aircraft, various different flight test conditions are selected. Altitude range is taken as between 10000 ft and 30000ft. Mach range is taken as 0.3 mach to 0.8 mach at each 10000ft increment. Usually between 0.4 mach to 0.6-0.7 mach is considerable as linear flight region for f16's aerodynamic qualities. Also, the parameters of the atmosphere are linear between 10000ft and 30000ft. Therefore, in order to distribute test points at linear and nonlinear regions evenly, test points at linear region of the 20000 ft are reduced and at the test pointes at the nonlinear ends of the flight envelope is increased.

2.2.2.1 Flight tests for longitudinal parameters

26 Short Period maneuvers are conducted for system identification studies

22 of them is used at prediction stage

4 flight test points are used at validation stage.

Combined flight test points are shown at the Figure 2.9:

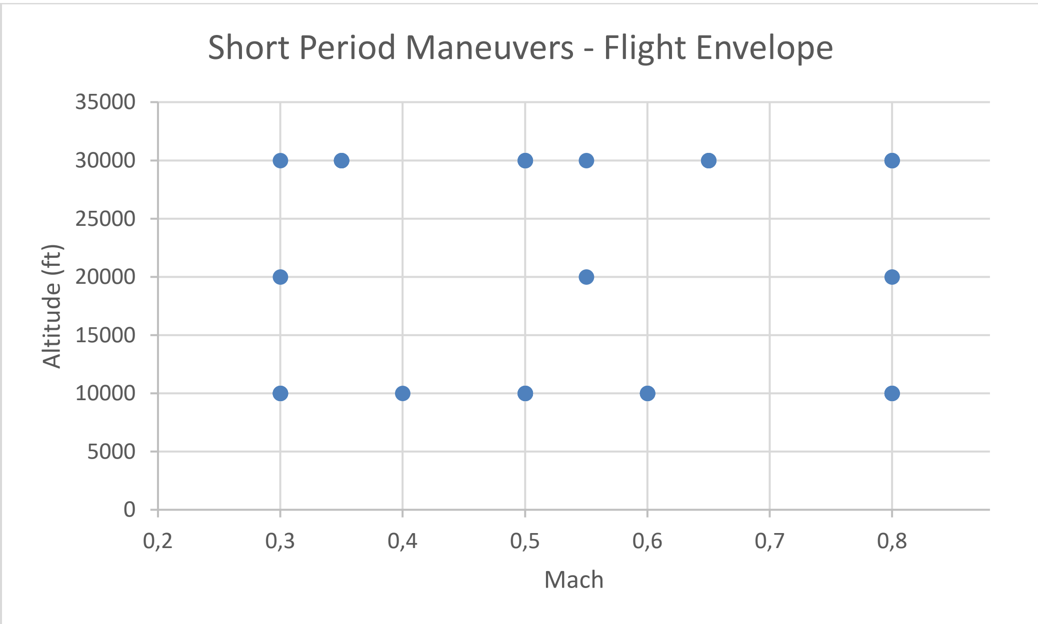

Figure 2.9 : Flight envelope for Short Period test maneuvers.

2.2.2.2 Flight tests for lateral parameters

53 Bank to Bank maneuvers are conducted for system identification

49 of them is used at prediction stage

4 flight test points are used at validation stage.

Combined flight test points are shown at the Figure 2.10:

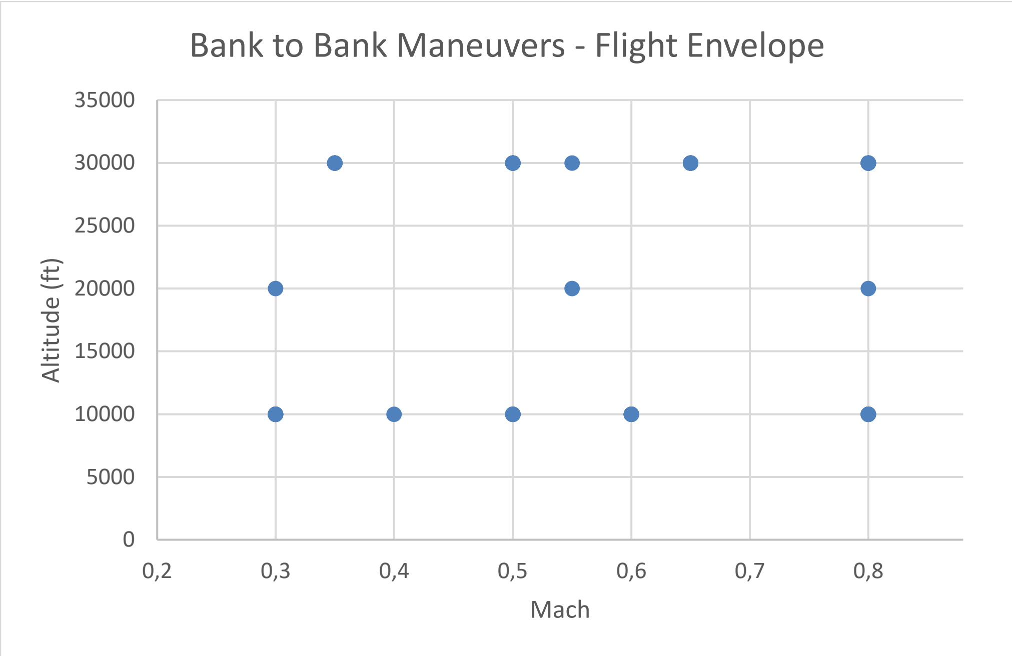

Figure 2.10 : Flight envelope for Bank-to-Bank test maneuvers.

2.2.2.3 Flight tests for directional parameters

49 Dutch Roll maneuvers are conducted for system identification

45 of them is used at prediction stage

4 flight test points are used at validation stage.

Combined flight test points are shown as:

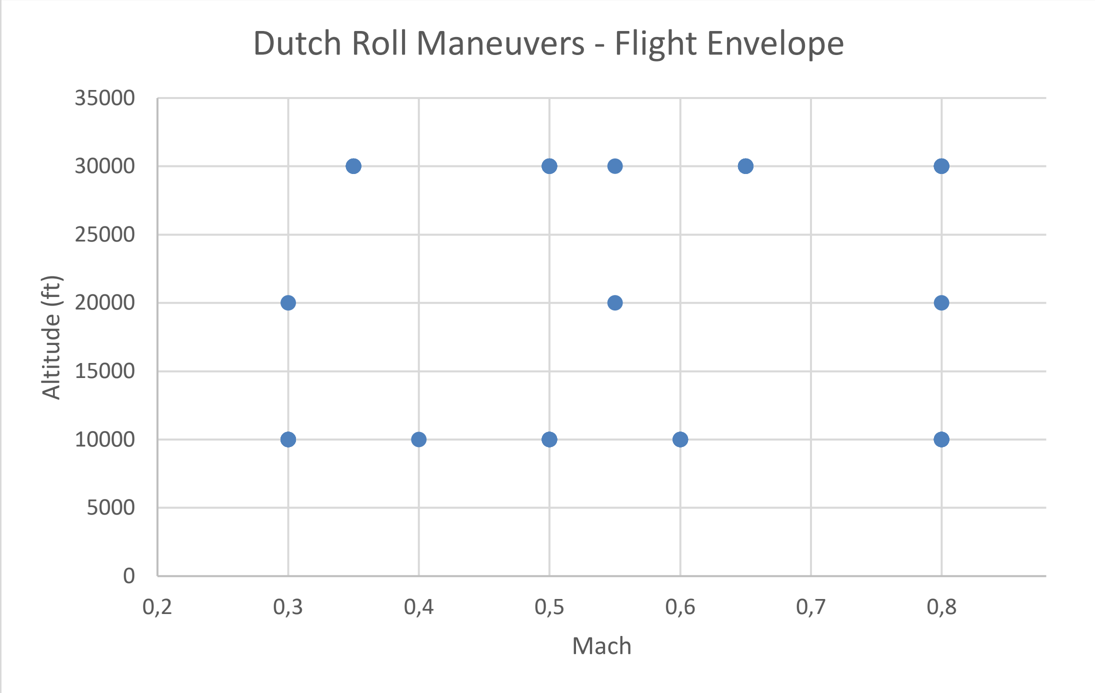

Figure 2.11 : Flight envelope for Dutch Roll test maneuvers.

2.2.3 Maneuver requirements and input design

To be able to thoroughly estimate the flight test data, it's crucial to use a variety of input excitation to the aircraft. With using pre-decided requirements for the flight test input, collection of the higher fidelity and diverse data is achieved, this leads to making detailed observation and analysis possible. To aid this process, it's important to simulate specific aircraft characteristics across a broad spectrum of aircraft states. This approach ensures that all necessary data is gathered, offering a solid basis for assessing the aircraft's performance and flight dynamics in different flight conditions.

2.2.3.1 Elevator 3-2-1-1 input for short period maneuver

To achieve a thorough analysis of the aircraft's performance and flight dynamics, it is necessary to excite the Angle of Attack (AoA) within a range of ±3 to 5 degrees from calculated trim angle. This approach aims to generate a sufficient and varied amount of pitch rate data while ensuring the AoA is scattered appropriately within the desired flight envelope. By stimulating these parameters, a comprehensive dataset can be collected, gives opportunity to a deeper understanding of the aircraft's aerodynamic characteristics and stability.

The 3-2-1-1 input desing was selected for this study due to the specific characteristics of the F-16 aircraft. The flight controller, designed to prevent oscillations, makes manual excitation of the aircraft's short-period dynamics necessary. This manual intervention is crucial for accurately capturing the data needed to analyze the F-16's performance and behavior under various conditions. The graphs of the elevator angle, angle of attack and pitch rate given at figure 2.12, 2.13 and 2.14 in order.

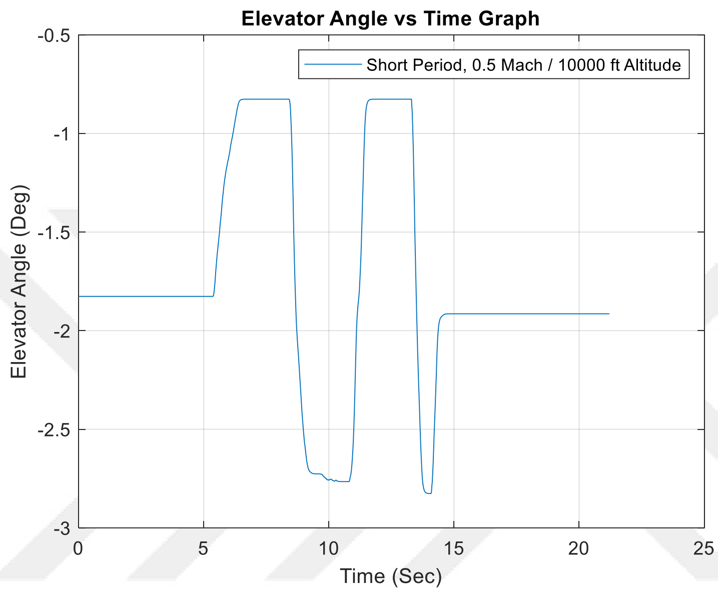

Figure 2.12 : Elevator angle vs time at Short Period maneuver.

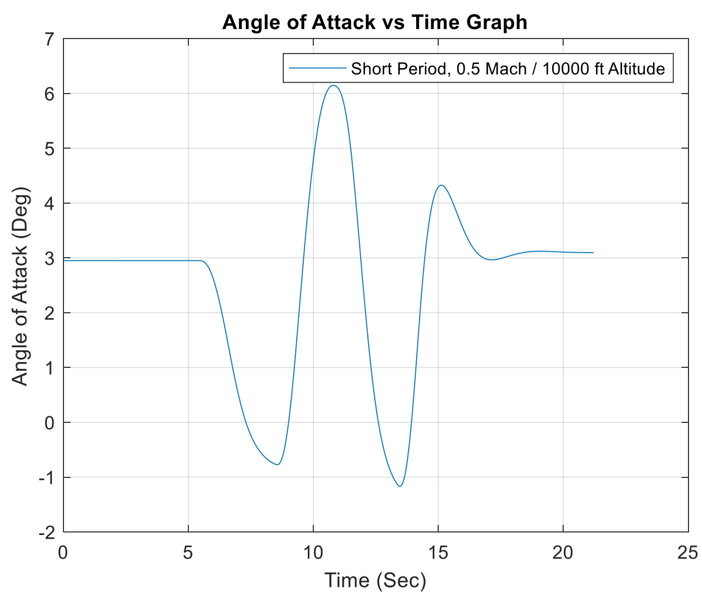

Figure 2.13 : Angle of attack vs time at Short Period maneuver.

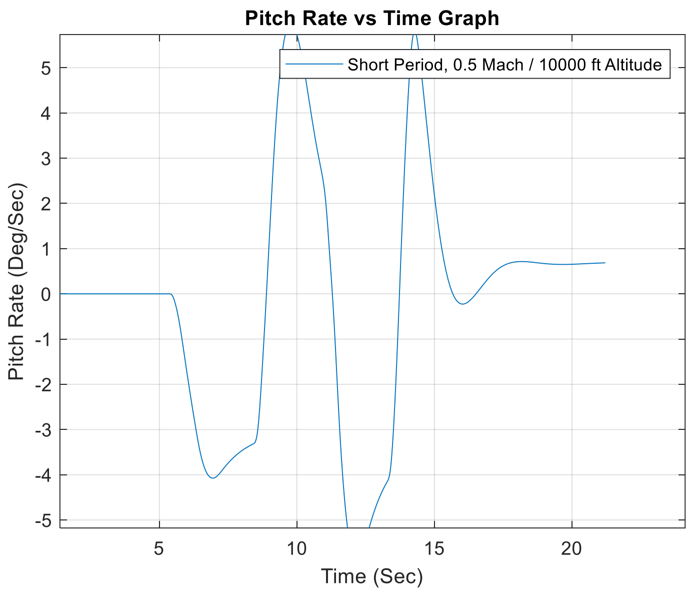

Figure 2.14 : Pitch rate vs time at Short Period maneuver.

2.2.3.2 Aileron 1-2-1 input for bank to bank maneuver

When it comes to the maneuver of Bank to Bank, main concern is to excite necessity bank angles within the given time frame. Therefore, the focus was on the exciting ±30 and ±60 bank angles in 1 second. Thus, aircraft will be excited in two different roll rates. This is crucial for to understand the effect of roll rate on both roll and yaw moment coefficients. The graphs of the aileron angle, bank angle and roll rate given at figure 2.15, 2.16 and 2.17 in order.

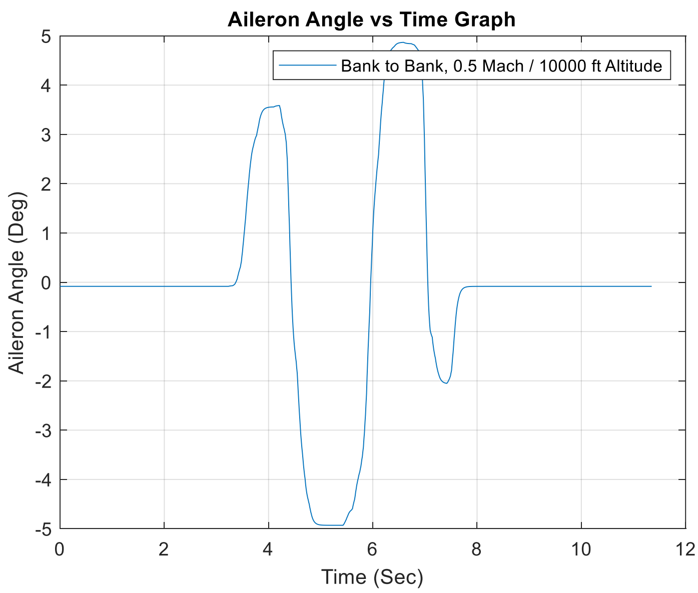

Figure 2.15 : Aileron angle vs time at Bank-to-Bank maneuver.

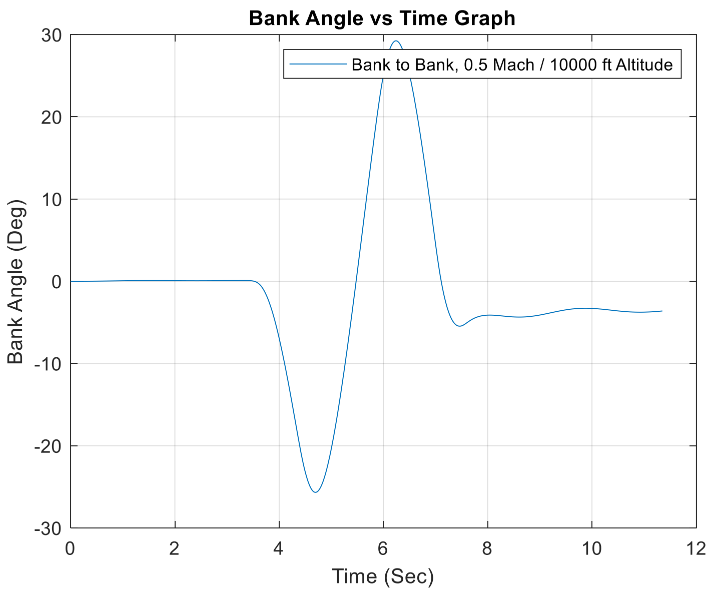

Figure 2.16 : Bank angle vs time at Bank-to-Bank maneuver.

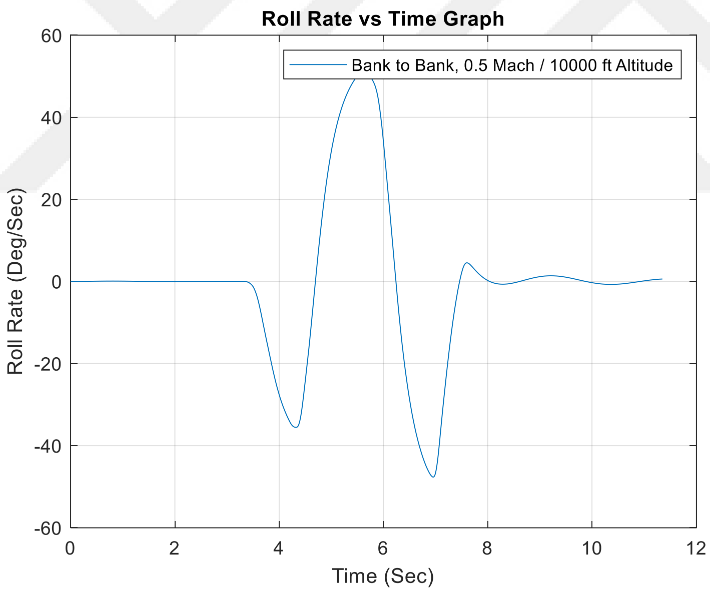

Figure 2.17 : Roll Rate vs time at Bank-to-Bank maneuver.

2.2.3.3 Rudder 1-2-1 input for dutch roll maneuver

At the Dutch Roll maneuvers, similar to the Bank to Bank maneuver, achieveing two different sideslip angle and yaw rate was the main focus. Therefore, maneuvers are conducted with two different magnitude of Rudder input. The graphs of the rudder angle, sideslip angle and yaw rate given at figure 2.15, 2.16 and 2.17.

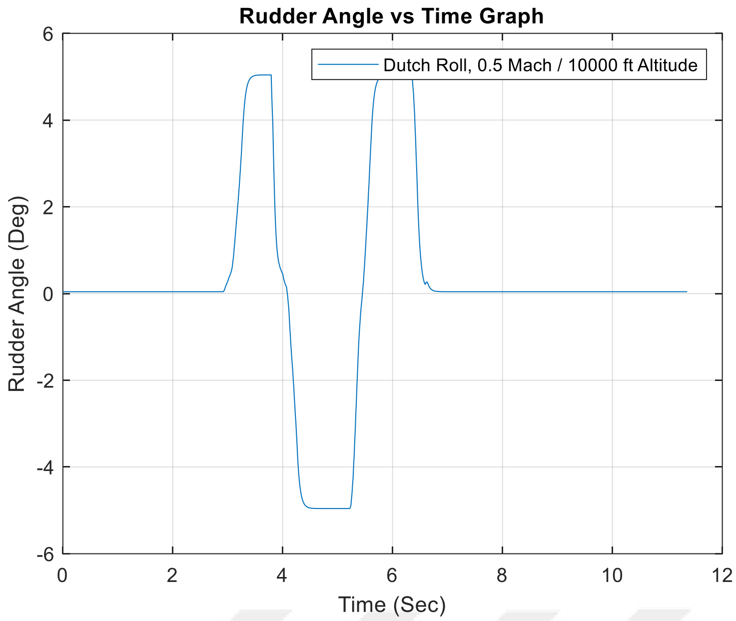

Figure 2.18 : Roll Rate vs time at Bank-to-Bank maneuver.

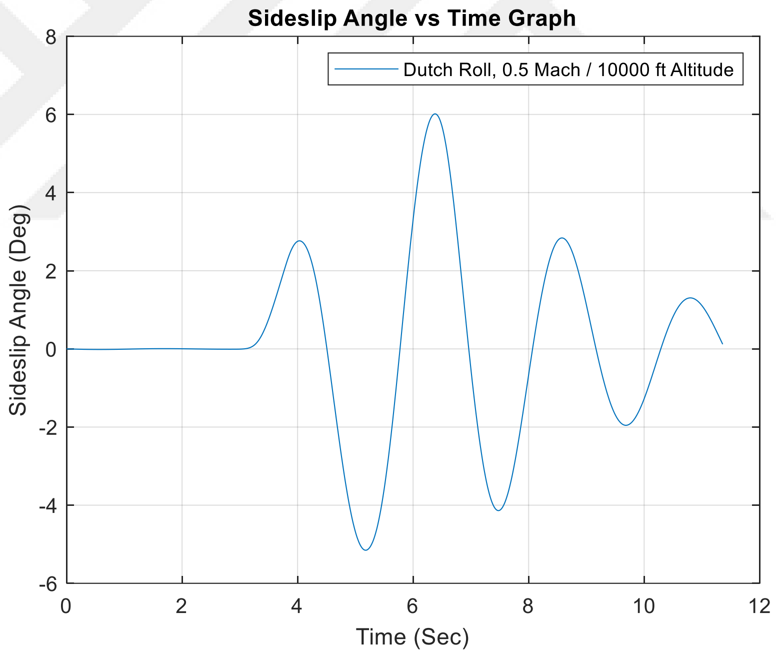

Figure 2.19 : Roll Rate vs time at Bank-to-Bank maneuver.

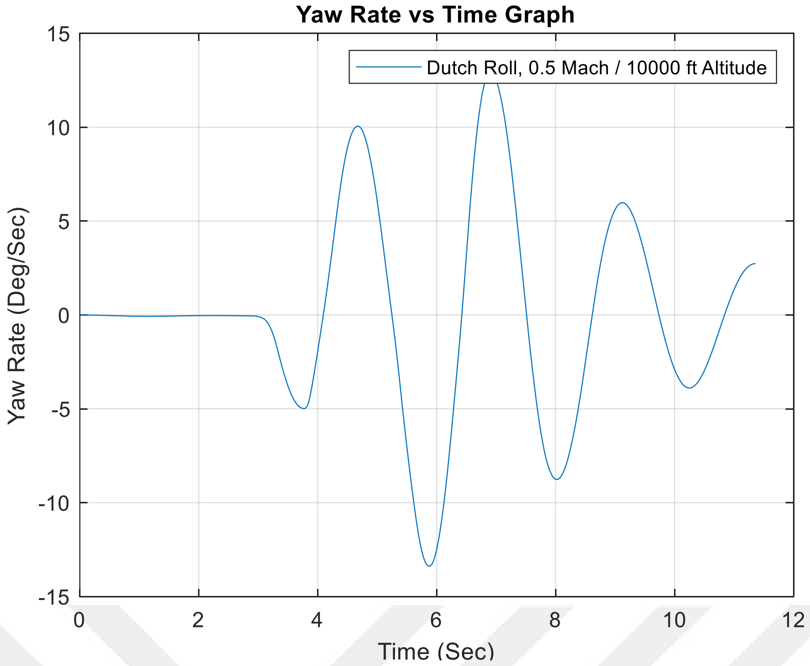

Figure 2.20 : Roll Rate vs time at Bank-to-Bank maneuver.

2.3 Flight Test Data

2.3.1 Measured parameters

Initially, aerodynamic state variables such as Alpha (angle of attack) and Beta (sideslip angle), which are critical for understanding airflow characteristics, are added to the observation block to be measured. Following this, true airspeed and Mach number, essential for determining the aircraft's performance across different flight regimes, are added. Subsequently, control surfaces, including the elevator, aileron, rudder, leading edge flaps (LEF), and throttle, are monitored to assess their effectiveness and response during various maneuvers. Linear accelerations (Ax, Ay, Az) and angular accelerations (P, Q, R, $\dot{P}$, $\dot{Q}$, $\dot{R}$), which provide insights into the aircraft's dynamic response to control inputs and external disturbances, are also included in the observation block. Finally, measurements of Euler angles (Phi, Theta, Psi) are utilized to describe the aircraft's orientation in space, which is vital for correlating aerodynamic forces and moments with the aircraft's attitude. These combined parameters enable a detailed and accurate identification of the aircraft's aerodynamic characteristics, crucial for design improvement, control, and performance optimization.

2.3.2 Flight test criteria

For each flight test maneuver, there are variety of different requirements need to be met. The aim to have these requirements is having a well-defined database. In the system identification studies, the algorithm’s estimation process depends solely on the data, therefore predictions will be acceptable only in the data range that provided to the system. If the observed flight test data does not cover enough flight envelope that aircraft model is wanted, the results in the uncovered region have risk of the low fidelity. Non-linear region analyses might diverge, unexpected tendencies can be observed from the aircraft model. Therefore, many different criteria are determined for Short Period, Dutch Roll and Bank to Bank maneuvers. They are shown at the table 2.1

Table 2.1 : Requirements for flight test maneuvers.

Maneuers	Inputs	AoA Desired	AoA Acceptable	AoS Desired	AoS Acceptable	Euler Angles Desired	Euler Angles Acceptable
Short Period	3-2-1-1 Pitch Stick Input	±5 Alpha	±8 Alpha	-	-	-	-
Dutch Roll	1-2-1 Pedal Input	-	-	±5 or ±10 Beta	%20 error band	-	-
Bank to Bank	1-2-1 Roll Stick Input	-	-		-	±30 or ±60 Phi Angle	%20 error band

3. DATA PRE-PROCESS

In the simulation stage, general observation of the control surfaces, states and atmospheric data is made. These data are useful for full black-box model system identification, however when it comes to the identification of the aerodynamic parameters, additional data process and mass-thrust dataset is needed.

To obtain total force and moment coefficients from the measured parameters such as linear-angular acceleration, Euler rates, angle of attack, sideslip angle etc., data of the thrust, total weight, cg positions and inertia values are needed.

Mass block which includes total weight, inertia, cg positions is critically important at producing all force and moment coefficients from force and moment. Also, weight and inertia data is critical to obtain total force and moments from measurement of the state parameters.

Thrust and its vectoring information is critical in all force and moment coefficients. In most cases for the single engine jet aircrafts, engines primary effect is visible on drag and pitch moment coefficients. The amount of thrust and its effective location according to the cg position is critical at producing these coefficients. However, if the engine has a tilt angle, it can create force and moment in other axes too.

3.1 Mass-Thrust Information Preperation

Mass – Thrust data is obtained from the plant of the 6DOF aircraft model developed by Russel (2003). After that integration of the subsystem blocks to the system identification codes are made.

3.1.1 Mass block preparation for mass – inertia – CG calculation

The momentary data of the mass inertia and cg positions in each second of the flight test points is crucial. The effect of each data point at the calculations will be explained in the following parts.

The data about the mass block is gathered from the nlpant.c code of the f16 model. At the code, mass information is defined as static table that stays same for the entire flight maneuver. Therefore, same table is applied to the data preparation process of the system identification studies.

In this study, mass – cg – inertia information is fed to the data at every time frame to obtain total force and moment coefficients.

The information is presented at Table 3.1 is as:

- Mass 9295.4 kg
- IXX 12875 kgm^2
- IYY 75674 kgm^2
- IZZ 85552 kgm^2
- IXZ 1331 kgm^2
- Chord 3.4503 m
- Span 9.1440 m
- Wing Area 27.87090 m^2
- xACCG (0.35-0.3)*Chord
- yACCG 0
- zACCG 0

3.1.2 Thrust block preparation

Gathering data about the thrust is very critical about the drag and pitch moment coefficients. While thrust is the main source of the drag coefficient, it also has an impact on the calculation of the pitch moment with the position of cg and center line of the thrust.

Required thrust and in-flight changes at the thrust values are recorded with as each time frame of the flight test points. Information about the usage of thrust information on the equations will be provided at the following chapter.

3.2 Obtaining Total Force And Moment Coefficients

In order to create a flight model that represents the aircraft in real life, model should be trained with the aerodynamics force and moments derived from the flight test data. Therefore, the obtained flight test data is processed to create aerodynamic force and moment coefficients. In this section, the methodology to obtain these coefficients is described. General representative of the diagram is at Figure 3.1.

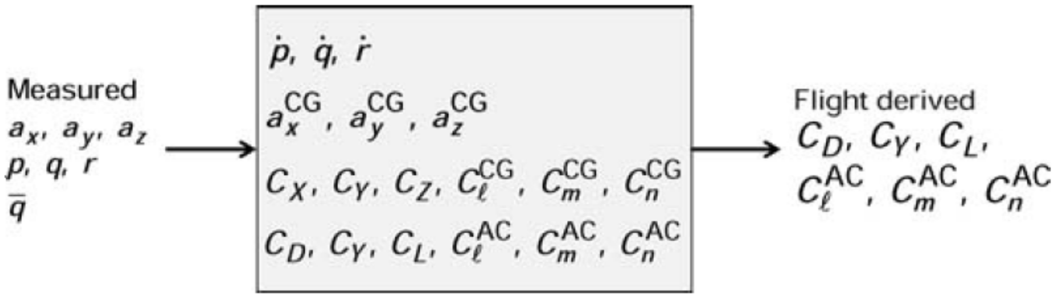

Figure 3.1 : Obtaining Total Force and Moment Coefficinets (Jategaonkar, 2006).

In the estimation of the total force and moment coefficients, main contributor parameters are the linear accelerations (axCG, ayCG, azCG) and the angular accelerations ($\dot{p}$, $\dot{q}$, $\dot{r}$). However, in the flight tests, most of the times measured parameters are linear accelerations and angular rates. In the system identification studies, angular accelerations are derived from the angular rates (Jategaonkar, 2006).

Calculation of total angular and translational accelerations:

In order to calculate the total coefficients. angular and linear accelerations must be calculated in the location of the center of gravity. Therefore, the measurements must be carried to the point of the center of gravity. The location of the cg is defined in the mass block of the model. In order to carry the measurement to the cg, the location of the sensors is crucial. After measurement of linear acceleration at sensor, the carrying to the cg formula is described by Jategaonkar with angular rates and accelerations as in the equations 3.1 to 3.3.

$$a_{X_{CG}} = a_X + x_{ASCG} * (q^2 + r^2) - y_{ASCG} * (p * q - \dot{r}) - z_{ASCG} * (p * r + \dot{q}) \tag{3.1}$$

$$a_{Y_{CG}} = a_Y - x_{ASCG} * (p * q + \dot{r}) + y_{ASCG} * (r^2 + p^2) - z_{ASCG} * (q * r + \dot{p}) \tag{3.2}$$

$$a_{Z_{CG}} = a_Z - x_{ASCG} * (p * r - \dot{q}) - y_{ASCG} * (q * r + \dot{p}) - z_{ASCG} * (p^2 + q^2) \tag{3.3}$$

Total linear accelerations calculated by product of the sensors to center of gravity (ASCG) with angular rates and accelerations.

Total angular accelerations are derived from the angular rates by using numerical differentiations. However, because of the sampling rate and frequency, some derivations can't define the angular accelerations precisely. For example, in some moments of the change, the difference in the measurement is smaller than the sensor's observing capabilities. Therefore, numerical differentiation with a filter needed to be used. In order to that, firstly, the measurement of each angular rate is gathered to the system. After that, ndiff_filter08 code that prepared by Jategaonkar (2006) is adapted to the system. This code represents the numerical differentiation with the filter of 8th order. Finally, the data size and test point information are fed to the system and total angular rates at the CG location is obtained.

Calculation of total force and moment coefficient

Thrust, Landing Gear effects are considered in the process of producing these body axes force coefficients. The equations used for calculating total force and moment coefficients given at the equation set 3.4 to 3.6:

$$C_X = \frac{m * a_{X_{CG}} - Thrust_X - LG_X}{q_{bar} * S_{ref}} \tag{3.4}$$

$$\mathrm{C_Y} = \frac{m * a_{X_{CG}} - LG_Y}{q_{bar} * S_{ref}} \tag{3.5}$$

$$\mathrm{C_Z} = \frac{m * a_{z_{CG}} - Thrust_Z - LG_Z}{q_{bar} * S_{ref}} \tag{3.6}$$

Generation of the lift, drag and side force coefficients from the body axes forces given at the equations 3.7 to 3.9.

$$C_D = -C_X * cos(a) - C_Z * sin\,(a) \tag{3.6}$$

$$\mathrm{C_L} = C_X * \sin(a) - C_Z * \cos\,(a) \tag{3.7}$$

$$\mathrm{C}_Y = C_Y \tag{3.9}$$

In order to produce rolling, pitching and yawing moment coefficients at the body-axes referred to CG position given at the equations 3.10 to 3.12.

$$C_{R_{CG}} = \frac{I_X * \dot{p} \; - \; I_{XZ} * \dot{r} \; - \; I_{XZ} * p * q \; - \; (I_Y - I_Z) * q * r - \; Thrust_R \; - \; LG_R}{q_{bar} * S_{ref} * B_{ref}} \tag{3.10}$$

$$C_{M_{CG}} = \frac{I_y * \dot{q} + \; I_{XZ} * (p^2 - r^2) \; - \; (I_Z - I_X) * p * r - \; \mathrm{Thrust_M} \; - \; \mathrm{LG}_M}{\mathrm{q_{bar}} * \mathrm{S_{ref}} * \mathrm{l_{ref}}} \tag{3.11}$$

$$C_{N_{CG}} = \frac{I_Z * \dot{r} \; - \; I_{XZ} * \dot{p} + \; I_{XZ} * q * r \; - \; (I_X - I_Y) * p * q - \; \mathrm{Thrust_N} \; - \; \mathrm{LG_N}}{\mathrm{q_{bar}} * \mathrm{S_{ref}} * \mathrm{B_{ref}}} \tag{3.12}$$

To make the comparison of the aerodynamic databases with the flight test data, calculations of the moment coefficients transferred to the aerodynamic center (moment reference point) by using eqations 3.13 to 3.15.

$$C_{R_{AC}} = C_{R_{CG}} - C_Z * \frac{y_{ACCG}}{B_{ref}} + C_Y * \frac{z_{ACCG}}{B_{ref}} \tag{3.13}$$

$$\mathrm{C}_{M_{\mathrm{AC}}} = C_{M_{CG}} - C_X * \frac{z_{ACCG}}{l_{ref}} + C_Z * \frac{x_{ACCG}}{l_{ref}} \tag{3.14}$$

$$\mathrm{C}_{\mathrm{N_{AC}}} = C_{N_{CG}} - C_Y * \frac{x_{ACCG}}{B_{ref}} + C_X * \frac{y_{ACCG}}{B_{ref}} \tag{3.15}$$

4. ESTIMATION WITH DEEP LEARNING

4.1 Data structure Development

After calculating the total force and moment coefficients, states and control surface data is combined with total coefficients at mat files. In the main python code at the estimation algorithm, the data called to the system to be able to manipulate data on the usage of system identification with deep learning. Firstly the data is divided into the groups of inputs and outputs. States and control surfaces are described as inputs of the deep learning models. Total force and moment coefficients are defined as outputs of the estimation algorithm. Secondly, normalization of the all parameters that will be used in the input section is realied. In order to estimate the model with high fidelity, normalization process is needed. Otherwise the effect of the some parameters will be much more visible than the other parameters. This causes estimation algorithm miss out some features of the aircraft, therefore it leads to low fidelity estimation. In order to prevent this, the scale of all parameters are normalized. At last, the data is divided as prediction and validation and set to the estimation algorithm.

4.2 Tensorflow Based Models

After the data prepared for the estimation of the aircraft's aerodynamics, the model structure that defines aerodynamics of the aircraft is determined. In order to apply neural network structure-based modelling into estimation, TensorFlow framework used in python environment. As a application programming interface (API) in this study, Keras API is selected for its easy and high level of consistency qualities. With this structure, chance of testing lots of different models, layers, feature sets is achieved. After this selection, model generation section is started. As the selection of model type, sequential model is selected. Many trials and errors section ran with the flight data to represent the aircrafts aerodynamics.

Due to the complexity of the aircrafts, layer is number of the Keras sequential model is selected as 10. Node number at each layer is selected as 128 with considering high number of parameters at each feature sets and aircraft states. Due to nonlinear correlation of the parameters with each other, Relu is selected as activation function at the all the inner layers. To represent the simplistic sum of each parameter at output layer, activation function is selected as linear. Lastly, optimizer option for the estimated model is selected as Adam algorithm and the loss function is selected as mean squared error. The show of them as list is given as

- Framework: TensorFlow framework
- API: Keras API
- Layers: 10
- Neurons: 128 each layer
- Model type: Sequential
- Act Function: Relu
- Optimizer: Adam algorithm
- Loss Function: Mean Squared Error

After defining the model, flight test data is arranged as prediction and validation. The amount of the flight data that will be used in train and test is described in Flight Test Envelope section of the chapter 2. After this model is compiled and trained with the selected data. At last, created models are tested with the test section of the flight data.

4.3 Different Feature Sets

In order to represent simplistic and complex feature sets, two different feature sets are prepared for every force and momemt coefficeints. Feature sets in the neural network-based system identification studies are the sets that include input and state parameters of the aircraft modeling. These parameters such as elevator, aileron, rudder angles, euler angles and rates, velocity, angle of attack, sideslip angle are critic at defining the characteristics of the aircraft. However, effects of these parameters to the aerodynamics of the aircraft is changing. Some of these parameters' effect on the force and moment coefficients are almost linear, while other parameters are highly non-linear. Therefore, in all of the system identification methodologies, there are other methodologies that includes the non-linearity of these parameters to the system identification. Especially in parameter estimation-based system identification methods, parameters' different powers, breakpoints through mach and angle of attack are commonly used. Neural network studies mainly include this non-linearity by additional layers where dependencies of the parameters to each other can be observed. In the next chapter, effect of adding additional parameters to the feature set by using flight dynamics information at deep learning-based system identification will be analyzed.

5. COMPARISON OF DEEP LEARNING BASED SYSTEM IDENTIFICATİON ESTIMATIONS WITH DIFFERENT FEATURE SETS

Within this study, Neural Network based system identification studies are conducted with different types of feature structures. Firstly, the relevant models are trained without manipulating the inputs. These input sets are including Euler angles, rates, angle of attack, sideslip and control surface angles according to the relevant force and moment coefficient. These parameters are presented at the section 5.1 as feature set 1.

Secondly, producing another feature set with adding exponential and coupled parameters. These parameters are gathered by using flight dynamics knowledge. For example, effectiveness of the Elevator angle depends on the angle of attack and mach of the aircraft. Therefore, coupled parameters of both elevator – angle of attack and elevator – mach are added to the new feature set. These parameters are presented at the section 5.1 as feature set 2.

After the generation of each feature sets, models are trained with same flight test data. Finally, models are compared with validation flight test maneuvers.

Used flight test envelopes for each parameters are presented at the section 5.2

Results of the estimations with validation test flights are presented at the section 5.3, it can create force and moment in other axes too.

5.1 Simplistic and Complex Feature Setsw

Simplistic and Complex feature sets are developed for each force and moment coefficients. Each feature sets can be grouped as longitudinal, lateral and directional. Explanation for the each parameter sets is described at 5.1.1 and 5.1.2 sections.

5.1.1 Longitudinal force and moment coefficients' feature sets

Longitudinal feature sets include parameters for the coefficients of Drag(CD), Lift (CL) and Pitch Moment (CM). Therefore, the main effective parameters on the longitudinal coefficients are selected.

Feature Set 1:

- Simpler Feature Set
- Consist of only required parameters
- 8 Parameters

Feature Set 2:

- Complex Feature Set
- Consist of exponential and coupled parameters of angle of attack, mach, elevator and pitch rate
- 15 Parameters

Table 5.1 : Feature Set for the Longitudinal force and moment coefficients

Parameters	Feature Set 1	Feature Set 2
1	AoA	AoA
2	AoS	AoS
3	Elevator	Elevator
4	Aileron	Aileron
5	Rudder	Rudder
6	LEF	LEF
7	Mach	Mach
8	PitchRate	PitchRate
9	-	AoA _ Square
10	-	AoA _ Cube
11	-	Elevator*AoA
12	-	AoA*Mach
13	-	PitchRate * AoA
14	-	Elevator*Mach
15	-	LEF*mach

5.1.2 Lateral and directional force and moment coefficients' feature sets

Longitudinal feature sets include parameters for the coefficients of Side Force (CY), Roll Moment (CR) and Yaw Moment (CN). Therefore, the main effective parameters on the longitudinal coefficients are selected

Feature Set 1:

- Simpler Feature Set
- Consist of only required parameters
- 5 Parameters

Feature Set 2:

- Complex Feature Set
- Consist of exponential and coupled parameters of angle of attack, mach, aileron, rudder, yaw rate and roll rate
- 15 Parameters

Table 5.2 : Feature Set for the Lateral and Directional force and moment coefficients

Parameters	Feature Set 1	Feature Set 2
1	AoS	AoS
2	Aileron	Aileron
3	Rudder	Rudder
4	Roll Rate	Roll Rate
5	Yaw Rate	Yaw Rate
6	-	AoS * AoA
7	-	Aileron * AoA
8	-	Rudder * AoA
9	-	Roll Rate * AoA
10	-	Yaw Rate * AoA
11	-	AoS * mach
12	-	Aileron * mach
13	-	Rudder * mach
14	-	Roll Rate * mach
15	-	Yaw Rate * mach

5.2 Flight Test Envelopes

The flight test data that will be used in model training must include all the region that model is intended to used. Therefore, flight test envelope is selected to make flight test data include necessary velocity and angle of attack values. Because the change in velocity and angle of attack is two most effective contributors from atmosphere to the aerodynamic database. At the higher speed – lower altitude flight test conditions, the effect of the compressibility on the aerodynamic database and nonlinearity that comes with being close to the transonic region are observable. Also, at the lower speed – higher altitude flight test conditions, the effect of the higher angle of attack values on the aerodynamic database and non-linearity that comes with near stall conditions can be examined. Furthermore, to be able to analyze linear aerodynamic region, the middle flight conditions also must be tested. With the consideration of these parameters and in defiance of F16 aircrafts own capabilities, necessary flight envelopes are determined. The detailed information about the regions of the flight envelopes will be discussed in following chapters.

5.2.1 Longitudinal flight test envelope

For the estimation of the longitudinal force and moment coefficients, longitudinal flight test envelope is selected to obtain flight data at both linear and non-linear regions of the F16 aircraft. The details about the flown test points and flight envelope graphic according to mach and altitude is given as:

26 Short Period Maneuver Conducted

- 22 Prediction – 4 Validation

Flight Envelope

- 0.3 Mach – 0.8 Mach
- 10000 ft – 30000 ft Altitude

Each flight test moment's altitude and mach graph is shown as:

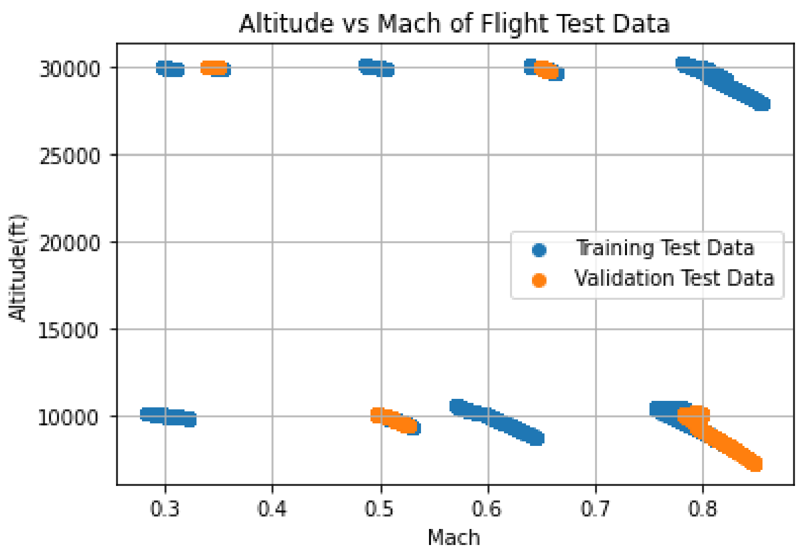

Figure 5.1 : Altitude and Mach values of the Short Period flight data

5.2.2 Lateral and directional flight test envelope

For the estimation of the lateral and directional force and moment coefficients, flight test envelope for lateral and directional maneuvers is selected to obtain flight data with different amount of input ranges and both linear and non-linear regions of the F16 aircraft. In Dutch Roll maneuvers, targeted sideslip angle were 5 and 10 degrees. In Bank-to-Bank maneuvers, targeted roll angle were 30 and 60 degrees. The details about the both flown test maneuvers and flight envelope graphic according to mach and altitude is given as:

102 Total Maneuver Conducted

- 53 Bank to Bank Maneuver
- 49 Dutch Roll Maneuver
- 94 Prediction – 8 Validation

Flight Envelope

- 0.3 Mach – 0.8 Mach
- 10000 ft – 30000 ft Altitude

Each flight test moment's altitude and mach graph is shown as:

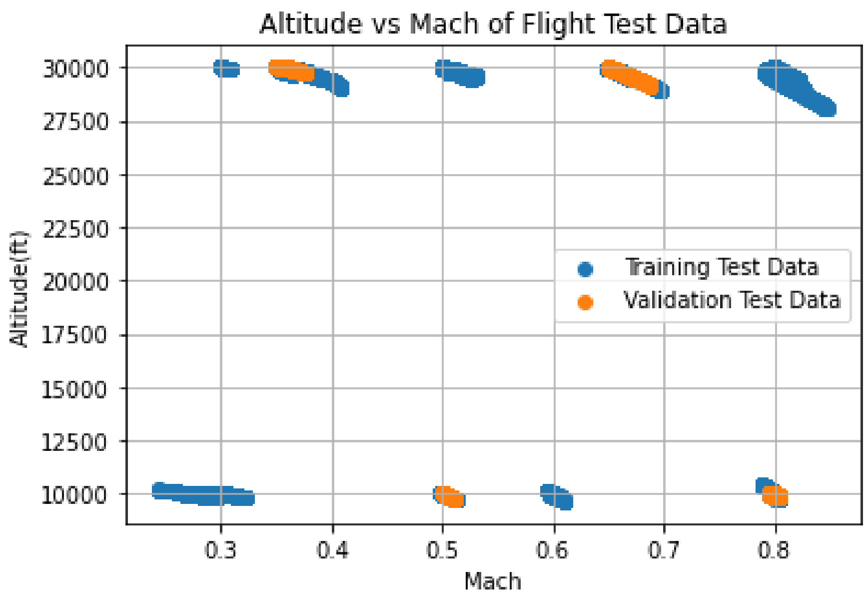

Figure 5.2 : Altitude and Mach values of Bank to Bank and Dutch Roll flight data

5.3 Force and Moment Comparisons

Comparisons of the both simplistic and complex models that prepared for each force and moment coefficients are explained in this section. Firstly, comparison for the longitudinal force and moment coefficients will be shown, then lateral and directional force and moment coefficients will be shown. In this chapter, the flight tests that graphics will be shown are from validation test points. At the training stage these maneuvers didn't used at the data set. In each test point, models that are trained from feature set 1 and 2 had ran and results are taken. Firstly, the trained models' loss and mean absolute error results will be given. After that, models result about how they followed each total coefficient will be shown in the graph.

5.3.1 Longitudinal force and moment comparisons

In this section, results of the drag coefficient (CD), lift coefficient(CL) and the pitching moment (CM) will be presented. The validation test points are selected to show the performance of the trained models at both linear and non-linear flight regions.

To represent the linear flight test regions, short period maneuvers of 0.65 Mach – 30000ft Altitude and 0.5 Mach – 10000ft Altitude are selected.

To represent the non-linear flight test regions, short period maneuvers of 0.8 Mach – 10000ft Altitude and 0.35 Mach – 30000ft Altitude are selected.

The results for the 4 different validation flights added at the following section. At the left, results of the model trained with simplistic feature set, at right results of the model trained with complex feature set are shown.

5.3.1.1 CD – Drag coefficient results

Loss function and mean absolute error model evaluation results according to defined validation test points of each feature set is given as:

Feature set 1:

- Loss: 1.7749e-06 MAE: 1.1369e-03

Feature set 2:

- Loss: 5.8797e-07 MAE: 3.7995e-04

Results of the simulations about CD coefficient given at the figures 5.3 to 5.10

Comparison for the Short Period maneuver – 1 (0.65 Mach – 30000 ft)

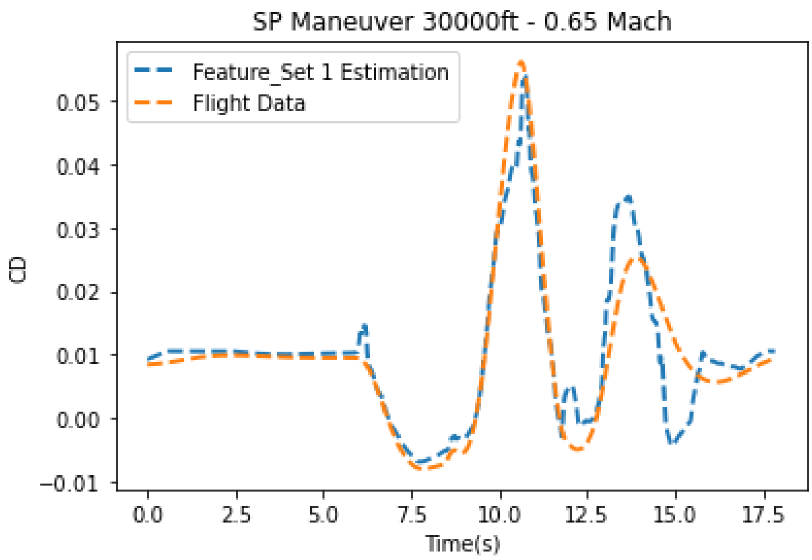

Figure 5.3 : SP-1, Feature Set 1 Simulation Result, 0.65 Mach – 30000 ft

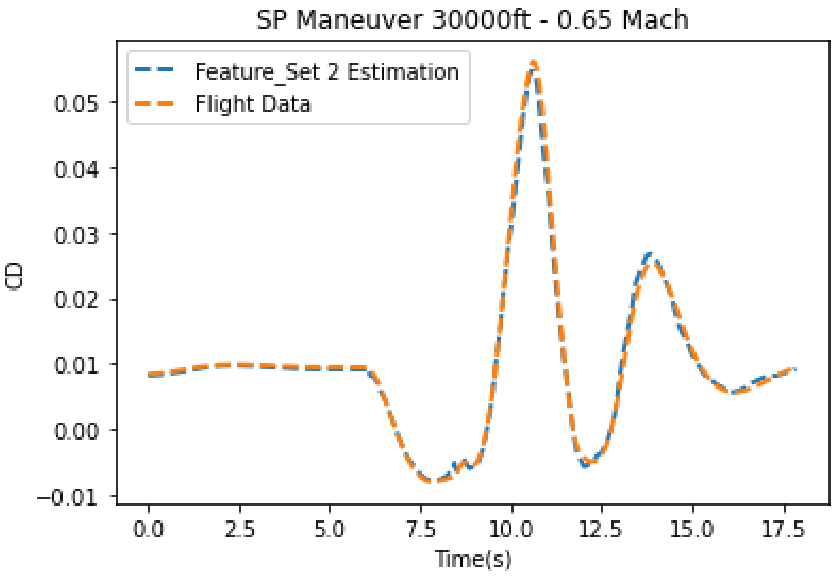

Figure 5.4 : SP-1, Feature Set 2 Simulation Result, 0.65 Mach – 30000 ft

Comparison for the Short Period maneuver – 2 (0.35 Mach – 30000 ft)

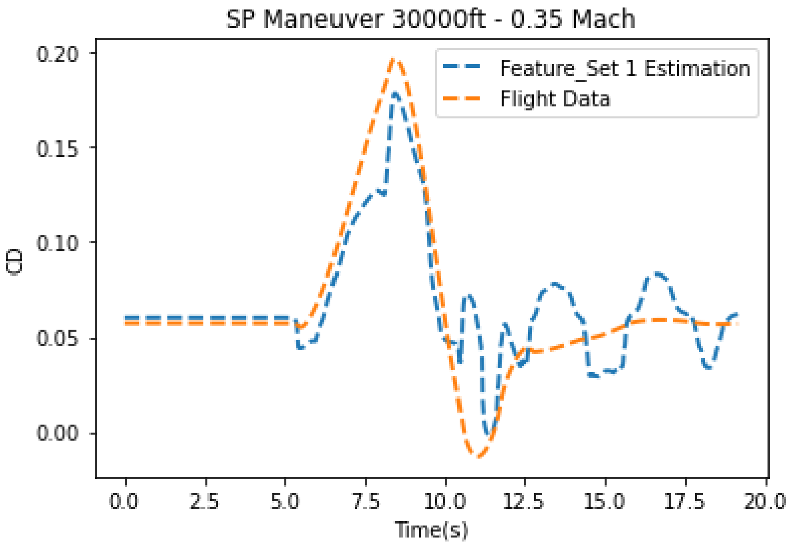

Figure 5.5 : SP-2, Feature Set 1 Simulation Result, 0.35 Mach – 30000 ft

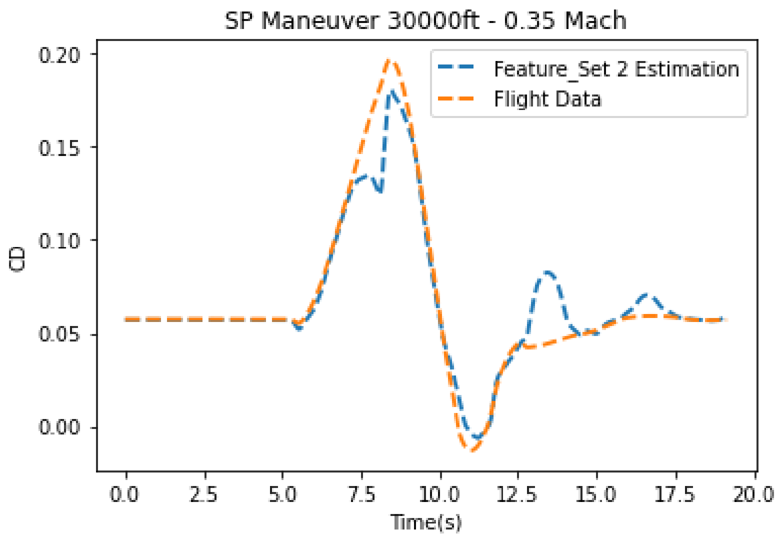

Figure 5.6 : SP-2, Feature Set 2 Simulation Result, 0.35 Mach – 30000 ft

Comparison for the Short Period maneuver – 3 (0.8 Mach – 10000 ft)

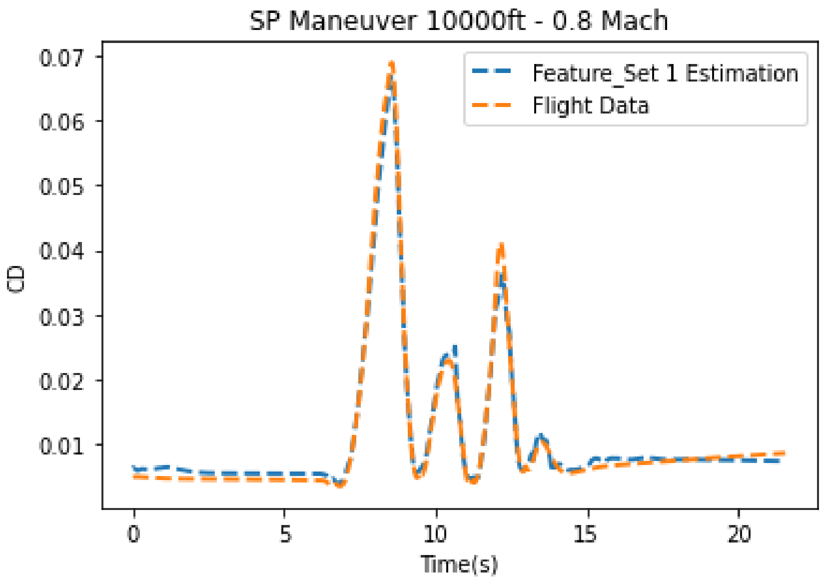

Figure 5.7 : SP-3, Feature Set 1 Simulation Result, 0.8 Mach – 10000 ft

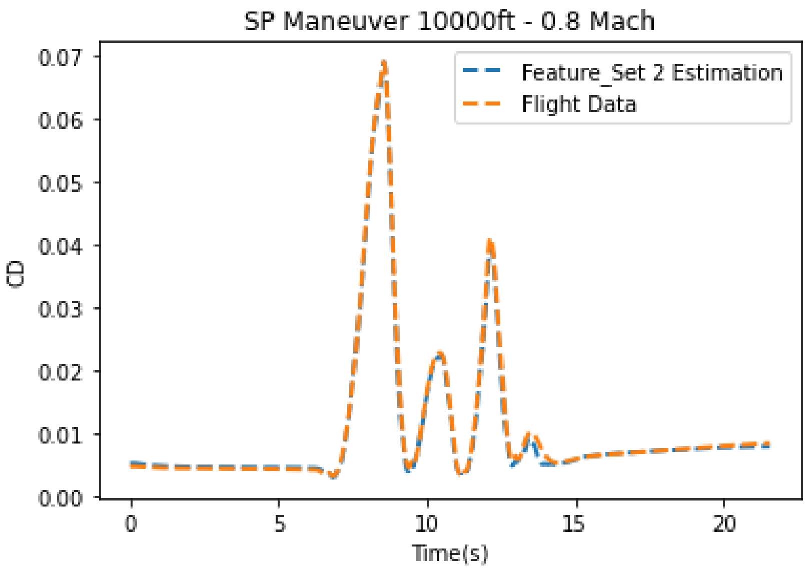

Figure 5.8 : SP-3, Feature Set 2 Simulation Result, 0.8 Mach – 10000 ft

Comparison for the Short Period maneuver – 4 (0.5 Mach – 10000 ft)

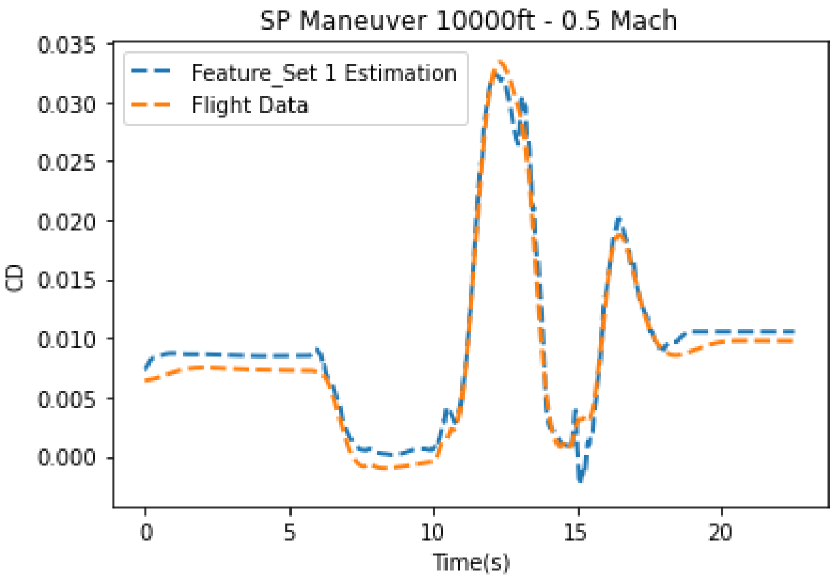

Figure 5.9 : SP-4, Feature Set 1 Simulation Result, 0.5 Mach – 10000 ft

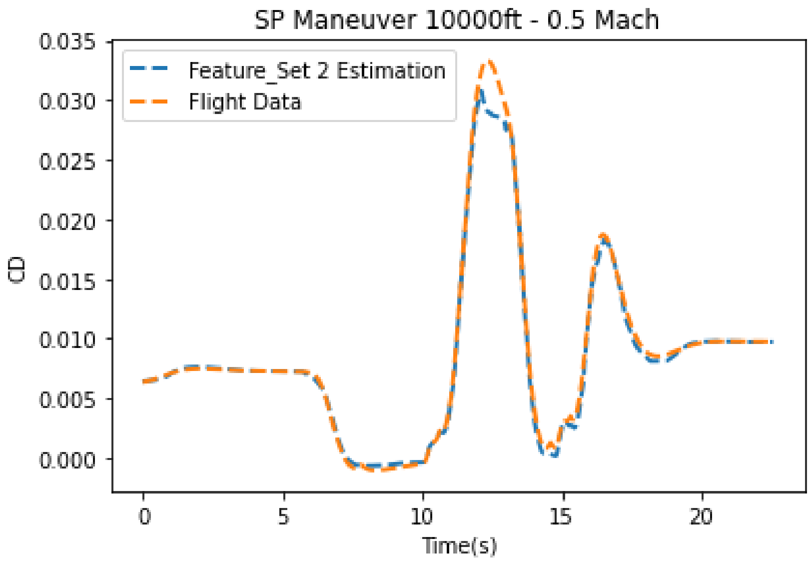

Figure 5.10 : SP-4, Feature Set 1 Simulation Result, 0.5 Mach – 10000 ft

5.3.1.2 CL – Lift coefficient results

Loss function and mean absolute error model evaluation results according to defined validation test points of each feature set is given as:

Feature set 1:

- Loss: 3.2122e-06 MAE: 0.00101

Feature set 2:

- Loss: 5.9862e-07 MAE: 5.994e-03

Results of the simulations about CL coefficient given at the figures 5.11 to 5.18

Comparison for the Short Period maneuver – 1 (0.65 Mach – 30000 ft)

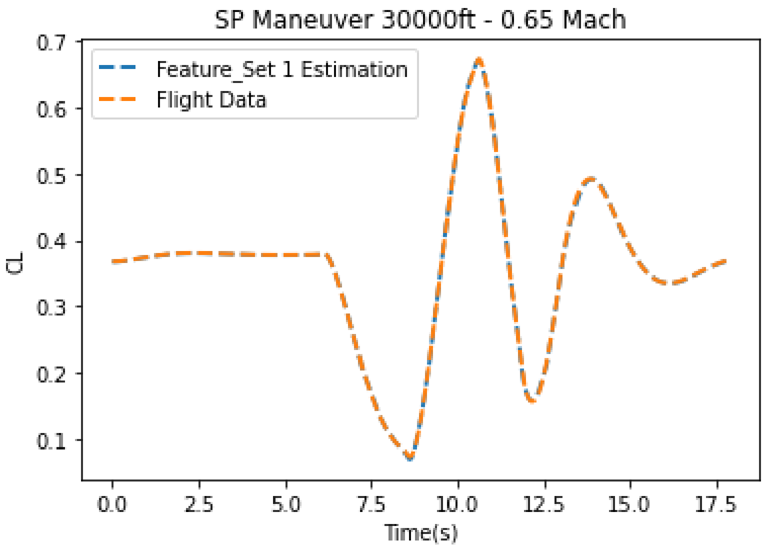

Figure 5.11 : SP-1, Feature Set 1 Simulation Result, 0.65 Mach – 30000 ft

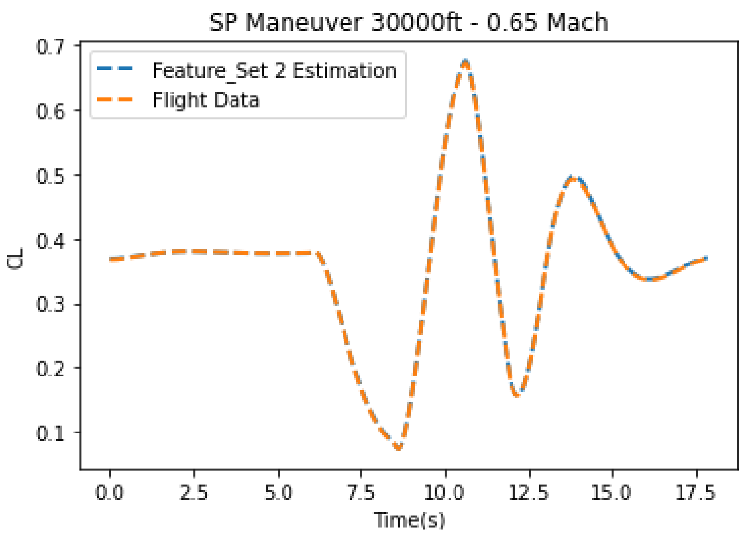

Figure 5.12 : SP-1, Feature Set 2 Simulation Result, 0.65 Mach – 30000 ft

Comparison for the Short Period maneuver – 2 (0.35 Mach – 30000 ft)

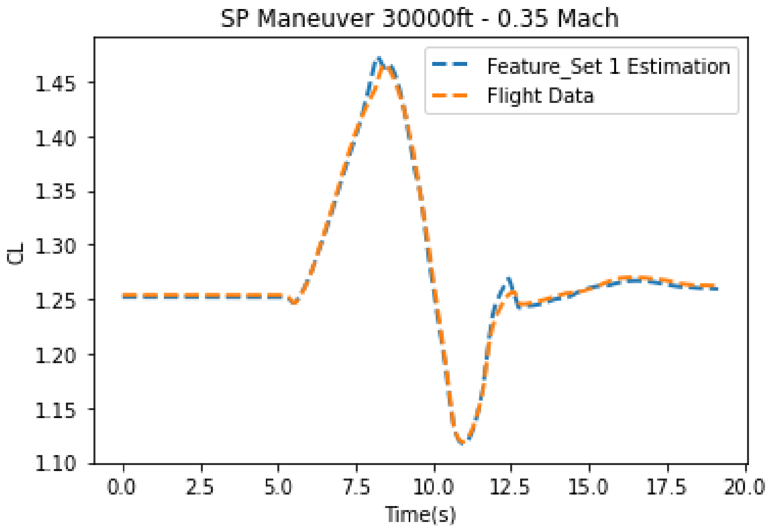

Figure 5.13 : SP-2, Feature Set 1 Simulation Result, 0.35 Mach – 30000 ft

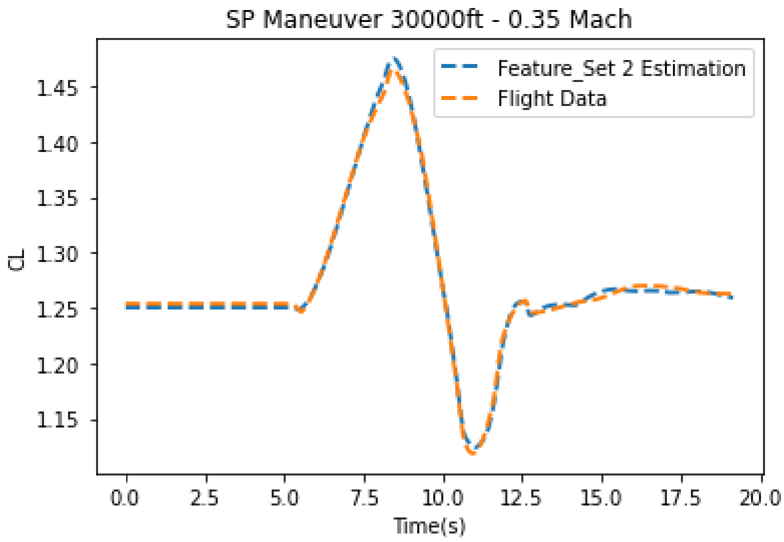

Figure 5.14 : SP-2, Feature Set 2 Simulation Result, 0.65 Mach – 30000 ft

Comparison for the Short Period maneuver – 3 (0.8 Mach – 10000 ft)

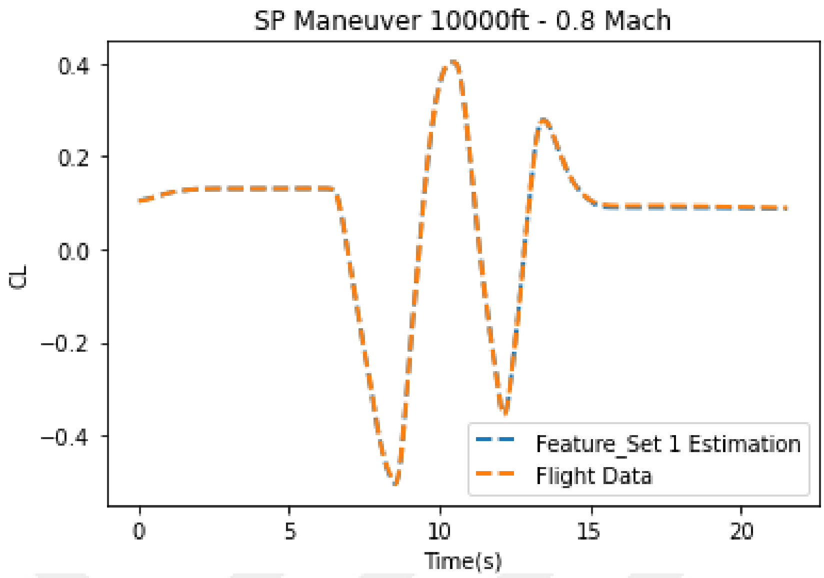

Figure 5.15 : SP-3, Feature Set 1 Simulation Result, 0.8 Mach – 10000 ft

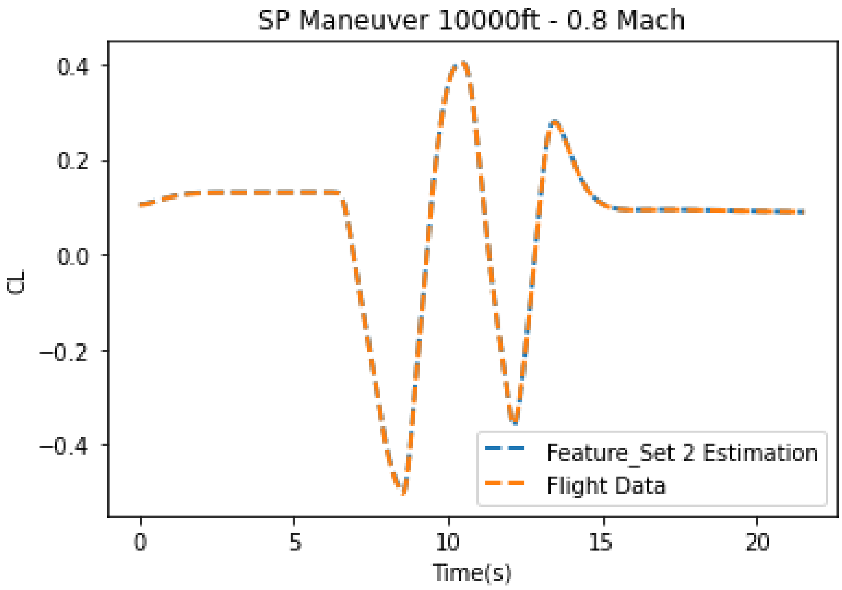

Figure 5.16 : SP-3, Feature Set 2 Simulation Result, 0.8 Mach – 10000 ft

Comparison for the Short Period maneuver – 1 (0.65 Mach – 30000 ft)

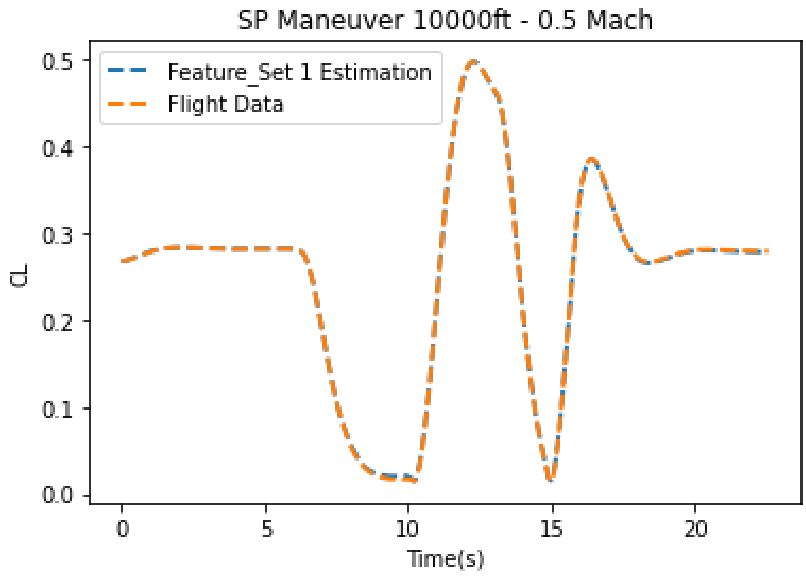

Figure 5.17 : SP-4, Feature Set 1 Simulation Result, 0.5 Mach – 10000 ft

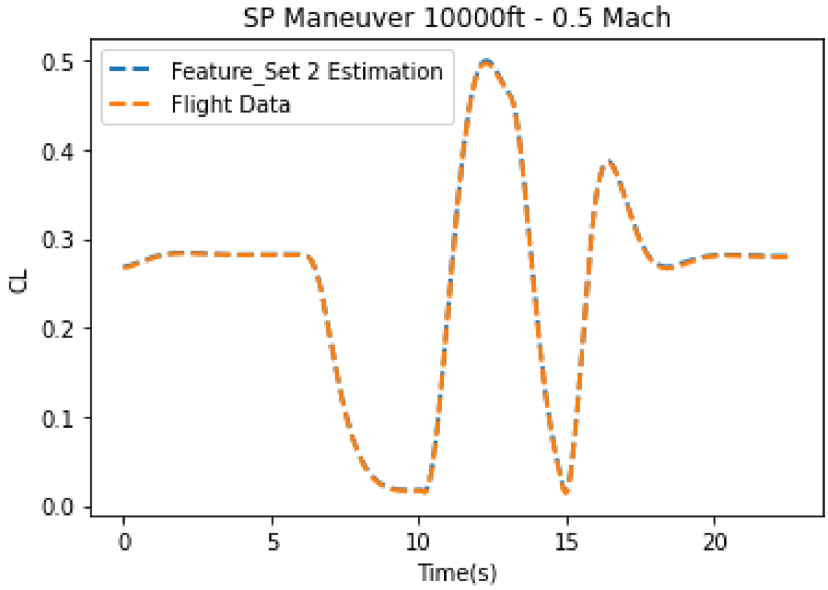

Figure 5.18 : SP-4, Feature Set 2 Simulation Result, 0.5 Mach – 10000 ft

5.3.1.3 CM – Pitch moment coefficient results

Loss function and mean absolute error model evaluation results according to defined validation test points of each feature set is given as:

Feature set 1:

- Loss: 2.2787e-05 MAE: 0.0033

Feature set 2:

- Loss: 1.7851e-05 MAE: 0.0029

Results of the simulations about CM coefficient given at the figures 5.19 to 5.26

Comparison for the Short Period maneuver – 1 (0.65 Mach – 30000 ft)

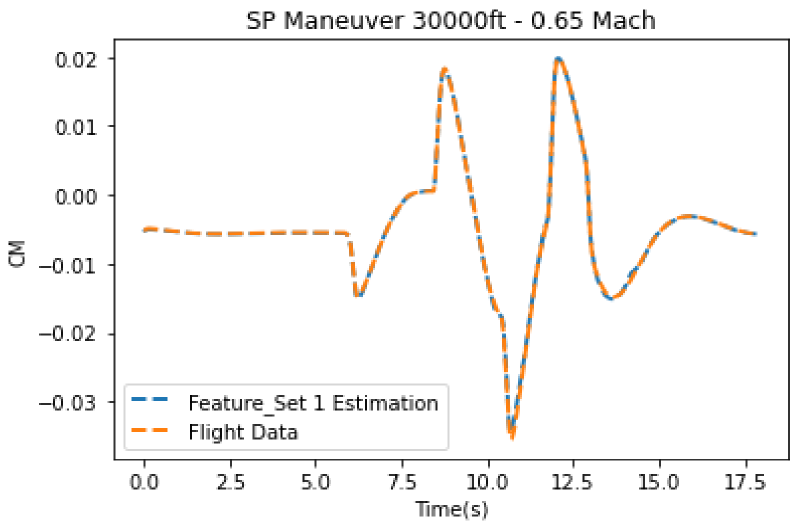

Figure 5.19 : SP-1, Feature Set 1 Simulation Result, 0.65 Mach – 30000 ft

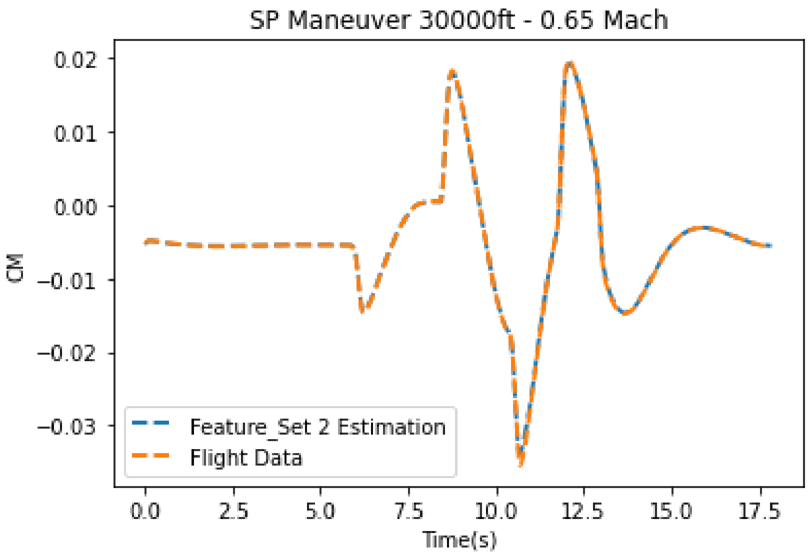

Figure 5.20 : SP-1, Feature Set 2 Simulation Result, 0.65 Mach – 30000 ft

Comparison for the Short Period maneuver – 2 (0.35 Mach – 30000 ft)

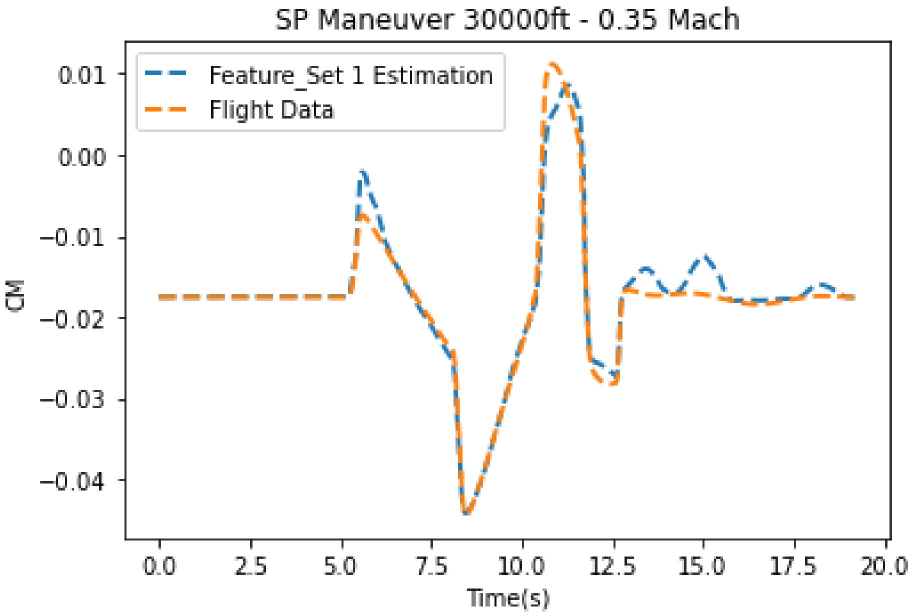

Figure 5.21 : SP-2, Feature Set 1 Simulation Result, 0.35 Mach – 30000 ft

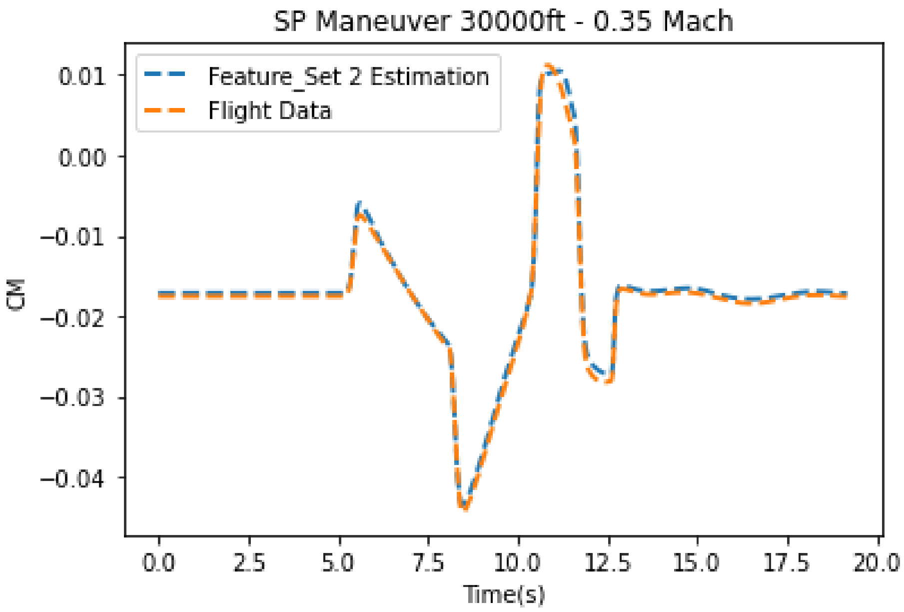

Figure 5.22 : SP-2, Feature Set 2 Simulation Result, 0.35 Mach – 30000 ft

Comparison for the Short Period maneuver – 3 (0.8 Mach – 10000 ft)

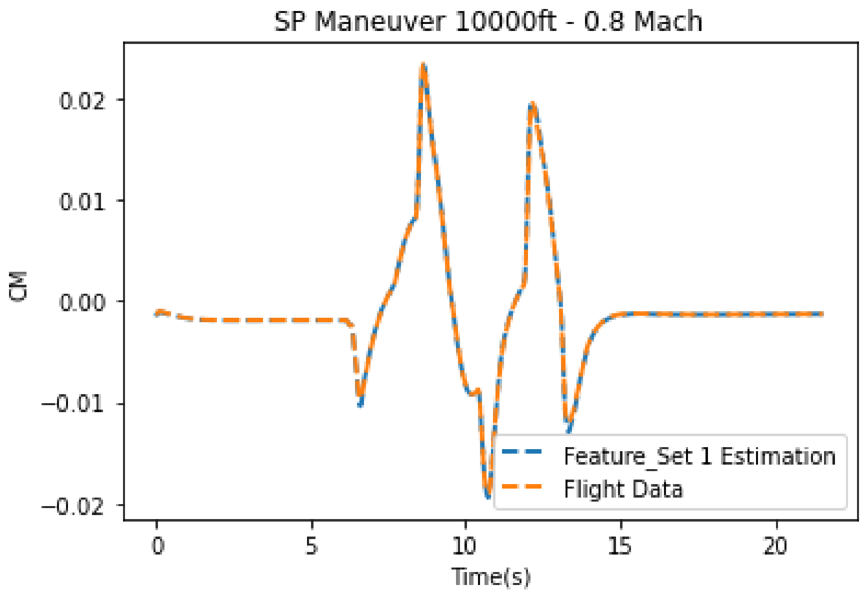

Figure 5.23 : SP-3, Feature Set 1 Simulation Result, 0.8 Mach – 10000 ft

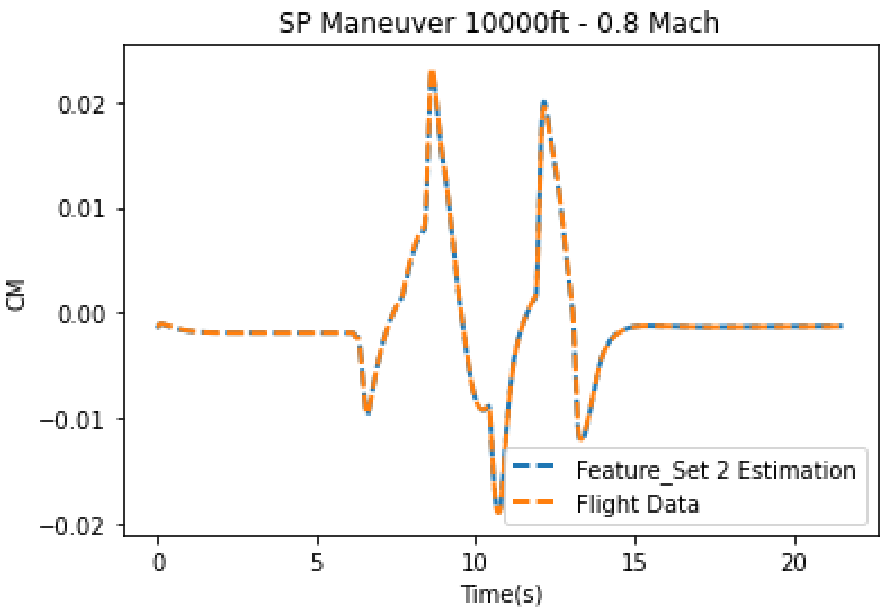

Figure 5.24 : SP-3, Feature Set 2 Simulation Result, 0.8 Mach – 10000 ft

Comparison for the Short Period maneuver – 4 (0.5 Mach – 10000 ft)

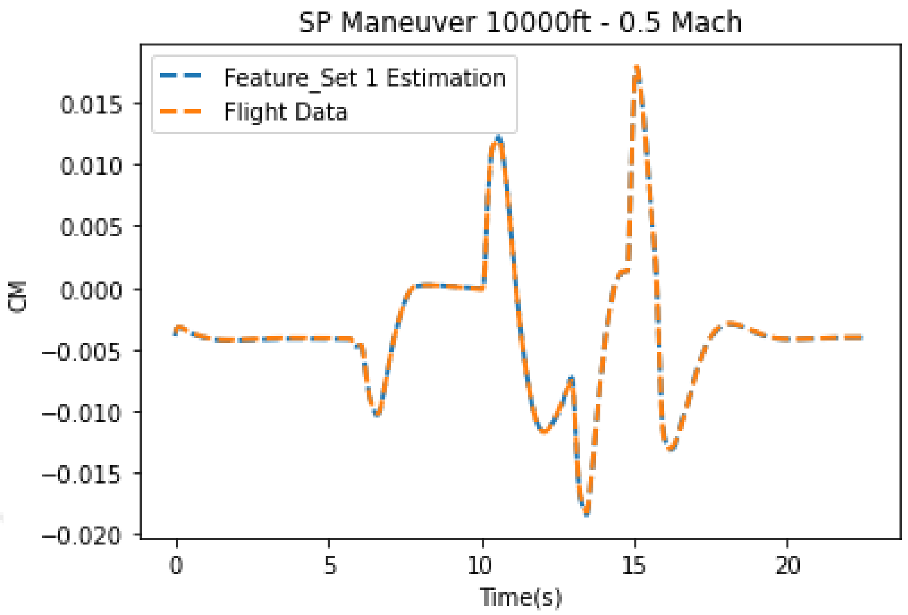

Figure 5.25 : SP-4, Feature Set 1 Simulation Result, 0.8 Mach – 10000 ft

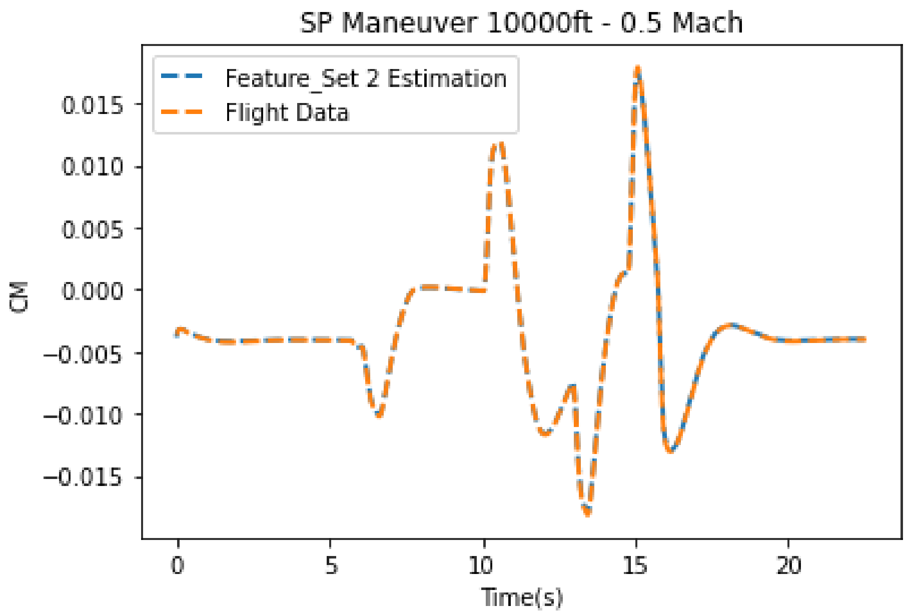

Figure 5.26 : SP-4, Feature Set 2 Simulation Result, 0.8 Mach – 10000 ft

5.3.1.4 – Conclusion for the longitudinal results

When analyzing short period flights at 0.5 Mach at 10,000 feet and 0.65 Mach at 30,000 feet, it is observed that both simple and complex feature sets yield similar results within the linear regime, indicating that simpler models can effectively capture the aircraft dynamics under these conditions.

However, when short period flights at 0.35 Mach at 30,000 feet and 0.8 Mach at 10,000 feet are examined, a significant increase in nonlinearity is noted as the extreme points of the flight envelope are approached. In these scenarios, crucially higher accuracy is demonstrated by the complex feature set compared to the simpler feature set.

This comparison reveals that to improve the accuracy in regions where nonlinearity increases, it is essential to incorporate complex parameters into the feature sets, in order to better estimate the moment and force coefficients. This approach ensures a more precise representation of the aircraft's aerodynamic behavior in nonlinear flight conditions.

5.3.2 Lateral - directional force and moment comparisons

In this section, results of the side force coefficient (CY), roll moment coefficient (CR) and the yaw moment (CN) will be presented. The validation test points are selected to show the performance of the trained models at both linear and non-linear flight regions. At the validation process of side force coefficient combination of the Dutch Roll and Bank to Bank maneuvers used, at the validation of roll moment coefficient Bank to Bank maneuvers are used and at the validation of yaw moment Dutch Roll maneuvers are used.

To represent the linear flight test regions, Dutch roll and bank to bank maneuvers of 0.65 Mach – 30000ft Altitude and 0.5 Mach – 10000ft Altitude are selected.

To represent the non-linear flight test regions, Dutch roll and bank to bank maneuvers of 0.8 Mach – 10000ft Altitude and 0.35 Mach – 30000ft Altitude are selected.

The results for the 4 different validation flights added at the following section. At the left, results of the model trained with simplistic feature set, at right results of the model trained with complex feature set are shown.

5.3.2.1 CY – Side force coefficient results

Loss function and mean absolute error model evaluation results according to defined validation test points of each feature set is given as:

Feature 1:

- Loss: 2.6168e-06 MAE: 9.5659e-04

Feature 2:

- Loss: 6.9633e-07 MAE: 4.7638e-04

Results of the simulations about CY coefficient given at the figures 5.27 to 5.34

Comparison for the Bank to Bank maneuver – 1 (0.8 Mach – 10000 ft)

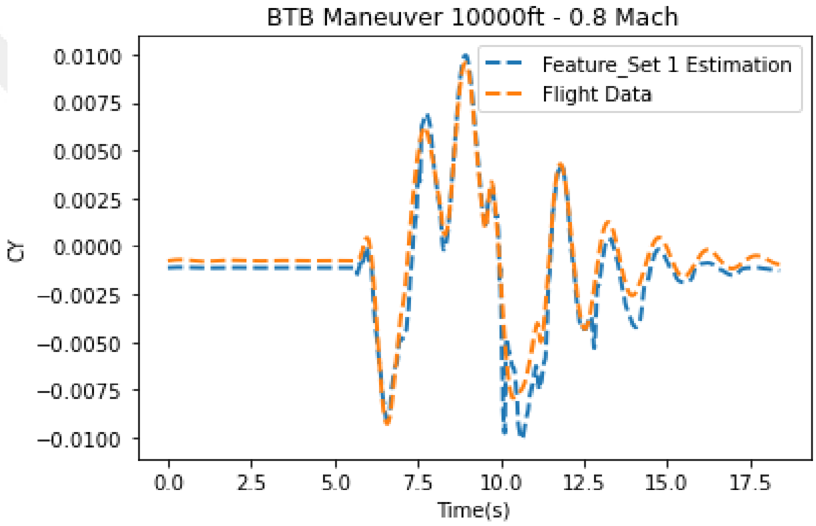

Figure 5.27 : BTB-1, Feature Set 1 Simulation Result, 0.8 Mach – 10000 ft

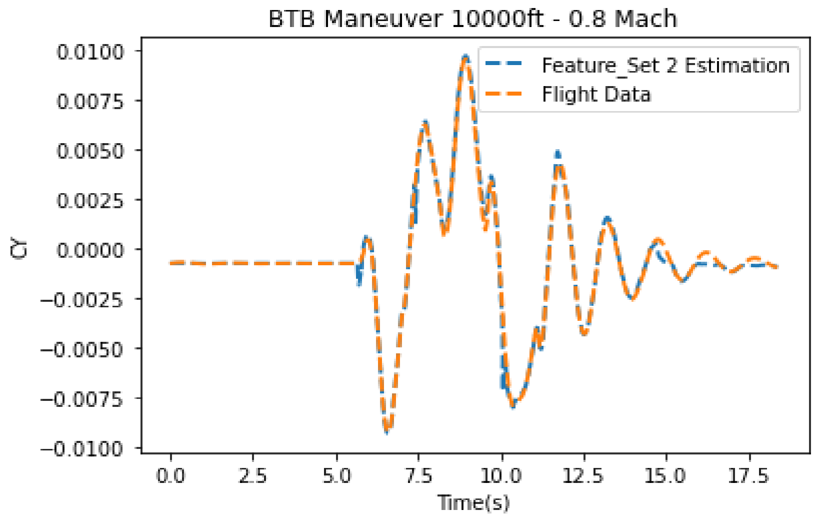

Figure 5.28 : BTB-1, Feature Set 2 Simulation Result, 0.8 Mach – 10000 ft

Comparison for the Bank to Bank maneuver – 2 (0.35 Mach – 30000 ft)

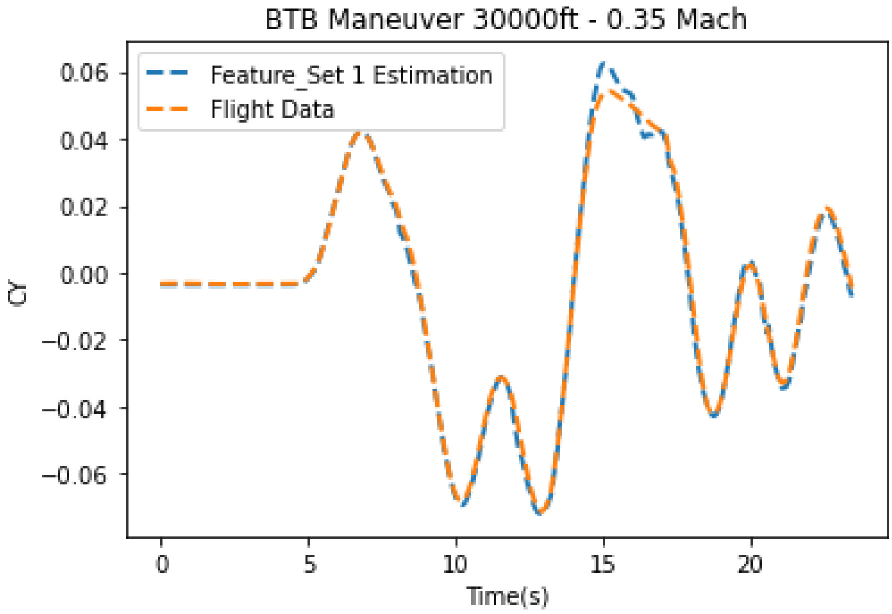

Figure 5.29 : BTB-2, Feature Set 1 Simulation Result, 0.35 Mach – 30000 ft

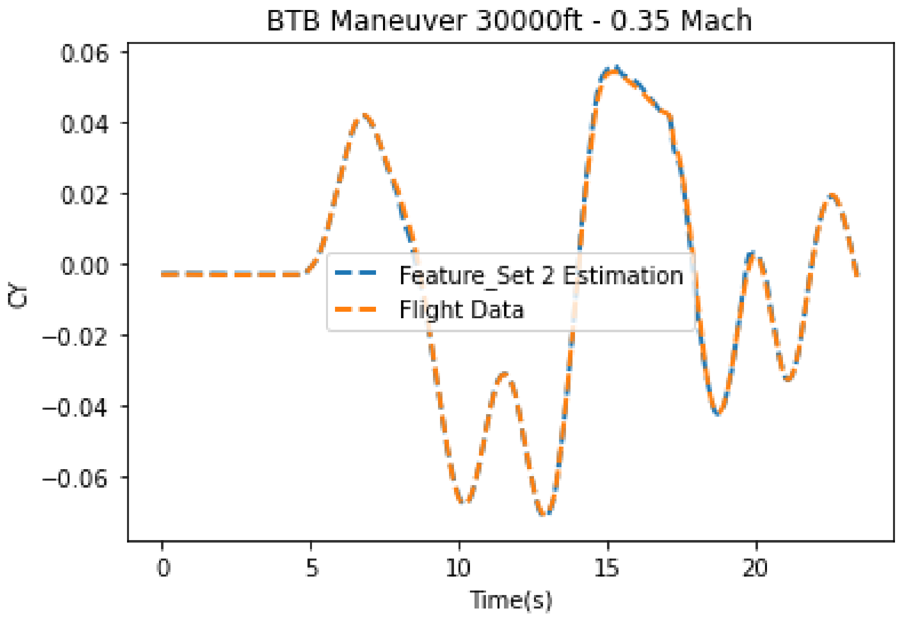

Figure 5.30 : BTB-1, Feature Set 2 Simulation Result, 0.35 Mach – 30000 ft

Comparison for the Dutch Roll maneuver – 1 (0.8 Mach – 10000 ft)

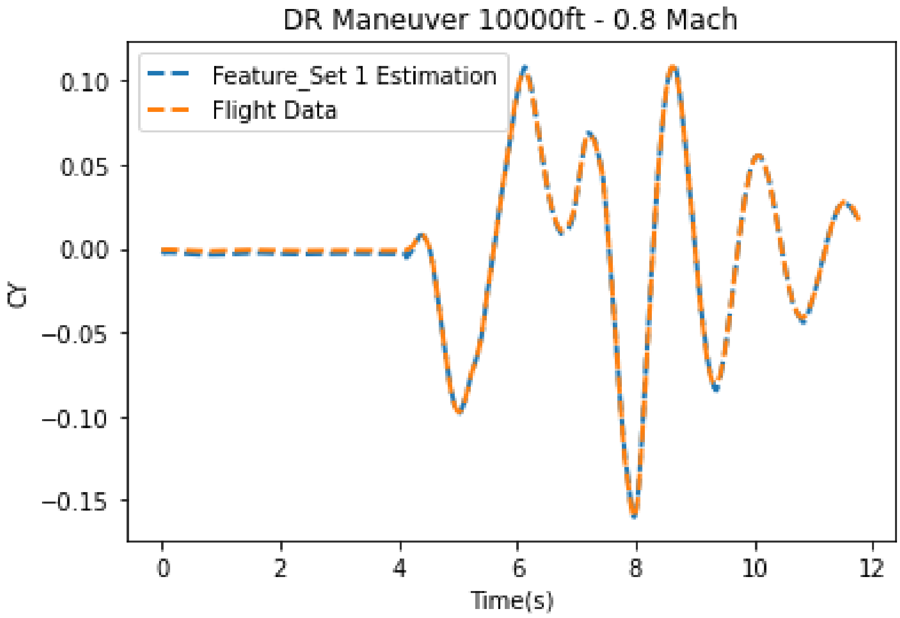

Figure 5.31 : DR-1, Feature Set 1 Simulation Result, 0.8 Mach – 10000 ft

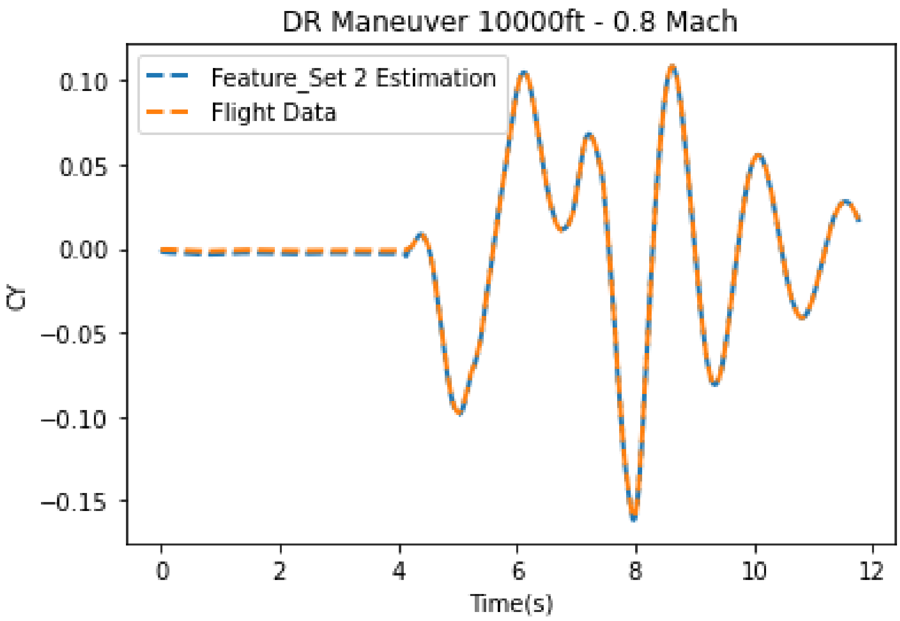

Figure 5.32 : DR-1, Feature Set 2 Simulation Result, 0.8 Mach – 10000 ft

Comparison for the Dutch Roll maneuver – 2 (0.5 Mach – 10000 ft)

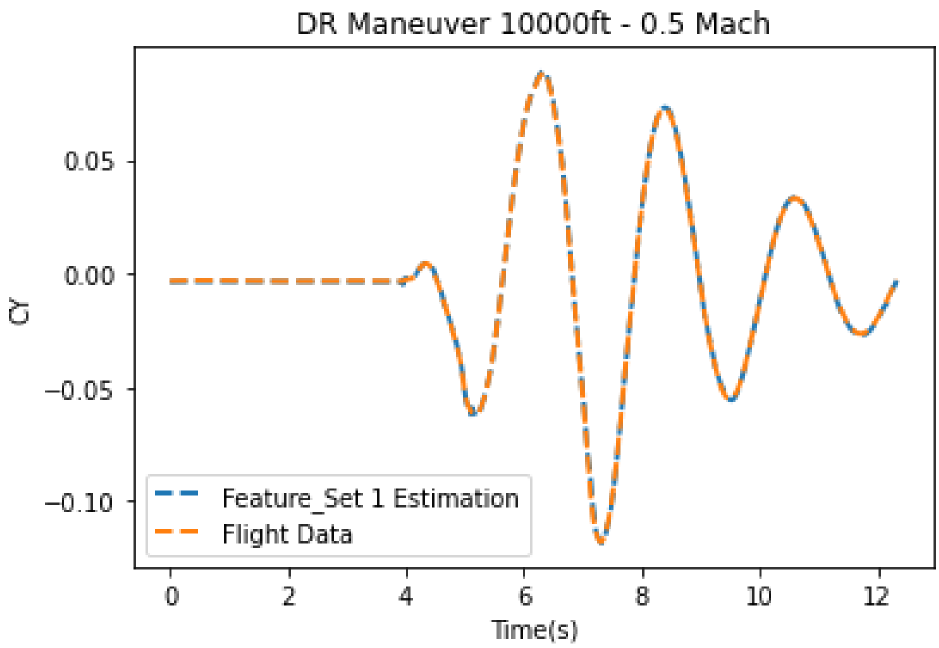

Figure 5.33 : DR-2, Feature Set 1 Simulation Result, 0.5 Mach – 10000 ft

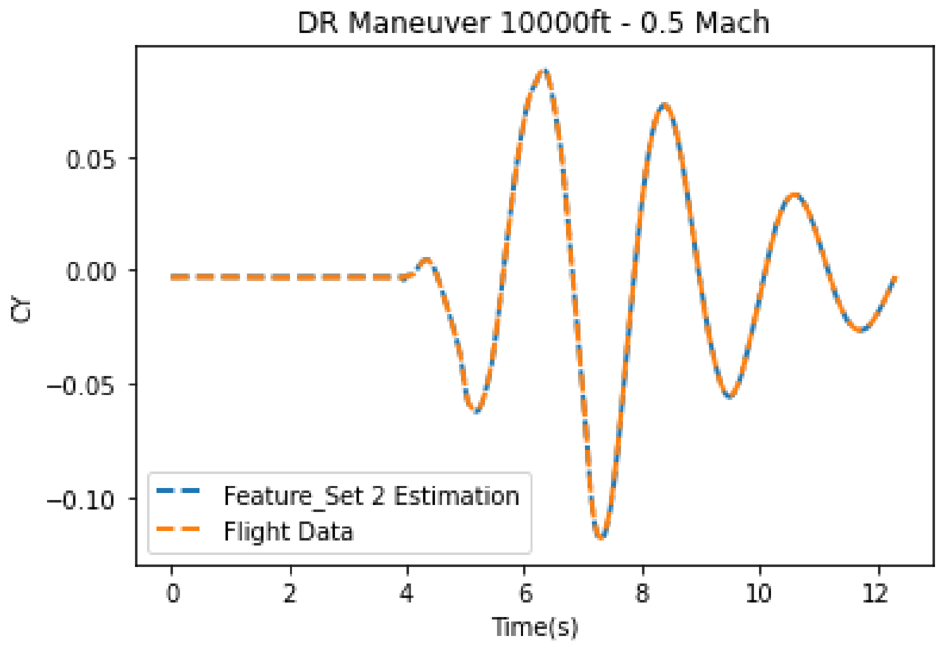

Figure 5.34 : DR-2, Feature Set 2 Simulation Result, 0.5 Mach – 10000 ft

5.3.2.2 CR – Roll moment coefficient results

Loss function and mean absolute error model evaluation results according to defined validation test points of each feature set is given as:

Feature 1:

- Loss: 6.8571e-07 MAE: 5.0453e-04

Feature 2:

- Loss: 1.8212e-08 MAE: 6.3345e-05

Results of the simulations about CR coefficient given at the figures 5.35 to 5.42

Comparison for the Bank to Bank maneuver – 1 (0.65 Mach – 30000 ft)

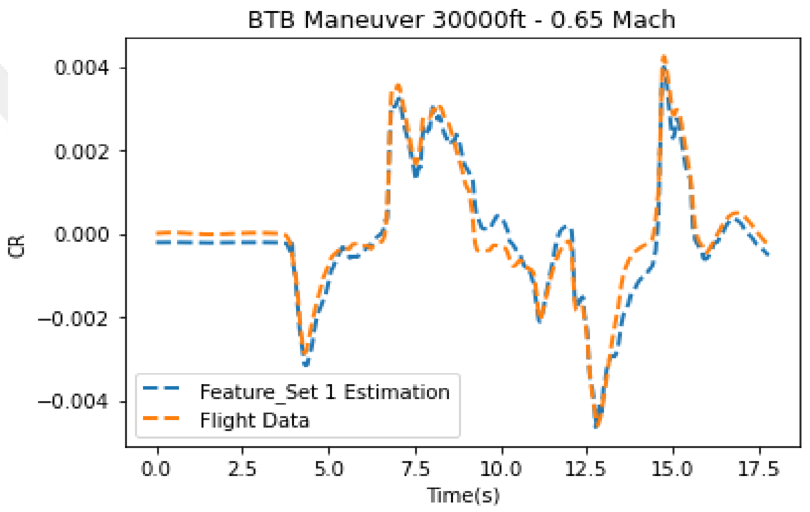

Figure 5.35 : BTB-1, Feature Set 1 Simulation Result, 0.65 Mach – 30000 ft

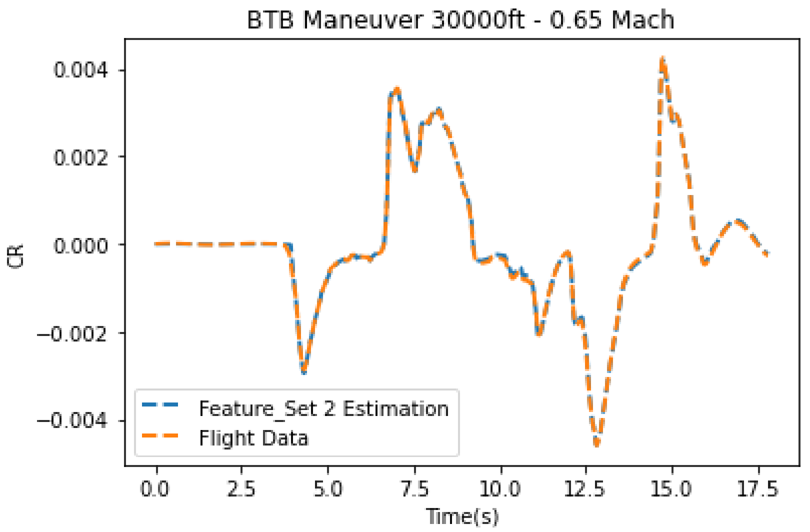

Figure 5.36 : BTB-1, Feature Set 2 Simulation Result, 0.65 Mach – 30000 ft

Comparison for the Bank to Bank maneuver – 2 (0.35 Mach – 30000 ft)

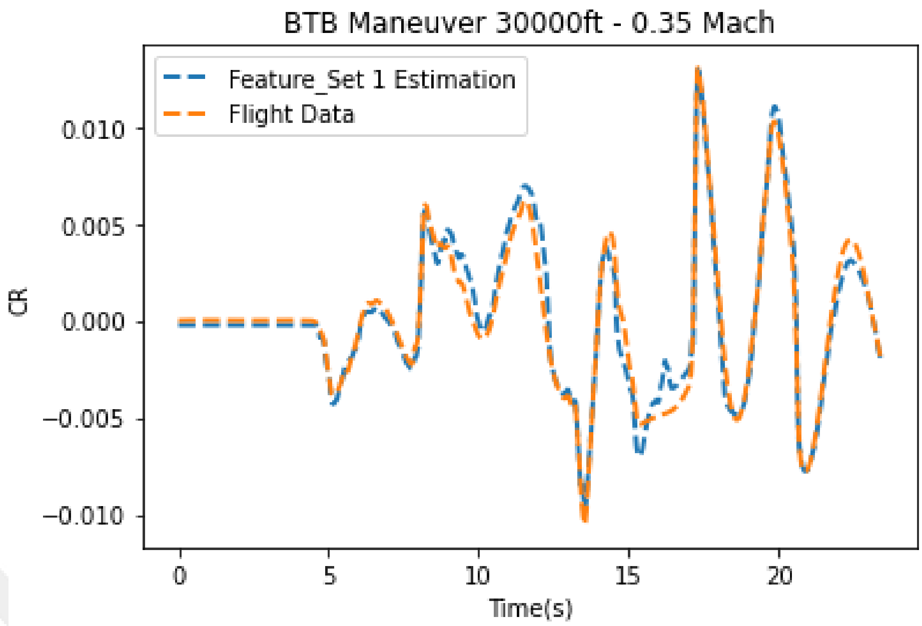

Figure 5.37 : BTB-2, Feature Set 1 Simulation Result, 0.35 Mach – 30000 ft

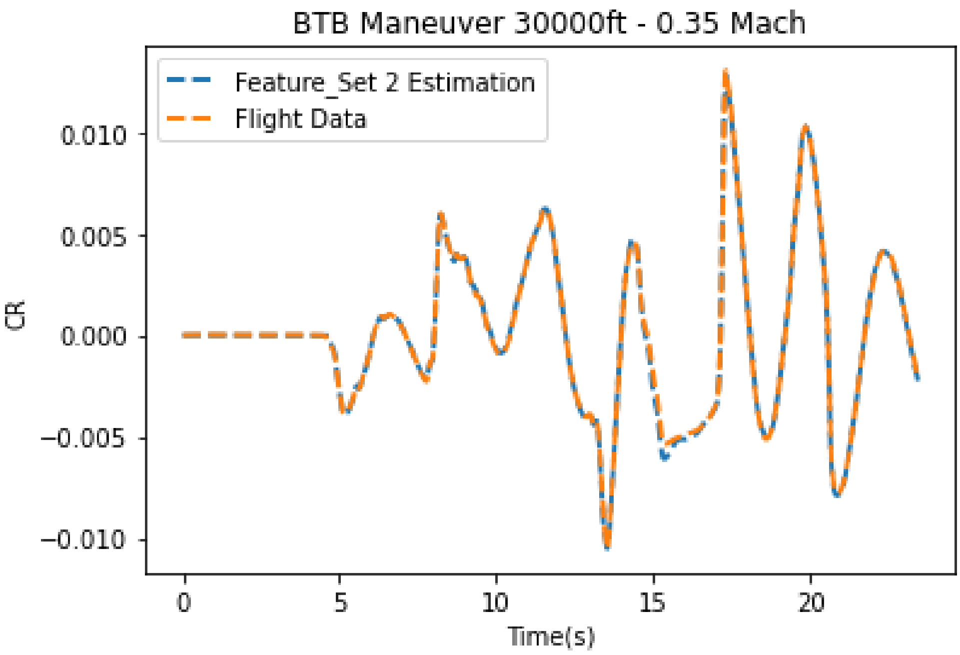

Figure 5.38 : BTB-2, Feature Set 2 Simulation Result, 0.35 Mach – 30000 ft

Comparison for the Bank to Bank maneuver – 3 (0.8 Mach – 10000 ft)

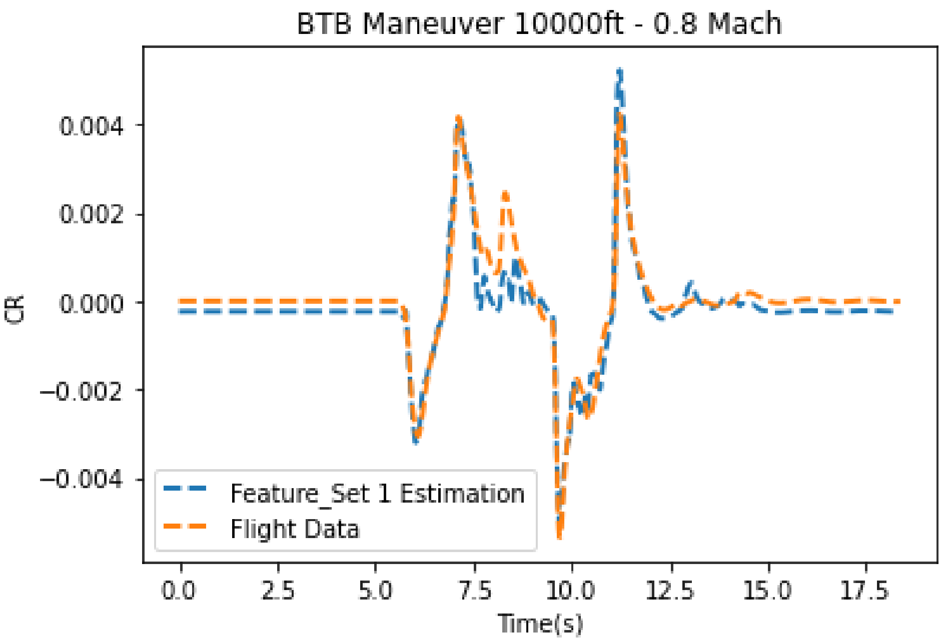

Figure 5.39 : BTB-3, Feature Set 1 Simulation Result, 0.8 Mach – 10000 ft

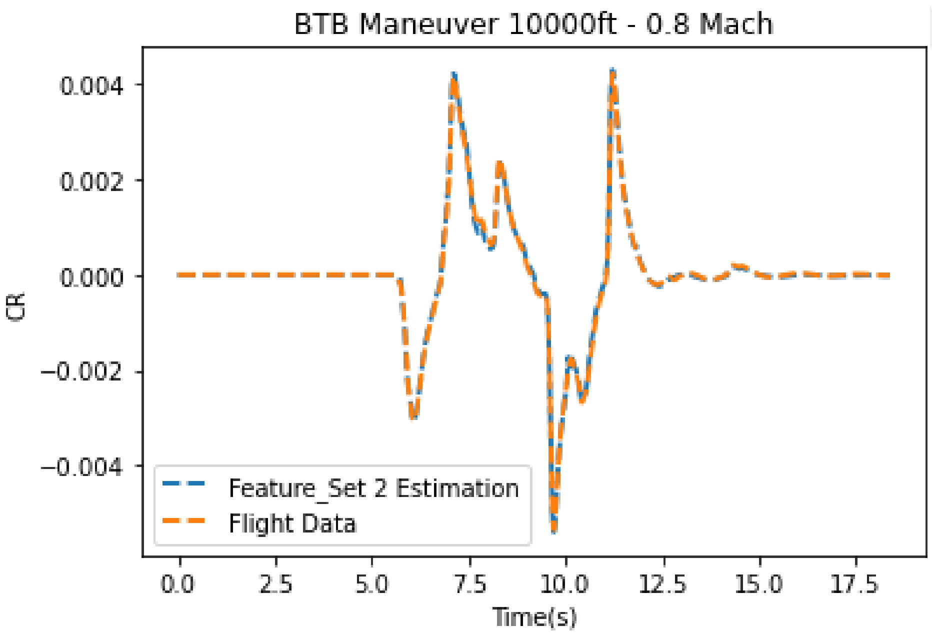

Figure 5.40 : BTB-3, Feature Set 2 Simulation Result, 0.8 Mach – 10000 ft

Comparison for the Bank to Bank maneuver – 4 (0.5 Mach – 10000 ft)

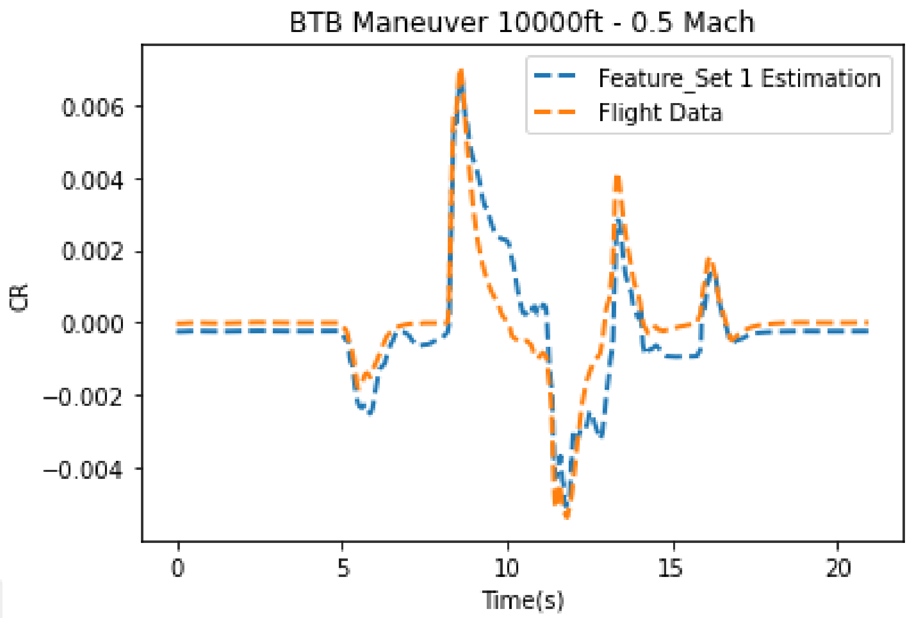

Figure 5.41 : BTB-4, Feature Set 1 Simulation Result, 0.5 Mach – 10000 ft

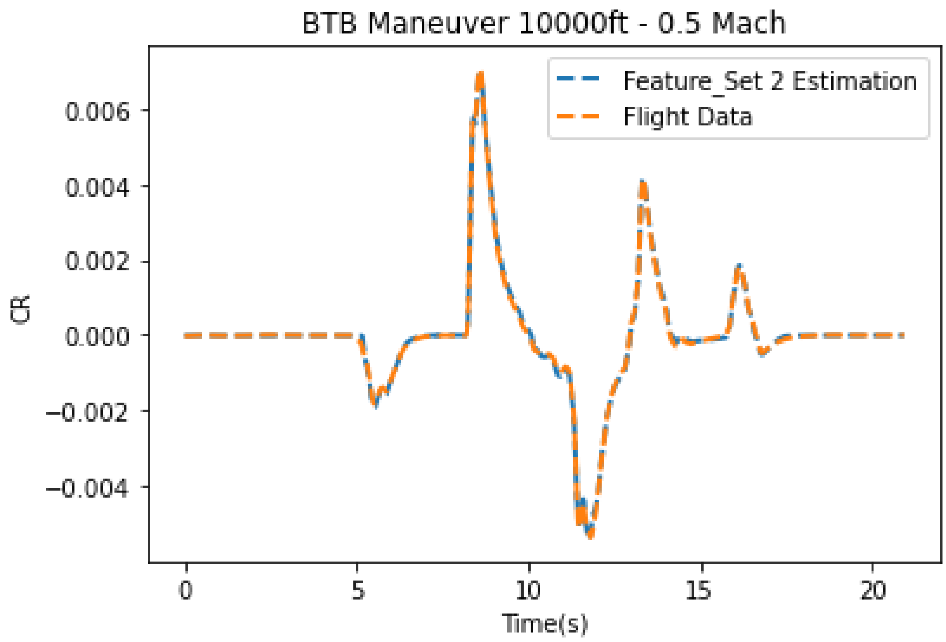

Figure 5.42 : BTB-4, Feature Set 2 Simulation Result, 0.5 Mach – 10000 ft

5.3.2.3 CN – Yaw moment coefficient results

Loss function and mean absolute error model evaluation results according to defined validation test points of each feature set is given as:

Feature 1:

Loss: 5.3152e-07 MAE: 3.2577e-04

Feature 2:

Loss: 5.6619e-08 MAE: 1.3118e-04

Results of the simulations about CN coefficient given at the figures 5.42 to 5.49

Comparison for the Dutch Roll maneuver – 1 (0.65 Mach – 30000 ft)

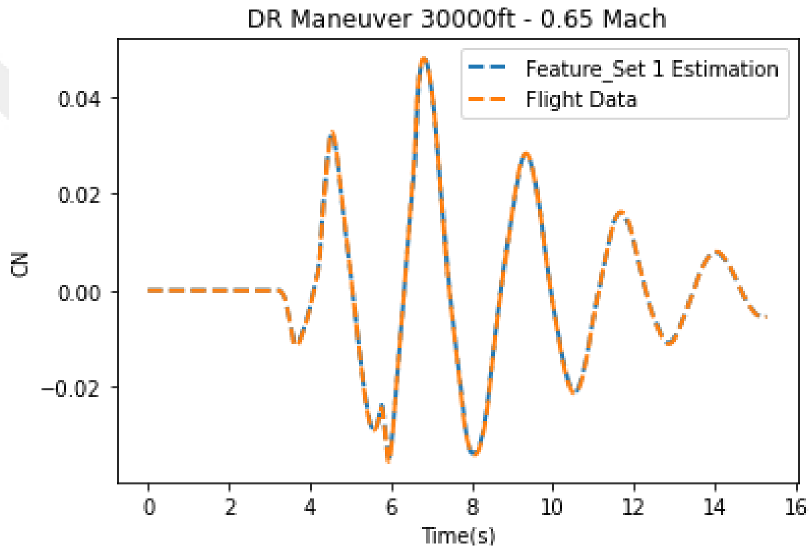

Figure 5.43 : DR-1, Feature Set 1 Simulation Result, 0.65 Mach – 30000 ft

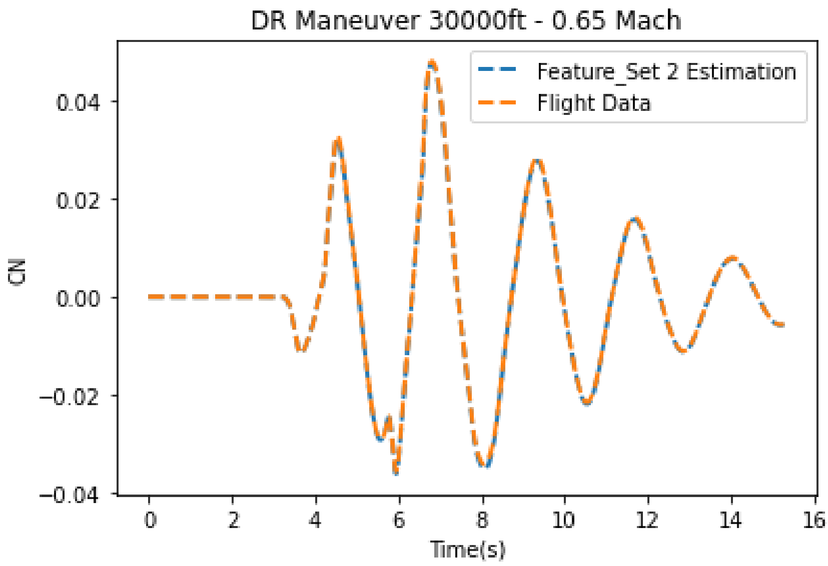

Figure 5.44 : DR-1, Feature Set 2 Simulation Result, 0.65 Mach – 30000 ft

Comparison for the Dutch Roll maneuver – 2 (0.35 Mach – 30000 ft)

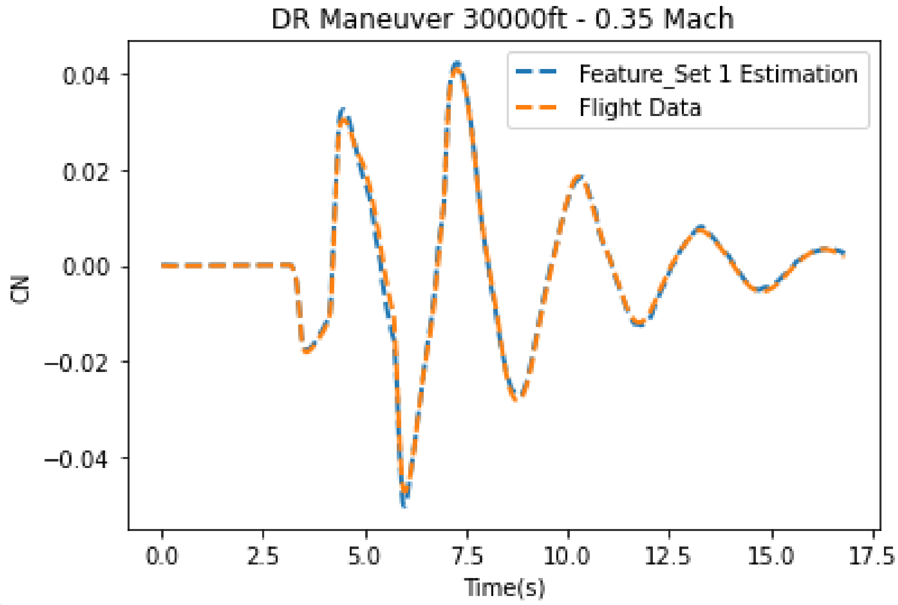

Figure 5.45 : DR-2, Feature Set 1 Simulation Result, 0.35 Mach – 30000 ft

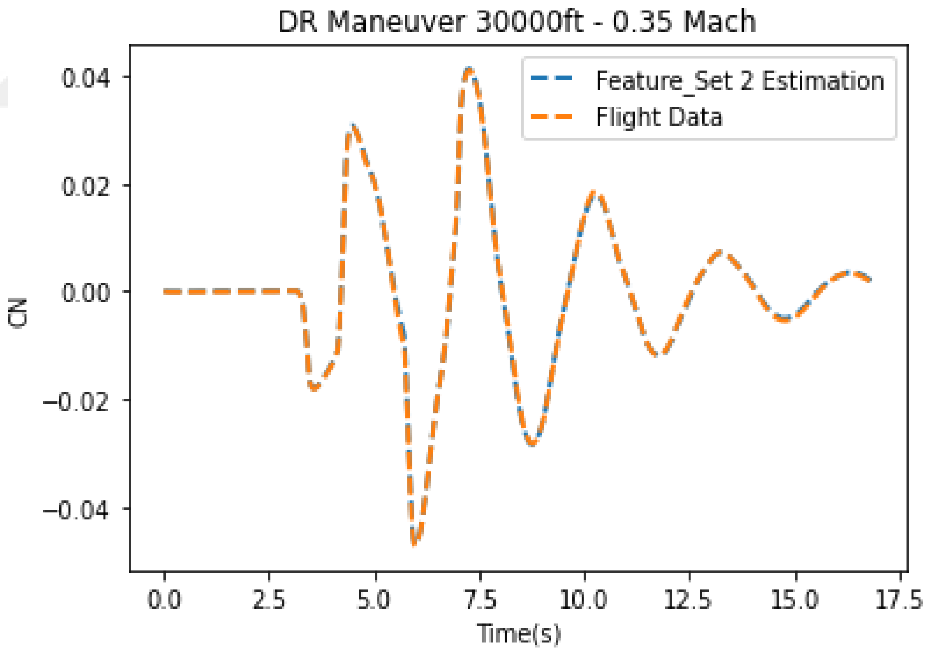

Figure 5.46 : DR-2, Feature Set 2 Simulation Result, 0.35 Mach – 30000 ft

Comparison for the Dutch Roll maneuver – 3 (0.8 Mach – 10000 ft)

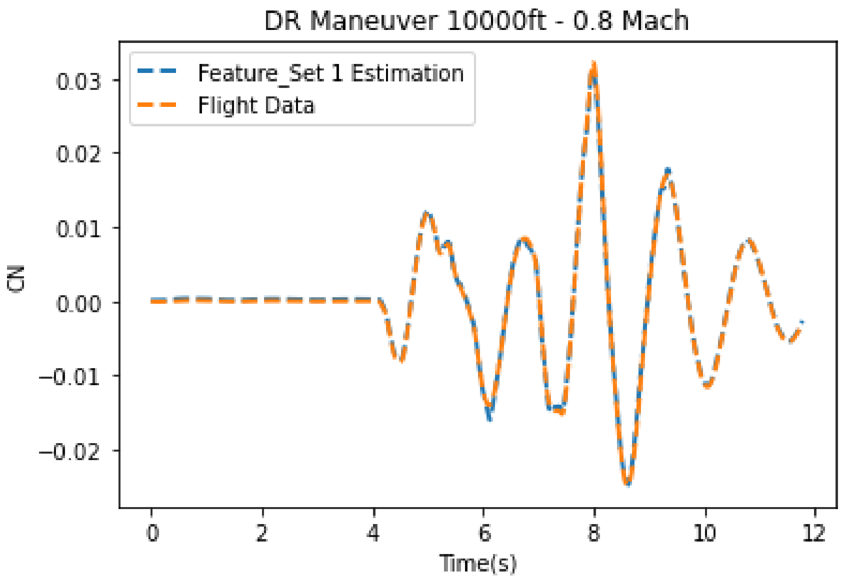

Figure 5.47 : DR-3, Feature Set 1 Simulation Result, 0.8 Mach – 10000 ft

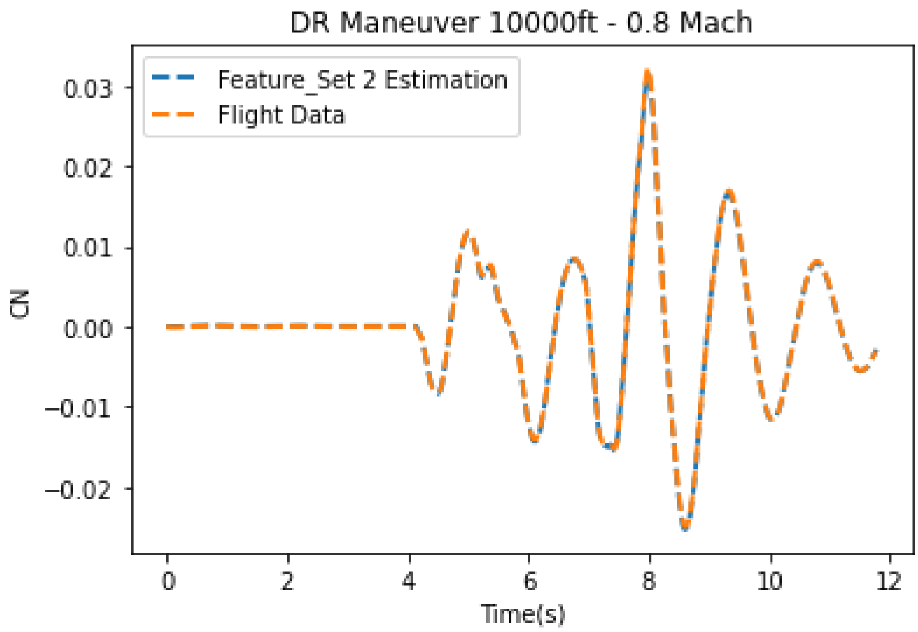

Figure 5.48 : DR-3, Feature Set 2 Simulation Result, 0.8 Mach – 10000 ft

Comparison for the Dutch Roll maneuver – 4 (0.5 Mach – 10000 ft)

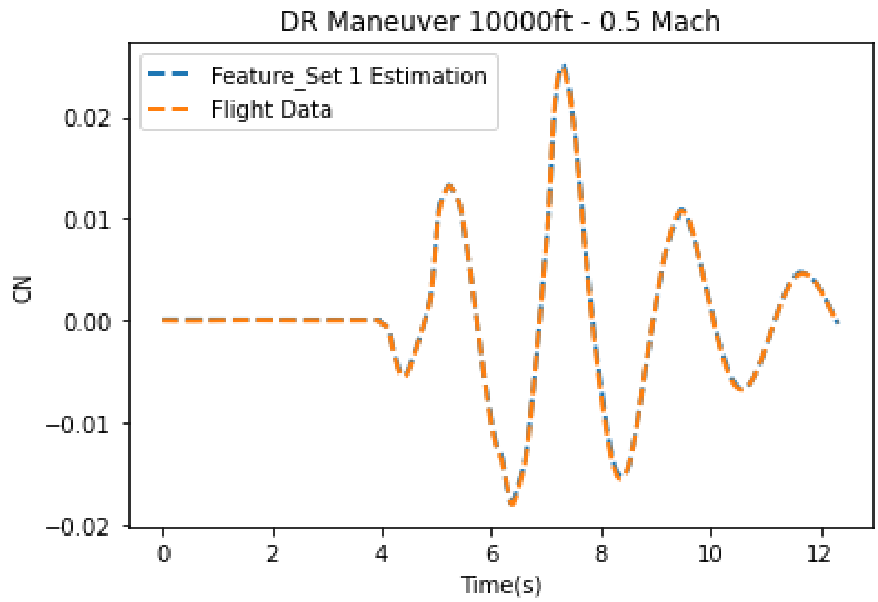

Figure 5.49 : DR-4, Feature Set 1 Simulation Result, 0.5 Mach – 10000 ft

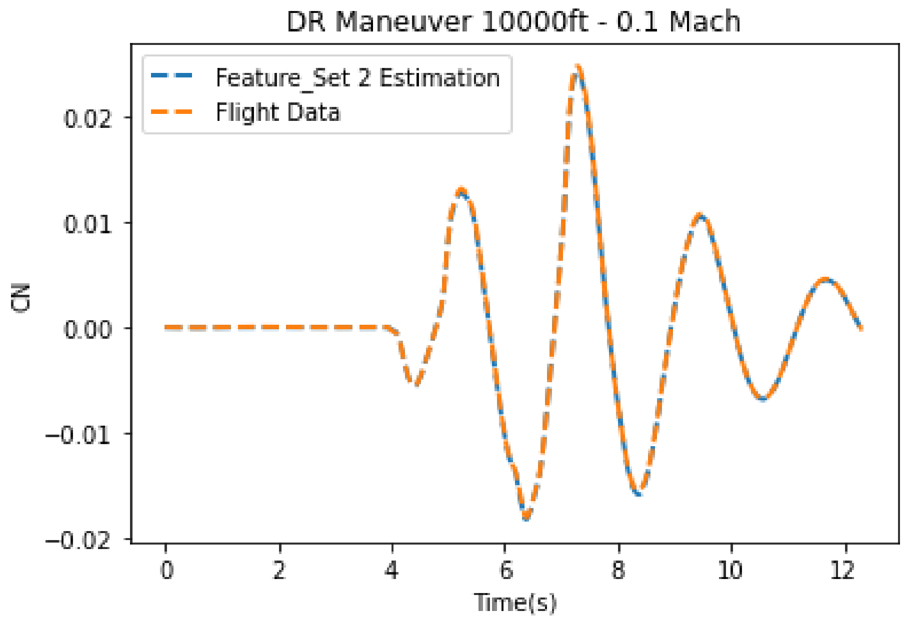

Figure 5.50 : DR-4, Feature Set 2 Simulation Result, 0.5 Mach – 10000 ft

5.3.2.4 Conclusion for lateral and directional results

When analyzing Dutch Roll and Bank-to-Bank flight maneuvers at 0.5 Mach at 10,000 feet and 0.65 Mach at 30,000 feet, it is observed that both simple and complex feature sets estimations are bringing close results at side force, yaw moment and roll moment coefficients within the linear regime. This reflects that simpler feature set trained models also be able to reflect the aircraft dynamics under linear flight conditions.

On the other hand, when Dutch Roll and Bank-to-Bank maneuvers at 0.35 Mach at 30,000 feet and 0.8 Mach at 10,000 feet are examined, a significant increase in nonlinearity is noted as the extreme points of the flight envelope are approached. Effects of the near stall angle of attacks and transonic region start to be seen on the aerodynamic characteristics. In these scenarios, results of the comparison of the feature sets shows that higher accuracy is demonstrated by the models are trained with complex feature set compared to the simpler feature set.

As in the longitudinal moment and force coefficient estimations, these comparison analyses indicates that in order to enhance the accuracy in flight test regions where nonlinearity increases, it is essential to complex feature sets to better estimate the characteristics of the aircraft in the whole flight envelope.

6. COMPARISON OF DEEP LEARNING BASED SYSTEM IDENTIFICATION ESTIMATIONS WITH DIFFERENT FLIGHT TEST REGIONS

In the next chapter, one of the most crucial aspects of System Identification studies, the cost of flight tests, is discussed. Optimizing flight test maneuvers and input sets for cost efficiency is essential. Various analyses in aircraft development require different levels of accuracy of the flight dynamics model, making it important to gather the necessary data.

In order to achieve optimization at the flight test survey, neural network studies conducted with different flight region data sets in this study. Therefore, the effects of the gathering different amount of flight data and different flight region data is observed for the fidelity of the aircraft modeling.

Firstly, the models that will be compared, trained with only non-linear region data. This region mainly includes the flight test region where the effects of near stall and transonic region start to be seen on the aerodynamic data. Which equals to high speed – low altitude and low speed – high altitude regions of the flight regime.

Secondly, the models trained with only linear region data. This region mainly includes where aircraft maneuvering tendencies are expected to stay similar for a certain amount of change in both angle of attack and velocity.

Finally, models trained with full-flight region flight data. That includes all the data that used both in linear and non-linear region specific data sets. With this way, the increase at the fidelity of models with the diversity and amount of data is observed.

Each of these steps are conducted with two different density of flight data cases. Firstly the models are trained with the low volume of the flight data. Secondly models are trained with the high volume of data. This means the flight conditions of those tests are same however the number of the flight test point are varies. Therefore, in total of this section of the study, 6 different cases tested. Flight envelope and the definations of these cases will be described in the following section.

magna aliquyam erat, sed diam voluptua. At vero eos et accusam et justo duo dolores et ea rebum. Stet clita kasd gub rgren, no sea takimata sanctus est

6.1 Flight Test Envelope & Case Definition

In this section, firstly, definitions of these cases and how many flight test points are used is described. After that, the used data's representation in the flight envelope graph is shown. Finally, performance of the model that created with the regarding case shown. In order to show performance, the loss function and mean absolute error results according the whole three different cases are presented.

6.1.1 Case 1: Non-linear region model (sparse data)

In this model, only the flight test points that is on the non-linear region used. And in order to show effect of the volume, only one test point from each corner of the flight test points is presented. Altitude and mach values of the test points given at Figure 6.1 and the total loss and mean absolute values are given at the Table 6.1.

- 4 Short Period Maneuver
- Non-Linear Region
- Sparse Data

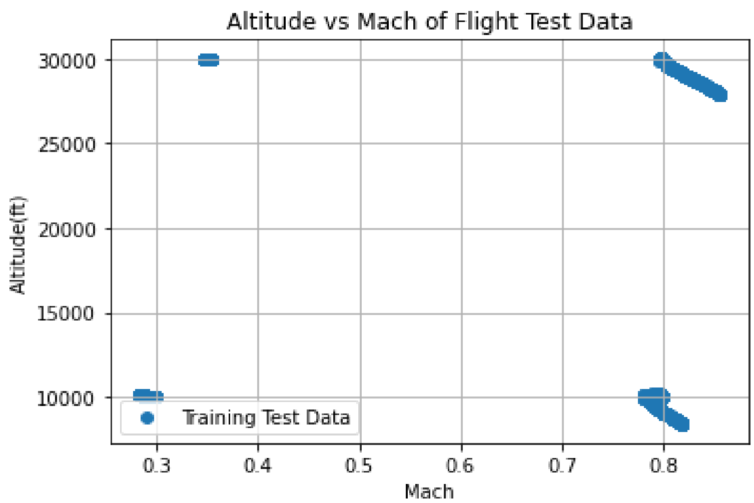

Figure 6.1 : Altitude vs Mach graph for the Case 1.

Table 6.1 : Loss and mean absoulte values for the analyses of Case 1.

	Linear Region		Nonlinear Region		Full Flight Region	
Cases	loss	mae	loss	mae	loss	mae
1	0,000028094	0,0025	1,0153E-05	0,0018	1,98E-05	0,0022

6.1.2 Case 2: Non-linear region model (dense data)

In this case, flight test points that are on the non-linear region used. And in order to show effect of the higher volume, all the test points are at the non-linear region are used. Altitude and mach values of the test points given at Figure 6.2 and the total loss and mean absolute values are given at the Table 6.2.

- 10 Short Period Maneuver
- Non-Linear Region
- Dense Data

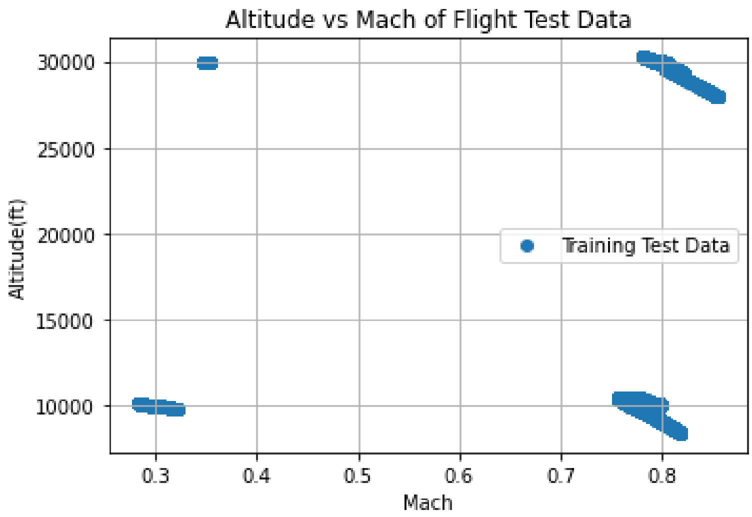

Figure 6.2 : Altitude vs Mach graph for the Case 2.

Table 6.2 : Loss and mean absoulte values for the analyses of Case 2.

	Linear Region		Nonlinear Region		Full Flight Region	
Cases	loss	mae	loss	mae	loss	mae
2	0,000017441	0,0016	6,7685E-06	0,0012	1,25E-05	0,0014

6.1.3 Case 3: Linear region model (sparse data)

In the case 3, flight test points that are on the linear region are used. And in order to show effect of the lower volume, only couple flight test points from the linear flight region are used. Altitude and mach values of the test points given at Figure 6.3 and the total loss and mean absolute values are given at the Table 6.3.

- 4 Short Period Maneuver Taken
- Linear Region
- Sparse Data

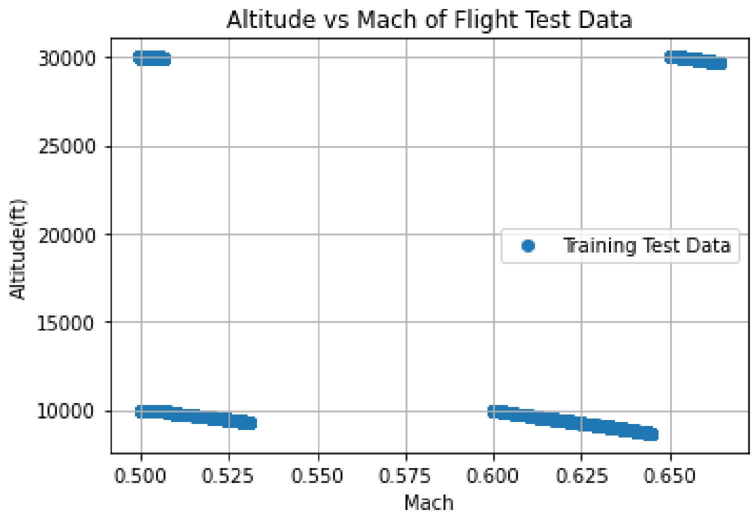

Figure 6.3 : Altitude vs Mach graph for the Case 3.

Table 6.3 : Loss and mean absoulte values for the analyses of Case 3.

	Linear Region		Nonlinear Region		Full Flight Region	
Cases	loss	mae	loss	mae	loss	mae
3	0,000015070	0,0013	3,7317E-05	0,0031	2,53E-05	0,0021

6.1.4 Case 4: Linear region model (dense data)

In the case 4, flight test points that are on the linear region are used. To show effect of the higher volume of the flight data, every flight test points from the linear flight region are used. Altitude and mach values of the test points given at Figure 6.4 and the total loss and mean absolute values are given at the Table 6.4.

- 11 Short Period Maneuver Taken
- Linear Region
- Dense Data

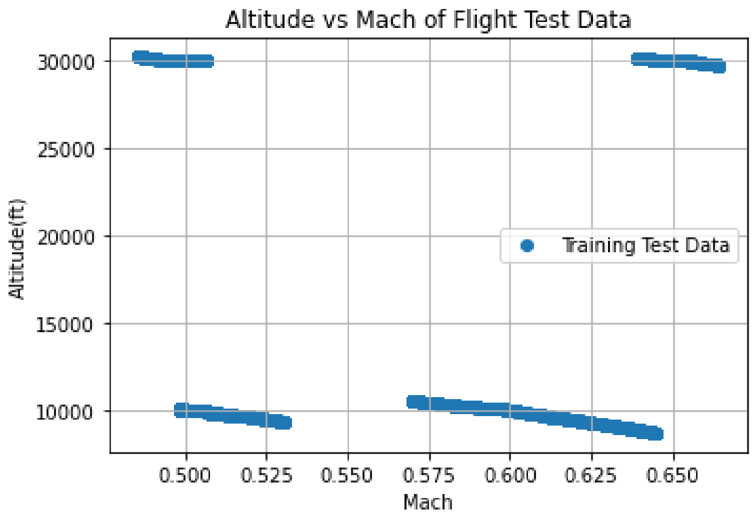

Figure 6.4 : Altitude vs Mach graph for the Case 4.

Table 6.4 : Loss and mean absoulte values for the analyses of Case 4.

	Linear Region		Nonlinear Region		Full Flight Region	
Cases	loss	mae	loss	mae	loss	mae
4	0,000007325	0,00083	1,4516E-04	0,0070	7,07E-05	0,0036

6.1.5 Case 5: Full flight region model (sparse data)

In the case 5, flight test points from both linear and non-linear regions are selected. To show effect of the lower volume of the flight data, only one test from each corner of the flight envelope and one test from the decided linear regions are used. Altitude and mach values of the test points given at Figure 6.5 and the total loss and mean absolute values are given at the Table 6.5.

- 8 Short Period Maneuver Taken
- Full Flight Region
- Sparse Data

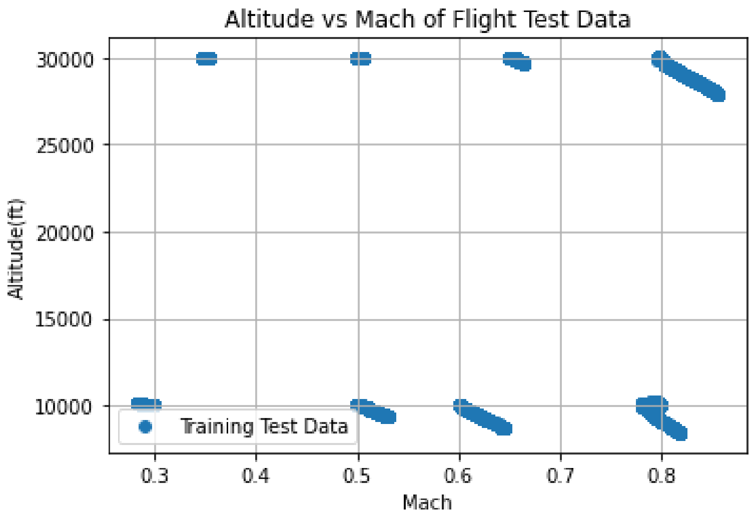

Figure 6.5 : Altitude vs Mach graph for the Case 5.

Table 6.5 : Loss and mean absoulte values for the analyses of Case 5.

	Linear Region		Nonlinear Region		Full Flight Region	
Cases	loss	mae	loss	mae	loss	mae
5	0,000011962	0,0012	5,9117E-06	0,0012	9,18E-06	0,0012

6.1.6 Case 6: Full flight region model (dense data)

In the case 6, flight test points from both linear and non-linear regions are selected. To show effect of the higher volume of the flight data, every flight test points from both linear and non-linear regions are used. Altitude and mach values of the test points given at Figure 6.6 and the total loss and mean absolute values are given at Table 6.6.

- 22 Short Period Maneuver Taken
- Full Flight Region
- Dense Data

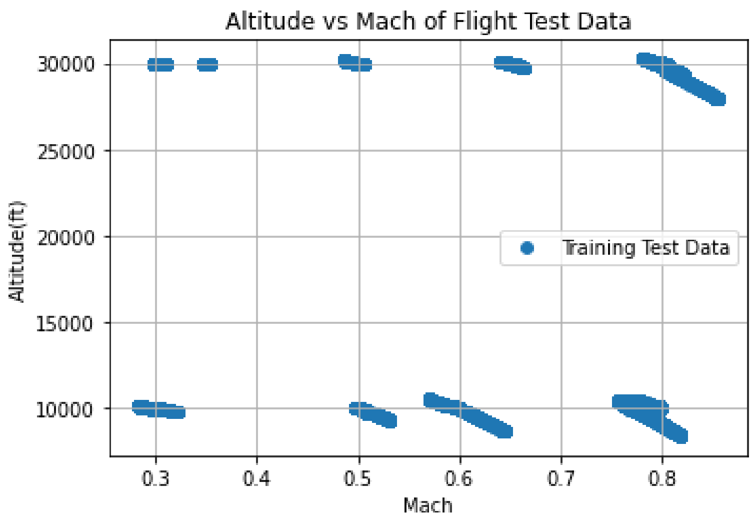

Figure 6.6 : Altitude vs Mach graph for the Case 6.

Table 6.6 : Loss and mean absoulte values for the analyses of Case 6.

	Linear Region		Nonlinear Region		Full Flight Region	
Cases	loss	mae	loss	mae	loss	mae
6	0,000007921	0,00091	3,8251E-06	0,0008	6,04E-06	0,0009

6.2 Flight Results of the Cases Comparison of Different Cases

In this section, flight test results of the models that trained with each case will be presented. In order to show the performance of the trained models, linear and non-linear flight test points are selected. Afterwards, trained models performance under both conditions are examined. In the following chapters, graphs of the flight tests results will be shown, on the left side linear region flights and on the right side non-linear region flight test points are presented. These test points are added sequentially regarding to time and total CM values shown at Short Period maneuvers.

6.2.1 Case 1: Non-linear region model (sparse data) – flight results

It can be seen in the following graphs that, the model that trained only at non-linear region data is not representing the linear region data sufficiently, however it presents better results at non-linear region. Simulation results for the Case 1 given at the Figure 6.7 and Figure 6.8.

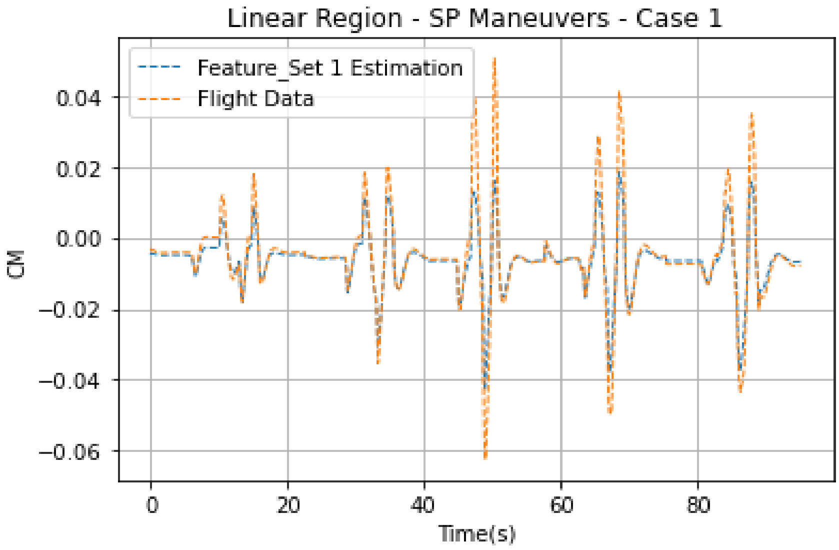

Figure 6.7 : Linear region Short Period simulation results for the Case 1.

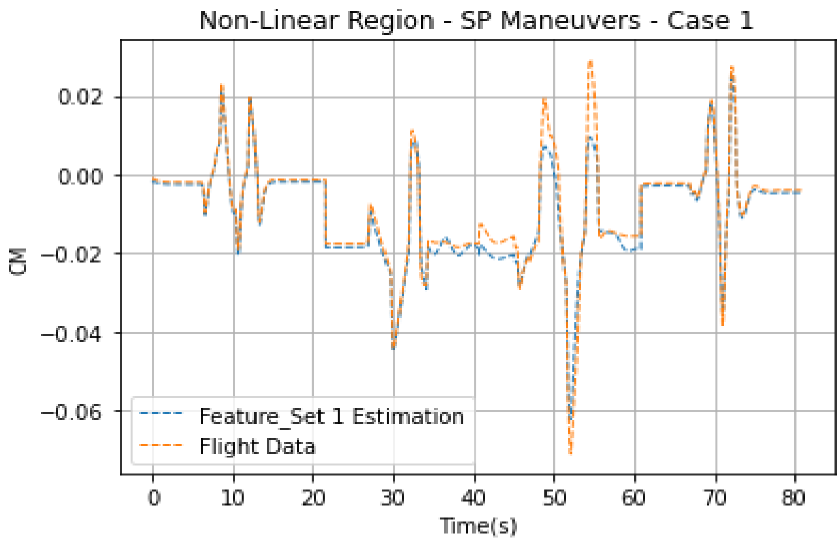

Figure 6.8 : Non-linear region Short Period simulation results for the Case 1.

6.2.2 Case 2: Non-linear region model (dense data) – flight results

In the case 2, model that trained with only non-linear region however with higher volume data. Effect of higher volume can be seen especially in some improvements that occurred in linear regions. It can be said the amount of the data plays crucial role however it is not an enough solution to be covering both regions. Simulation results for the Case 2 given at the Figure 6.9 and Figure 6.10.

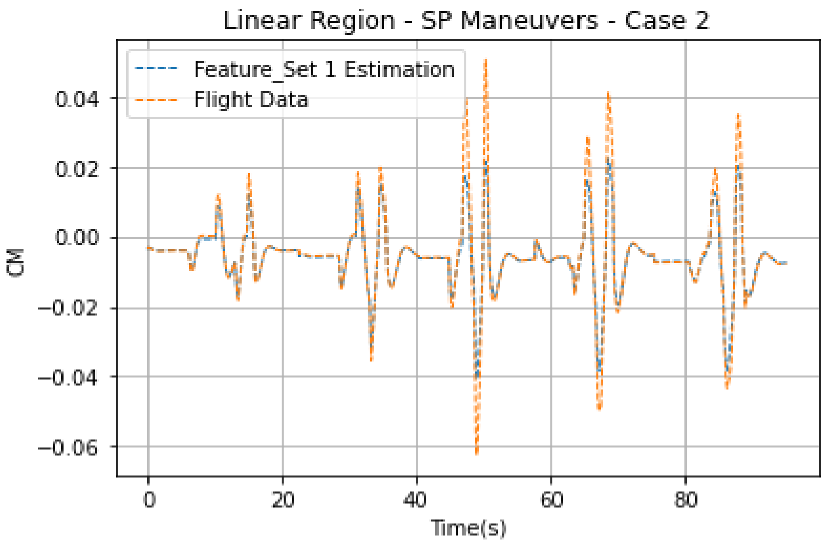

Figure 6.9 : Linear region Short Period simulation results for the Case 2.

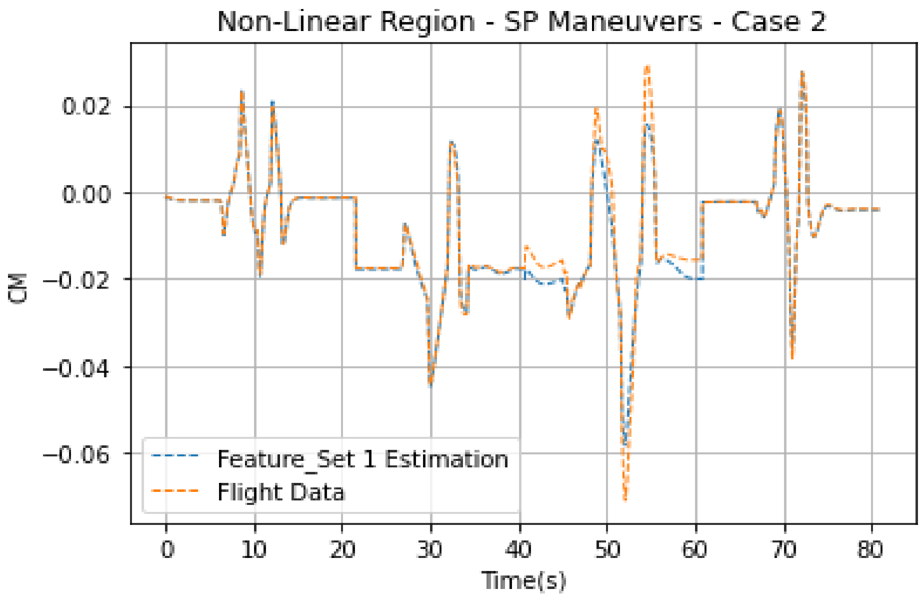

Figure 6.10 : Non-linear region Short Period simulation results for the Case 2.

6.2.3 Case 3: Linear region model (sparse data) – flight results

In the case number 3, the model is trained with only linear region and sparse data. When the graphs that represent the result of the maneuvers is analyzed, it can be seen that trained model is showing adequate results in the linear flight test maneuvers, however in non-linear region the model shows a necessary in the improvements. Simulation results for the Case 3 given at the Figure 6.11 and Figure 6.12.

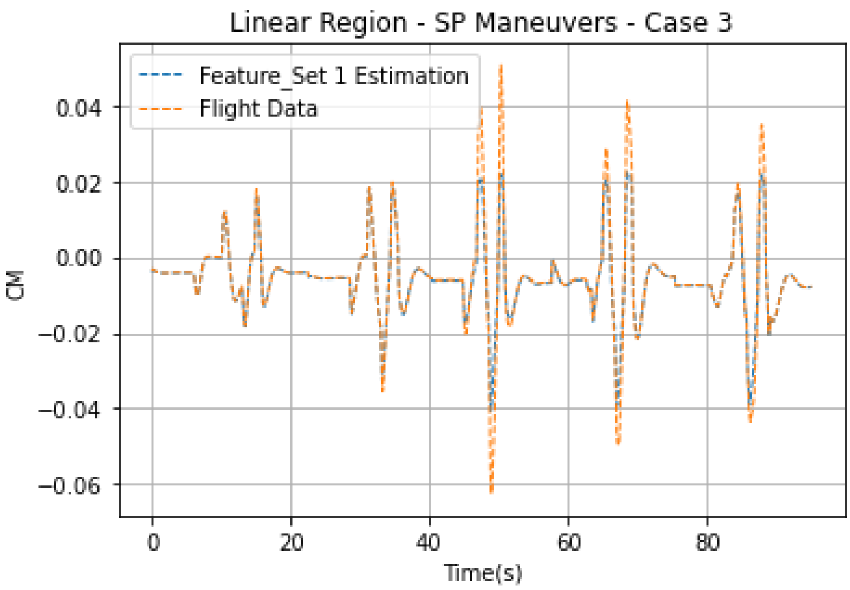

Figure 6.11 : Linear region Short Period simulation results for the Case 3.

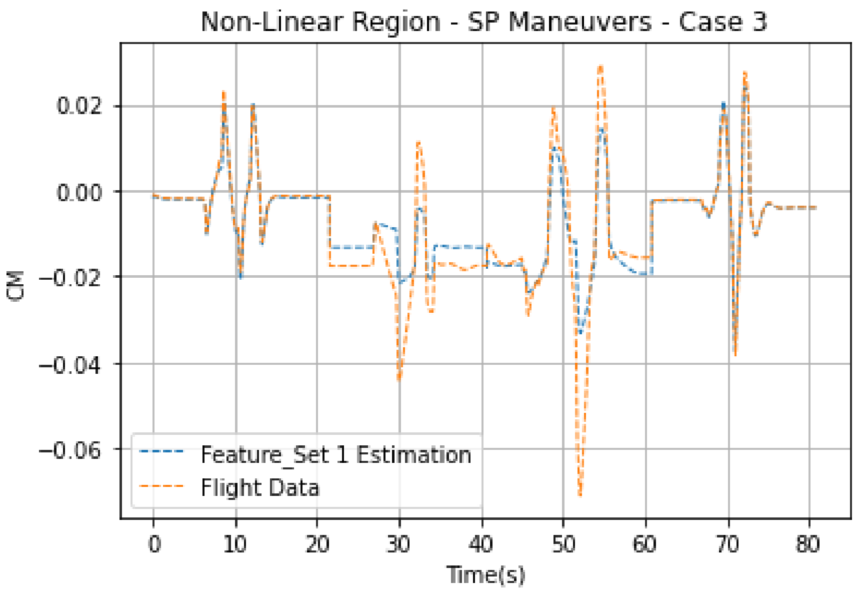

Figure 6.12 : Non-linear region Short Period simulation results for the Case 3.

6.2.4 Case 4: Linear region model (dense data) – flight results

In the case 4, the model only trained with linear region flight test data but with the higher amount of the data. Therefore while we can see improvements in the linear region, some of the non-linear region data shows that the more data in the linear region might diverge the non-linear region even more. Simulation results for the Case 4 given at the Figure 6.13 and Figure 6.14.

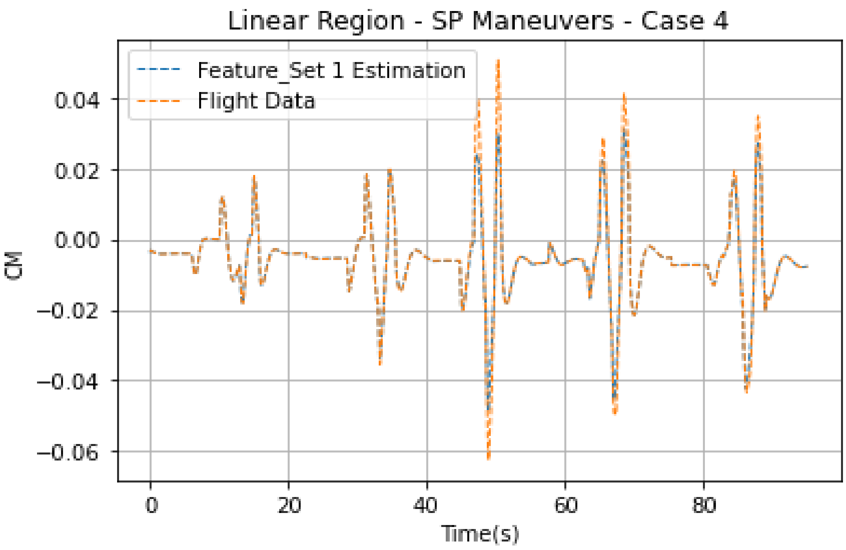

Figure 6.13 : Linear region Short Period simulation results for the Case 4.

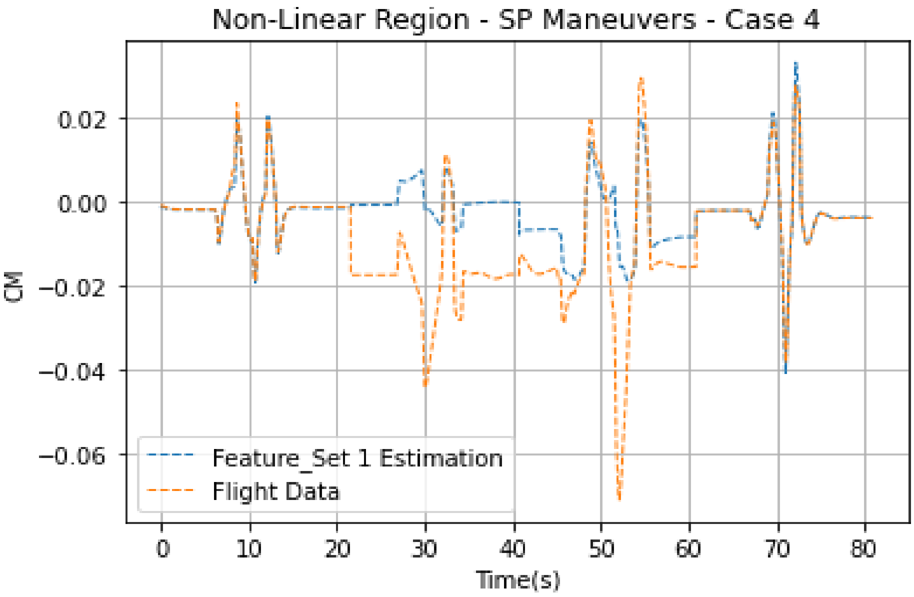

Figure 6.14 : Non-linear region Short Period simulation results for the Case 4.

6.2.5 Case 5: Full flight region model (sparse data) – flight results

In the case number 5, the model is trained with both flight test points from linear region and non-linear region. In order to show the effect of the low volume of the flight test data, only one from the each flight test condition is selected. When the graphs that represent the result of the maneuvers is analyzed, it is clear that the trained model is showing adequate results in most of the both linear and non-linear flight test maneuvers, however it can be also seen that the model needs to be trained with higher amount data to correspond to each flight test maneuver. Simulation results for the Case 5 given at the Figure 6.15 and Figure 6.16.

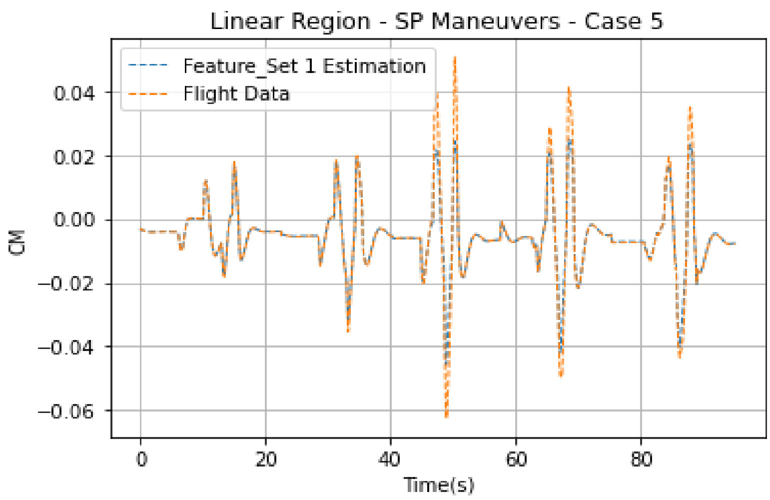

Figure 6.15 : Linear region Short Period simulation results for the Case 5.

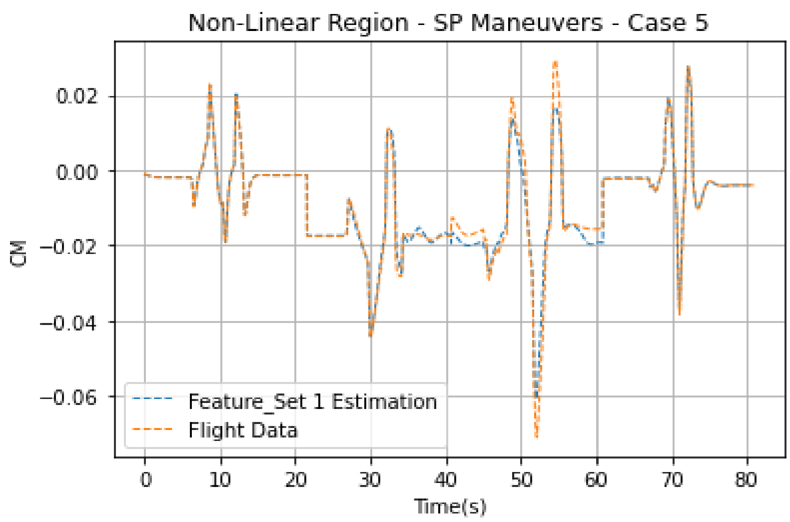

Figure 6.16 : Non-linear region Short Period simulation results for the Case 5.

6.2.6 Case 6: Full flight region model (dense data) – flight results

In this model, only the flight test points that is on the non-linear region used. And in In the last case, the model is trained with the all the flight test points from both flight test points from linear region and non-linear region. In order to show the effect of the dense flight test data, all of the test points that described in the prediction area are used. When the graphs that represent the result of the maneuvers is analyzed, it is clear that the trained model is showing best results in the all the cases are tested. It also improved the results in both linear and nonlinear compared to the case5. Simulation results for the Case 6 given at the Figure 6.17 and Figure 6.18.

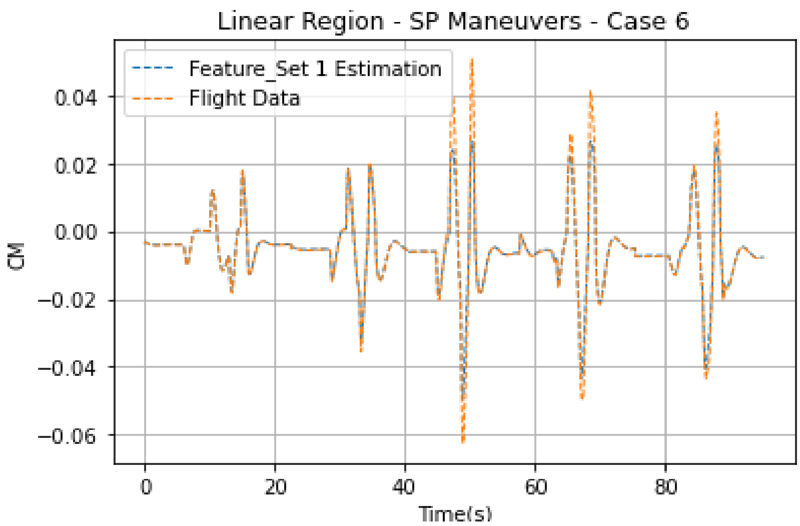

Figure 6.17 : Linear region Short Period simulation results for the Case 6.

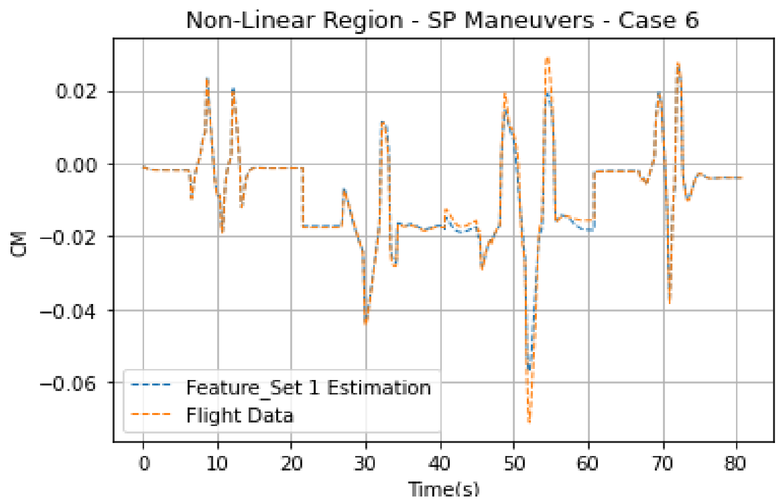

Figure 6.18 : Non-linear region Short Period simulation results for the Case 6.

6.3 Comparison of Different Cases

In this In this section, names and the loss functions of the each cases are given. Firstly, in order to compare which parameter belong to which cases, name of the cases are given in the following paragraph. Later, each cases' loss function results in linear, non-linear and all flight test results are presented.

- Case 1: Non-Linear Region Model (Low Data)
- Case 2: Non-Linear Region Model (Dense Data)
- Case 3: Linear Region Model (Low Data)
- Case 4: Linear Region Model (Dense Data)
- Case 5: Full Flight Region Model (Low Data)
- Case 6: Full Flight Region Model (Dense Data)

6.3.1 Model comparison in linear flight region

It can be seen In this section, loss functions are compared of the each model that prepared with different cases. Results of the models with all linear flight test points are shown at the Figure 6.19.

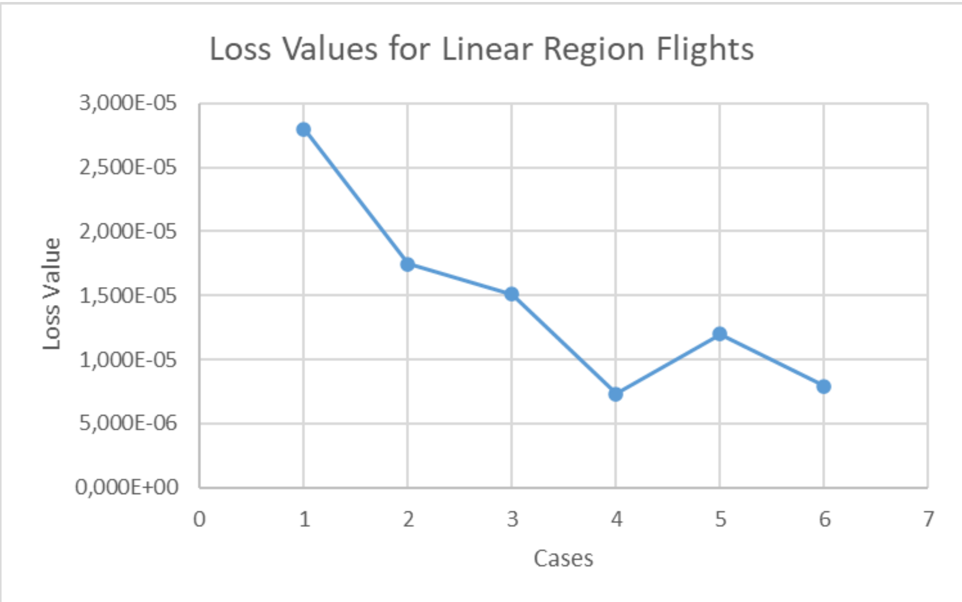

Figure 6.19 : Loss Value comparison of the different Cases at linear flight region.

It can be seen that the loss function result of the models trained with non-linear only flight data is significantly high. Therefore it can be said that the models trained in non-linear only data might diverge in linear conditions. After that, when both linear only and full flight data cases are analyzed, it can be seen that those cases show similar characteristics. The region selection becomes correct and the significance of the amount of data starts to increase.

6.3.2 Model comparison in linear flight region

Results of the models that trained with each cases regarding to the all nonlinear flight test points are shown at the Figure 6.20.

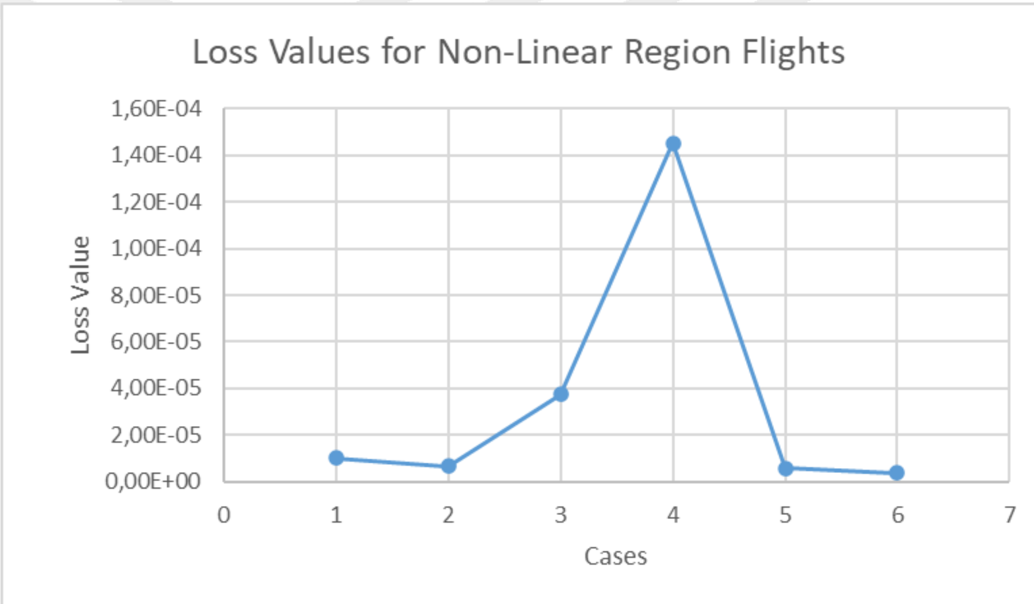

Figure 6.20 : Loss Value comparison of the different Cases at non-linear flight region.

According to the graph above, its clear that the situation is opposite for the first four cases, where linear only data trained models loss functions become significantly higher. Similar to the linear case, both non-linear only data trained models and full flight test trained models show the similar results.

6.3.3 Model comparison in linear flight region

Results of the models that trained with each cases regarding to the all nonlinear flight test points are shown at the Figure 6.21.

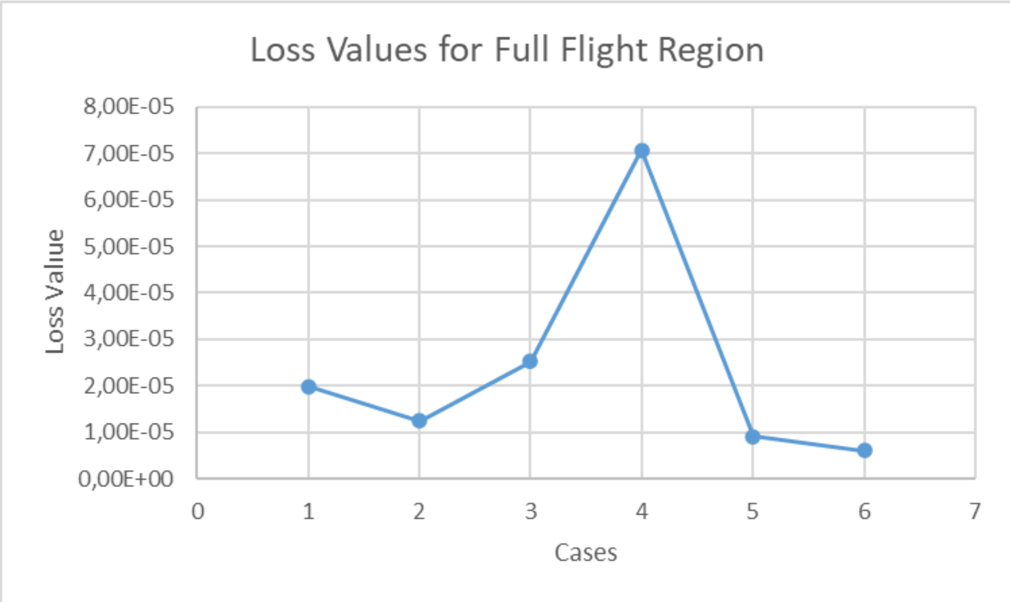

Figure 6.21 : Loss Value comparison of the different Cases at full flight region.

When loss function values are compared for the full flight test regions, it can be observed that the models trained with full flight test region performance critically better. This shows that, the flight test data that the models that will be trained must include and scan all the flight region the model wanted to be used.

7. CONCLUSIONS

In this thesis, comprehensive analyses of the aircraft dynamics under various flight conditions are conducted and the effectiveness of simple and complex feature sets in capturing aerodynamic behaviors are examined. Final results reveal deliberate insights into the performance of predictive models across different flight envelopes.

Firstly, for the analysis of longitudinal aerodynamic parameters with short period flights, it is observed that both simple and complex feature sets yield comparable results within the linear regime. However, as flight conditions approach extreme points of the envelope, nonlinearities become prominent. This indicates a necessity for the inclusion of the complex parameters to the feature set for higher accuracy. With this way, the importance of considering the full flight envelope becomes clearer when developing predictive models that accurately represent aerodynamic behavior under diverse conditions.

Secondly, in the examination of Dutch Roll and Bank-to-Bank maneuvers, similar trends emerged, with simple feature sets performing adequately within linear regimes. However, it shows limitations in capturing nonlinear effects near stall angles and in transonic regions. Complex feature sets proved essential for achieving higher accuracy in these challenging flight scenarios. Therefore, it becomes clear that the feature sets need to be preparade considering the entire flight envelope.

Lastly, the analyses of loss function values showed the significance of which regions that models are trained. The results indicate the overachievement of the flight test data of the full range of flight envelope. Models trained with data from the complete flight envelope consistently outperformed those trained with partial data of linear or non-linear regions, emphasizing the importance of thorough data coverage for robust predictive modeling.

In conclusion, this thesis contributes valuable insights into the development of predictive models for aircraft dynamics, demonstrating the critical role of complex feature sets and comprehensive training data in accurately representing aerodynamic behavior across various flight conditions. These findings have implications for aircraft design, flight simulation, and control system development, paving the way for improved performance and safety in aviation.

REFERENCES

Andersson, C., Ribeiro, A. H., Tiels, K., Wahlström, N., & Schön, T. B. (2019, December). Deep convolutional networks in system identification. In 2019 IEEE 58th conference on decision and control (CDC) (pp. 3670-3676). IEEE.

Bagherzadeh, S. A. (2018). Nonlinear aircraft system identification using artificial neural networks enhanced by empirical mode decomposition. Aerospace Science and Technology, 75, 155-171.

Behera, S. K., & Rana, D. (2014). System identification using recurrent neural network. Int. J. Adv. Res. Electr. Electron. Instrum. Eng, 3(3).

Çetin, E. (2018). System identification and control of a fixed wing aircraft by using flight data obtained from x-plane flight simulator (Master's thesis, Middle East Technical University).

Chauhan, R. K., & Singh, S. (2017, January). Application of neural networks based method for estimation of aerodynamic derivatives. In 2017 7th International Conference on Cloud Computing, Data Science & Engineering-Confluence (pp. 58-64). IEEE.

Dubois, G. (2018). Modeling and simulation: challenges and best practices for industry. CRC Press.

Echevarría Corrales, F. (2021). Artificial intelligence methods for identification of aerodynamic coefficients from flight data.

Grauer, J. A., & Morelli, E. A. (2015). Generic global aerodynamic model for aircraft. *Journal of Aircraft*.

Harris, J., Arthurs, F., Henrickson, J. V., & Valasek, J. (2016, June). Aircraft system identification using artificial neural networks with flight test data. In 2016 international conference on unmanned aircraft systems (ICUAS) (pp. 679-688). IEEE.

Jategaonkar, R. V. (2006). Flight vehicle system identification: A time domain methodology. American Institute of Aeronautics and Astronautics.

Kirkpatrick, K., May, J., & Valasek, J. (2013, January). Aircraft system identification using artificial neural networks. In 51st AIAA Aerospace Sciences Meeting including the New Horizons Forum and Aerospace Exposition (p. 878).

Kumar, M. V., Omkar, S. N., Ganguli, R., Sampath, P., & Suresh, S. (2006). Identification of helicopter dynamics using recurrent neural networks and flight data. Journal of the American Helicopter Society, 51(2), 164-174.

Liu, Q., Zhang, P., Xiao, W., & Diao, J. D. (2019, July). Correction methods of aerodynamic force and moment coefficients based on the identification data. In 2019 Chinese Control Conference (CCC) (pp. 1581-1586). IEEE.

Millidere, M., Akgül, F., & Leblebicioğlu, K. (2021). F16 savaş uçağının boylamsal aerodinamik veritabanının tanımlanması ve doğrulanması. In Ulusal Havacılık ve Uzay Konferansı. Virtual Conference.

Millidere, M., Cakin, U., & Yigit, T. (2019). Generating aerodynamic database from closed loop simulated flight data. In European Conference for Aeronautics and Space Sciences. Madrid, Spain.

Millidere, M. (2021). Optimal input design and system identification for an agile aircraft.

Moreira, L., & Soares, C. G. (2003). Dynamic model of manoeuvrability using recursive neural networks. Ocean Engineering, 30(13), 1669-1697.

Morelli, E. A., & Klein, V. (2006). Aircraft system identification: Theory and practices. Reston, VA: AIAA.

Nguyen, L. T. (1979). Simulator study of stall/post-stall characteristics of a fighter airplane with relaxed longitudinal static stability (Vol. 12854). National Aeronautics and Space Administration.

Paris, A. C., & Bonner, M. (2004). Nonlinear model development from flight-test data for F/A-18E Super Hornet. *Journal of Aircraft, 41*(4), 692-702.

Patel, D. (2007). System Identification of General Aviation Aircraft Using The Filter Error Technique (Doctoral dissertation).

Putra Amiruddin, Brilian. (2020). Deep Learning Methods for System Identification of UAV. 10.31224/osf.io/adr97.

Roudbari, A., & Saghafi, F. (2016). Generalization of ANN-based aircraft dynamics identification techniques into the entire flight envelope. IEEE Transactions on Aerospace and Electronic Systems, 52(4), 1866-1880.

Russell, R. S. (2003). Non-linear F-16 simulation using Simulink and Matlab. University of Minnesota.

Schoukens, J., Pintelon, R., & Rolain, Y. (2004, June). Time domain identification, frequency domain identification. Equivalencies! Differences?. In Proceedings of the 2004 American Control Conference (Vol. 1, pp. 661-666). IEEE.

Stevens, B. L., Lewis, F. L., & Johnson, E. N. (2015). Aircraft control and simulation: Dynamics, controls design, and autonomous systems. John Wiley & Sons.

Tischler, M. B., & Remple, R. K. (2012). *Aircraft and rotorcraft system identification: Engineering methods with flight test examples* (2nd ed.). Reston, VA: AIAA.

Zheng, Y., & Xie, H. (2018). Review on neural network identification for maneuvering UAVs. In 2018 International Conference on Sensing, Diagnostics, Prognostics, and Control (SDPC) (pp. 362-366). IEEE.

CURRICULUM VITAE

Name Surname : **Mehmet Can ŞEN**

EDUCATION :

- **B.Sc.** : 2019, Istanbul Technical University, Aeronautical Engineering, Aeronautical and Aerospace Department

PROFESSIONAL EXPERIENCE AND REWARDS:

- 2017-2019 Modeling and Simulation Engineer / Student for VLA Aircraft project at Turkish Aerospace and ISTANBUL Technical University cooperation
- 2019-Present Modeling and Simulation Engineer for Turkish Aerospace